



מכון ויצמן למדע

WEIZMANN INSTITUTE OF SCIENCE

Thesis for the degree
Doctor of Philosophy

עבודת גמר (תזה) לתואר
דוקטור לפילוסופיה

Submitted to the Scientific Council of the
Weizmann Institute of Science
Rehovot, Israel

מוגשת למועצה המדעית של
מכון ויצמן למדע
רחובות, ישראל

By
Marija Vucelja

מאת
מריה ווצליה

פרקטלים ואירועים נדירים במערכות רחוקות משיווי משקל
Fractals and rare events in non-equilibrium systems

Advisor:
Prof. Gregory Falkovich

מנחה:
פרופ' גריגורי פלקוביץ

July, 2010

אב תש"ע

Contents

List of Figures	vi
Abstract	vii
Acknowledgements	viii
Introduction	1
Clustering of particles in flows	2
Two examples of two-dimensional turbulence	3
Passive scalar contours	3
Point vortices as a discretization of a 2D flow	4
Non-equilibrium mixing accelerates computations	5
I Clustering of particles in flows	7
1 Clustering of matter in waves and currents	9
1.1 Weakly nonlinear waves	12
1.2 Contribution of the surface curvature	12
1.3 The Green-Kubo formula for the clustering rate	13
1.4 Relating Eulerian and Lagrangian averages	14
1.5 The clustering rate λ for weakly-interacting waves	15
1.6 The clustering of matter in surface waves	16
1.6.1 The velocity field of the floaters	17
1.6.2 Results on clustering in surface waves	18

1.7	Conclusions on clustering with surface waves	19
1.8	Interplay of waves and currents	19
1.8.1	The ballistic limit	22
1.8.2	The diffusive limit	22
1.8.3	Limit of fast-oscillating waves	22
1.9	Results on clustering with waves and currents	24
1.10	Remark on entropy production rate in dynamical systems	25
2	Particles in a flow with time correlations	26
2.1	The model	27
2.1.1	Telegraph noise	29
2.2	Results	31
2.2.1	The statistics of the particle-velocity gradient	31
2.2.2	The Lyapunov exponent	36
2.2.3	Lyapunov moments	37
2.2.4	Short-correlated flows	37
2.2.5	Long-correlated flows	39
2.3	Conclusions	41
2.3.1	Further directions	41
II	Two-dimensional turbulence	43
3	Passive scalar contours	45
3.1	Heuristic arguments for fractal dimension $D_0 = 3/2$	48
3.2	The numerical algorithm	50
3.2.1	Generating the passive scalar field	50
3.2.2	Analysing the contours	51
3.3	Results	52
4	2D turbulence of point vortices	54
4.1	Point vortices	55

4.1.1	Cloud-in-cell algorithm	56
4.2	Concluding remarks	57
III	Non-equilibrium mixing accelerates computations	59
5	Efficient Sampling with Irreversible Monte Carlo Algorithms	61
5.1	The irreversible MCMC algorithm	63
5.2	Testbed - a ferromagnetic spin-chain	65
5.2.1	Results	66
5.3	Relation of proposed irreversible MCMC to previous studies	67
5.4	Conclusions	68
	Bibliography	69
	List of Publications	80
	Statement about independent collaboration	81
	Appendix	82
A	Derivation of the Green-Kubo formula for the clustering rate λ	82
B	Note on the Gaussianity of weak wave turbulence	85
C	The diagrammatic technique	86
C.1	Correlation functions of normal coordinates	90
C.2	Rules and vertices	95
C.3	Correlation function $\langle a'^* a' \rangle$	96
C.4	Correlation function $\langle a' a' \rangle$	98
C.5	Correlation function $\langle a_1 a_2 a_3 \rangle$	99
C.6	Correlation function $\langle a_1^* a_2 a_3 \rangle$	100
C.7	Correlation function $\langle \tilde{a}_1^* \tilde{a}_2^* \tilde{a}_3 \tilde{a}_4 \rangle$	100
C.8	Four wave interaction	101
C.9	Higher than ϵ^4	101
C.10	Calculating the sum of Lyapunov exponents	101

C.11	Term λ_{aaaa}	108
C.12	The sum of Lyapunov exponents for gravity-capillary waves	117
D	The velocity field of floaters	118
E	Calculation of the clustering rate of surface waves	120
E.1	Calculation of λ_4	120
E.2	Reduction to terms involving interactions and the zero frequency field . .	122
E.3	The expression for ψ	123
E.4	Calculation of the quadratic term	124
E.5	Calculation of terms in λ involving products of four fields	125
E.6	Calculation of the fourth-order terms in λ_2	125
E.7	Calculation of the fourth-order terms in λ_3	127
E.8	Summary	128
F	Interaction terms containing the products of three fields	129
G	Continuity of the PDF of particle-velocity gradient for $St = St^*$	131
H	The derivation of Lyapunov moments	134

List of Figures

1.1	North Pacific subtropical convergence zone	9
1.2	Clustering of hollow glass particles in a water tank	10
1.3	Satellite image of a swirl near Japan with a plankton bloom	20
1.4	Isolines of the clustering rate in the presence of waves and currents	21
2.1	Clouds over Jordan river	27
2.2	Particle aggregation in a turbulent Keplerian flow	28
2.3	The Lyapunov exponent on the Kubo-Stokes number plane	30
2.4	The phase transitions in the PDF of x on plane (St,Ku)	33
2.5	PDF of the particle-velocity gradient at small Stokes number	34
2.6	PDF of the particle-velocity gradient in the large Stokes regime	35
2.7	The Lyapunov exponent as a function of Kubo number	36
2.8	Lyapunov exponent $\lambda \equiv \langle x(t) \rangle - \tau/2$ in short-correlated flows.	38
2.9	Lyapunov exponent in long-correlated flows	40
3.1	Passive scalar occurrences in nature	45
3.2	Instances of passive scalar in experiment and simulations	46
3.3	Snapshot of the passive scalar field	49
3.4	Sketch of the passive scalar isolines	50
3.5	Sketch of creation of fjords on passive scalar contours	50
3.6	A typical long passive scalar isoline	52
3.7	The box-counting fractal dimension of passive scalar contours	53
4.1	The energy spectra and the energy of point vortices	56

5.1	Schematic representation of the replication deformation	63
5.2	Correlation time of the total spin de-correlation in the spin-cluster model.	65

Abstract

I studied several physical situations in which turbulence plays a key role. By turbulence we mean a state of a physical system with many degrees of freedom strongly deviated from equilibrium. Each problem is a separate story and common to all is that the systems considered are out of equilibrium and that the focus is on fractal distributions in either physical or phase space. I begin by discussing clustering of particles in flows due to compressibility and due to inertia. I then switch to two-dimensional turbulence and investigate the fractal nature of contours of a passive scalar in a smooth, temporally uncorrelated, Gaussian velocity field and the energy cascade in a forced system of point vortices. The last problem introduces a method which utilizes non-equilibrium mixing to accelerate the convergence of a Markov Chain Monte Carlo algorithm towards equilibrium.

Acknowledgements

First time I came to Israel it was in 2002, and I was invited to spend a summer at the Weizmann Institute of Science. The visit was so impressive that I decided this was the place to continue my studies. By now, I have spent seven years in this magnificent country and consider it my second home. I am in debt to all of the wonderful people, that I have met during these years, who embraced me with their hospitality and warm heartedness. I owe my deepest gratitude to Grisha Falkovich for all the knowledge, support, guidance and care, that he provided me with. Grisha's unparalleled intuition in physics is only one of many things that have drawn me to work with him, and by now I hope I have inherited some of this "magic" myself. I spent almost a year of my Ph.D. at Los Alamos, where I worked with Misha Chertkov and Kostya Turitsyn. I have learned a lot from Misha and Kostya, and consider them as my co-advisers. This collaboration was possible, because of the hospitality of the Los Alamos National Laboratory. Over the years I received numerous valuable advices from Elisha Moses and David Mukamel. Together with Grisha and Eran Bouchbinder they formed my thesis committee, and I benefited greatly from the committee's comments on my work. I had many illuminating discussions with Itzhak Fouxon, Victor Steinberg, Misha Stepanov, Volodya Lebedev, Pasha Wiegmann, Ildar Gabitov, Jeremie Bec, Dario Vincenzi and Israel Klich. My colleagues also helped me with their questions and suggestions, among them I should mention Yair Shokef, Raphael Chetrite, Agnese Seminara, Karen Michaeli, Zohar Komorgodskii, Assaf Avidan and Roni Ilan. I am grateful to Karen Michaeli and Israel Klich for translating the abstract of my thesis to Hebrew. Many thanks goes to numerous friends from Israel and abroad who colored these years; especially I want to thank the Novosibirsk "quartet": Alesha Lyashenko, Timich Shegai, Vasya Kantsler and Max Naglis for their friendship and for teaching me Russian. I am in debt to my family Otilija and Andjelko, brother Petar and grandmother Stefania and my relatives for their love, constant support and encouragement. Finally, I would like to thank Ralik (Israel Klich) for being his wonderful self and for making these years so beautiful.

*If the doors of perception were cleansed every thing would appear to man as it is,
infinite.*

William Blake

"The Marriage of Heaven and Hell", 1794

Introduction

Turbulence is a state of a physical system with many degrees of freedom strongly deviated from equilibrium. Historically, the term was used to describe exclusively motions of fluids, but in contemporary scientific jargon turbulence describes a chaotic, highly non-equilibrium state of a nonlinear physical system. Examples of turbulence in nature are abundant: ocean waves after a storm, rivers, vortices behind ships or cars, clouds, far-from-equilibrium states in solids, Bose-Einstein condensates or nonlinear optics etc; most fluids in nature are turbulent. Although omnipresent in the world around us, turbulence still lacks a unified theoretical description, and this is one of the central problems of modern physics. On the other side, the enormous amount of excited and interacting degrees of freedom involved, nonlinearity and lack of scale separations make computational efforts to realistically model turbulence futile. Understanding turbulence is of unprecedented importance for both theoretical and applied science.

Different realizations of turbulence from the same experiment do not look alike at all; common to them is that they appear disordered, unpredictable, irreproducible and irreversible. Ample empirical experience has convinced us that the appropriate language to study turbulence is the language of probability theory. Surprisingly enough, it appears that descriptions of many physical phenomena related to turbulence allow their understanding without detailed knowledge of the structure of turbulence. Sufficient to know is that one deals with the random flow possessing some general properties. In other words, there are universal laws describing the effects of a random flow.

In this thesis, I focus on fractal distributions appearing in turbulent states in either physical space or phase space. I study both fractal contours produced by incompressible random flows and fractal measures produced by compressible random flows. A deeper pursuit behind my work is finding universal aspects of turbulence. The paragraphs bellow, provide brief intro-

ductions to the problems considered in this thesis, and state the main results.

Clustering of particles in flows

We begin by presenting new analytical results related to the statistics of particles suspended in turbulent flows (see Chapters 1 and 2). These particles can be water droplets in clouds, dust in air, planetesimals in the early Solar system, concentration of plankton or an oil slick on the ocean surface etc. Spontaneous formation of clusters of particles suspended in chaotic flows may originate from two different physical processes: compressibility of the fluid flow and particle inertia. In the first case particles are trapped in regions of ongoing compression, while in the second case inertia causes their ejection from vortical regions. The underlying link between these phenomena is manifested in the limit of weak inertia, in which the particle dynamics in incompressible flows can be approximated by that of tracers in a weakly compressible velocity field [6, 72]. The following two paragraphs describe scenarios of clustering of particles due to compressibility and inertia, respectively.

Together with G. Falkovich and I. Fouxon, we looked into causes of patchiness of pollutants on the surfaces of oceans, seas and lakes. In most cases these water basins are stably stratified (convection is severely suppressed), yet patchiness is often present. Thus, a mechanism of producing inhomogeneities of floaters involves only the top layer of water. This hint lead us to consider flows of surface waves. We have shown that turbulence of surface waves is weakly compressible, and alone it cannot account for the clustering of matter on liquid surfaces, i.e. the timescales on which clustering occurs due to waves alone are too long compared to those observed in nature [103]. We made estimates of the rate and the fractal dimension of the density distribution. Lastly, we have shown that the interplay between waves and currents gives realistic timescales, and therefore can act as a source of inhomogeneities in natural environments [104].

Small impurities like dust, droplets or bubbles suspended in a flow, are finite-size particles whose density often differs from that of the underlying flow. Their behavior is vastly different from that of the point-like tracers. In the same small portion of the fluid one can find particles moving with substantially different velocities, which means that essentially the problem of inertial particles in a flow is more difficult than the related problem of tracers - it is kinetic,

rather than hydrodynamic [11, 12, 46]. Recently significant analytical progress was possible, by utilizing the Lagrangian approach, in one-dimensional temporally uncorrelated flows [33]. Following, G. Falkovich, S. Musacchio, L. Piterbarg and I have managed to obtain analytical results on the Lagrangian dynamics of inertial particles in a one-dimensional random flow with particular finite-time correlations [47]. The velocity gradients of the flow were set to obey the telegraph noise statistics. The motivation behind our work was to study the effects of time correlations on the dynamics of inertial particles. We discussed the asymptotic of short- and long-correlated flows, as well as the fluid-tracer limit [47]. The dependence of the Lyapunov exponent of particle trajectories on dimensionless parameters of the model revealed the presence of a region in parameter space, where the Lyapunov exponent changes sign, thus signaling the aggregation-mixing transition. Extensions of this model might turn out to be useful in describing rain formation, clustering of dust in air, optimization of combustion processes in engines etc.

Two examples of two-dimensional turbulence

Passive scalar contours

In many natural and engineering settings one encounters the advection of a passive substance by a flow. The concentration of such a substance can exhibit complex dynamic behavior that shows many phenomenological parallels with the behavior of a turbulent velocity field. The "substance" could be a pollutant, as in the familiar case of smoke dispersing in the air; or it could be heat, when a hot object is cooled in the flow; or a fluorescent dye mixed by a turbulent jet etc. Yet the statistical properties of this so-called *passive scalar* turbulence are decoupled from those of the underlying velocity field.

Few years ago passive scalar turbulence had yielded to mathematical analysis¹. A close link was discovered between the multipoint statistics of the advected fields and the collective behavior of the separating Lagrangian (fluid) particles. Essential for this progress has been the observation that anomalous scaling properties and coherent structures in a scalar field occur

¹ More information on the passive scalar problem one can get from references in review articles, such as [45, 91].

even for a scalar advected by a simple random Gaussian velocity field [60, 61, 63]. Now that we know much about the statistics of moments of the passive scalar field in different velocity fields, the question is can one go beyond moments and multi-point correlations functions of the fields advected by a flow and consider an infinite-point object, a line? Statistics of the isolines of passive scalar is of considerable practical importance, as it is the best characteristic of convective mixing (what was inside the isoline stays inside).

A recent discovery in mathematics, the so called *Schramm Loewner Evolution* (SLE) lead to an explosive growth of new results in mathematics, field theory and the theory of critical phenomena [10, 23, 67]. In fluid dynamics SLE was used to characterize the isolines of vorticity in the inverse cascade of two-dimensional flows [17, 24] and the isolines of temperature in surface-quasi-geostrophic flows [18]. This discovery motivated G. Falkovich, K. S. Turitsyn and myself to look at passive scalar contours in the case where the passive substance is carried by a two-dimensional, incompressible, smooth, Gaussian and delta-correlated in time velocity field (see Chapter 3). Such velocity fields are dubbed incompressible *Kraichnan* velocity fields in *Batchelor regime*, c.f. [8, 60]. Most of the analytical results on the statistics of passive scalar have been obtained for these flows. At present, even in this simplest case, there are no analytical results about individual contours. The problem is notoriously difficult since we are interested in single contours, and not the whole field of isolines. Objects of this kind are non-local structures, parametrized with infinite number point, which can recombine and disappear under the influence of forcing, advection and molecular diffusion. In [105] we have numerically obtained the box-counting fractal dimension of the passive scalar contours at scales much larger than the forcing scale. Within numerical accuracy, the result matches our heuristic prediction: $D_0 = 3/2$. We report on this work in Chapter 3.

Point vortices as a discretization of a 2D flow

With G. Falkovich and A. Shafarenko, we looked at an idealized two-dimensional turbulent flow [106]. In nature there are many examples of nearly two-dimensional turbulence, for instance large-scale motions in the atmosphere, shallow layers of a fluid, soap films etc. The steady state of 2D-turbulence has two integrals of motion balancing it, and these cascade through scales.

The energy flows upscale in an *inverse cascade*, while the enstrophy (integral of the square of the curl of velocity) cascades down toward smaller scales (*direct cascade*). One of the most relevant results in turbulence, since A. N. Kolmogorov's 1941 work [58], is the discovery, of R. H. Kraichnan, of the velocity spectrum ($\langle k|\mathbf{v}_k|^2 \rangle \propto k^{-5/3}$) in the inverse cascade of two-dimensional incompressible turbulence [59].

Some properties of two-dimensional ideal flows can be modeled by a point vortex gas on a plane, which is a variant of the Coulomb gas. The Coulomb gas description has been remarkably effective in condensed matter physics and quantum field theory. In particular, numerous results were obtained for the equilibrium statistics of point vortex gases. However, nobody ever managed, either numerically or analytically, to describe far-from-equilibrium states including turbulence. In 1981 for a forced system of point vortices E. G. Siggia and H. Aref performed, back then the state of the art numerics, and obtained what looked like an inverse cascade of energy (the scaling matched the expected $k^{-5/3}$; see [92]). Chapter 4 summarizes our efforts to repeat this classical result. We have used the same numerical method as E. G. Siggia and H. Aref, made larger runs that they did and nevertheless did not recover the $k^{-5/3}$ scaling. At this point it is unclear, whether $k^{-5/3}$ was not observed, because of the approximations introduced by the numerical method employed ("cloud-in-the-cell") or maybe not all aspects of two-dimensional turbulence can be modeled with point vortices. This inconsistency invites a more fundamental question - as to what extent the model point vortices is an exemplar of two-dimensional turbulence. For example, we know that a point vortex gas is dynamically conformally invariant, while the realistic two-dimensional turbulence is not (only certain features of it have been conjectured to be conformally invariant [17, 81]). Answers to such profound questions, regarding conformal symmetry in turbulence remain a matter of future research.

Non-equilibrium mixing accelerates computations

The last problem, presented in this thesis, is about Monte-Carlo (MC) sampling [100]. A guiding principle in the development of MC sampling techniques has been the notion that equilibrium systems evolve according to detailed balance. However it is known that detailed balance is a sufficient, but not a necessary condition, for MC to converge to a steady state. If so, a

question naturally arises: Can one utilize non-equilibrium mixing to reach a given steady state faster? The answer happens to be affirmative in many cases. Indeed, our work shows how to build an irreversible deformation of a reversible algorithm, after which the sampling procedure is substantially improved. To illustrate the general scheme M. Chertkov, K. S. Turitsyn and myself have designed an Irreversible version of a well known Metropolis-Hastings algorithm (which we will abbreviate as IMH) and have tested it on the example of a ferromagnetic spin-chain with long-range interactions. The standard Metropolis-Hastings (MH) algorithm suffers from the critical slowdown (a phenomena that, the mixing time diverges in the vicinity of a phase transition), while IMH is free from it. The advantages of our algorithm, over many other proposals, with likewise impressive convergence rates, is that it is generic (opposed to model-specific suggestions) and rather easy to implement. With some further development the ideas presented in Chapter 5 have the potential to be useful in studies of phase transitions, soft matter dynamics, protein structures, granular media and etc.

Part I

Clustering of particles in flows

1. Clustering of matter in waves and currents



Figure 1.1: Left: The Great Pacific waste patch is a gyre of marine litter in the central North Pacific Ocean. It is characterized by high concentrations of plastics, chemical sludge, and other debris that have been trapped by the currents of the North Pacific Gyre. It was first noticed by passing ships and believed to be located roughly between $135 - 155^\circ\text{W}$ and $35 - 42^\circ\text{N}$. Its size is alleged to be humongous. The area is not visible on satellite images, since plastic poorly reflects light. To the best of our knowledge, up to now no scientific studies on the size and density of the patch have been done. **Right:** Leaves on water, Mint Springs Park, Virginia.

Propagating waves create drifts in fluids. Understanding how drifts produced by many waves disperse pollutants has broad implications for geophysics and engineering. Clustering of matter (debris, oil slicks, seaweeds or etc) on the surfaces of lakes, seas or pools, is well-known empirically, yet there is no theory to explain this ubiquitous phenomena. Dynamical processes like wave breaking and Langmuir circulations produce streaks of flotsam [99]. In a random flow, such as sea stirred by wind or a storm, waves of various wavelengths and directions are running about on the surface and interacting, and regions of compression and expansion are constantly emerging and disappearing. Patchiness, in random flows, is presumed to be a signature of a fractal measure forming on the surface (see e.g. [30, 32, 77, 94, 96] and Figure 1.2). Our work established the role of small-amplitude waves (omnipresent on water surfaces) in that process

and estimated how fast the fractal set on the surface is formed and what is its fractal dimension.

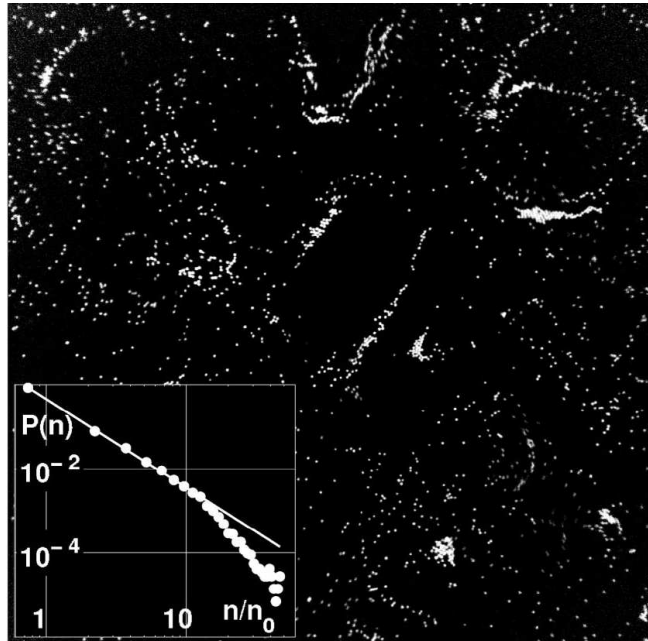


Figure 1.2: *Inhomogeneous distribution of hollow glass particles floating in a water tank. A central part (20×20 mm) is taken from a typical image of particle distribution in random waves at high mean concentration (3.8 particles per square mm). Inset: the histogram of particle concentration in the boxes 0.96×0.96 mm at low mean concentration (1.46 particles per square mm, $n_0 = 1.35$ particles per box). The straight line is $P \propto n^{-2}$ presumably due to caustics. The picture is taken from the experiment, analyzed in [32].*

Since surface flows are compressible even for incompressible fluids ($\partial_x v_x + \partial_y v_y = -\partial_z v_z$), a theory describing this clustering phenomena should be based on the general description of the development of density inhomogeneities in a compressible flow. An important characteristic of the formation of small-scale inhomogeneities is minus the sum of the Lyapunov exponents, λ . It gives the asymptotic logarithmic growth rate of the density on fluid particle trajectories at large times, in other words λ is minus the average value of the velocity divergence seen by a fluid particle. Notice that λ is always nonnegative. The physics behind this sign-definiteness is apparent, namely there are more Lagrangian particles¹ in the contracting regions, leading to negative average velocity gradients in the Lagrangian frame [6, 86–88]. The two averages, Lagrangian (average along fluid trajectories) and Eulerian average (space average), coincide

¹ Lagrangian (or fluid) particles are infinitesimal fluid volume elements.

only in the incompressible case. In our case, at initial time they coincide and are equal to zero, since we assume that the measure was uniform at the beginning. Actually if one takes density to be the phase space density and starts from equilibrium (which is characterized by a uniform measure), then λ is the entropy production rate, and $\lambda \geq 0$ is the consequence of the second law of thermodynamics.

The density grows on most trajectories. In the limit of infinite time, it concentrates on a constantly evolving fractal set characterized by a singular measure, the so-called Sinai-Ruelle-Bowen measure (see e.g. [37]). For floaters, this means that they form a multi-fractal structure on the surface². This structure is the attractor of the two-dimensional dissipative dynamics obeyed by the particles on the surface. The Kaplan-Yorke dimension of the attractor, $D_{KY} \equiv 1 + \lambda_1/|\lambda + \lambda_1|$, is between one and two, assuming that the principal Lyapunov exponent λ_1 is positive [78].

The Eulerian compressibility, measured by the dimensionless ratio $\varphi \equiv \langle (\partial_i v_i)^2 \rangle / \langle (\partial_j v_j)^2 \rangle$, of surface flows is of order one, cf. [19]. Here angular brackets stand for spatial averaging, \mathbf{v} is the floaters velocity field, and φ changes from zero for an incompressible flow to one for a potential flow. One expects $\lambda \sim \lambda_1$ from $\varphi \sim 1$, so that the deviation of D_{KY} from the surface dimension 2 is also of order one, $2 - D_{KY} \sim 1$. The expectation holds true for the flow on the surface of three-dimensional turbulence. Performing numerical simulations with the full three-dimensional Navier-Stokes equations, Boffetta et al. [19] found $\varphi \approx 0.5$, $D_{KY} \approx 1.15$ and observed strong clustering on the surface, see also [20, 31, 39]. However, due to stable stratification, underwater turbulence is relatively rare in the natural environment, and it is important to consider other cases of surface flows, of which the small-amplitude surface waves are probably the most wide-spread. Despite the amplitude smallness, a small-but-finite λ produces a strong effect over time-scales of order $1/\lambda$ or larger. Thus to evaluate the role of surface waves in the formation of the floaters inhomogeneities in the natural environment, one needs to know how small is λ . In [103] we show that λ is of sixth or higher order in wave amplitude. Let us note that for surface waves the degree of compressibility φ is due to linear waves, which produce potential flow with $\varphi = 1$. Thus one could expect that the estimates

² Some of the relevant theoretical papers are [4, 6, 13, 39, 41, 42, 45, 88, 111], while for experiments see [7, 30, 32, 77, 83, 89, 95, 96].

$\lambda \sim \lambda_1$ and $2 - D_{KY} \sim 1$ would hold for surface waves, as they do for the underwater turbulence. We show that in fact for surface waves $\lambda \ll \lambda_1$, under some natural non-degeneracy assumptions [103].

1.1 Weakly nonlinear waves

The calculation of λ for random non-interacting waves was the subject of [4]; we considered it in the case of weakly-interacting waves in [104]. In the first order in the wave amplitude, the particles carried by surface waves stay in place after the wave passes. The mass transfer (Stokes drift) and net clustering are nonlinear effects (see e.g. [9]), therefore an analysis of clustering of floaters should take into account the nonlinearity of waves. In [4] the authors assumed a linear relation between the velocity field of the floaters and the wave amplitudes, and considered a Gaussian ensemble of non-interacting waves. The system nevertheless was nonlinear, since the calculation involved expressing Lagrangian objects in terms of Eulerian ones. It was shown that λ vanishes in the fourth order in the wave amplitude for longitudinal waves, whose dispersion relation does not allow the same frequency for two different wave-vectors (e.g. sound, gravity, capillary waves). On the other hand, the lowest order non-vanishing contribution into λ_1 was shown to be of the fourth order in the wave amplitude. Under the same assumption of the linear relation between the velocity and the wave amplitudes, in [104] we demonstrated that the account of the wave interactions does not change the conclusion of [4] on the vanishing of λ in the fourth order in the wave amplitude.

1.2 Contribution of the surface curvature

The results mentioned above were inconclusive as far as surface waves are concerned, for which the relation between the velocity and the amplitudes is nonlinear, due to a small but finite curvature of the surface, see [112, 113]. For this case a separate calculation of λ was needed, and in [103] we provide such a calculation. We consider weakly nonlinear surface waves and show that neither the wave interactions, nor the nonlinear relation between the velocity and the amplitudes, are sufficient to create a nonzero sum of the Lyapunov exponents up to the fourth order in the wave amplitudes.

1.3 The Green-Kubo formula for the clustering rate

The main tool of our analysis is a Green-Kubo type formula for the sum of the Lyapunov exponents [41, 42]. This formula expresses λ in terms of the correlations of the flow divergence in the particle frame. It describes the interplay between the particle motion and the local flow compressions in accumulating density inhomogeneities, which become pronounced as a result of the long-time evolution.

The evolution of the density field $n(t, \mathbf{x})$ in a flow $\mathbf{v}(t, \mathbf{x})$ is governed by the continuity equation $\partial_t n + \nabla \cdot (\mathbf{v}n) = 0$, see [9]. In the Lagrangian frame this equation has a formal solution: $n[t, \mathbf{X}(t, \mathbf{x})] = n(0, \mathbf{x}) \exp \left\{ - \int_0^t dt' w[t', \mathbf{X}(t', \mathbf{x})] \right\}$, where $\mathbf{X}(t, \mathbf{x})$ is a Lagrangian particle trajectory starting at time $t = 0$ from $\mathbf{X}(0, \mathbf{x}) = \mathbf{x}$ and $w(t, \mathbf{x}) \equiv \nabla \cdot \mathbf{v}(t, \mathbf{x})$ is the divergence of the velocity.

In the previous section we argued that one can characterize the growth of spatial inhomogeneities at large times by the asymptotic logarithmic growth rate λ , which is defined like

$$\lambda \equiv \lim_{t \rightarrow \infty} \frac{1}{t} \ln \left[\frac{n[t, \mathbf{X}(t, \mathbf{x})]}{n(0, \mathbf{x})} \right] = - \lim_{t \rightarrow \infty} \frac{1}{t} \int_0^t dt' w[t', \mathbf{X}(t', \mathbf{x})]. \quad (1.1)$$

The above limit is well-defined, see e.g. [37], and it gives minus the sum of the Lyapunov exponents of the flow $\mathbf{v}(t, \mathbf{x})$. It was shown in [41, 42] that if $\mathbf{v}(t, \mathbf{x})$ is a random, spatially homogeneous, stationary flow, then one can express it likewise as

$$\lambda = \int_0^\infty dt \langle w(0, \mathbf{x}) w[t, \mathbf{X}(t, \mathbf{x})] \rangle, \quad (1.2)$$

where angular brackets designate spatial averaging. This expression is the central formula we use to derive our conclusions. The derivation of Eq. (1.2), starting from the definition of λ was published in [41]. In Appendix A we repeat the key steps of this proof.

1.4 Relating Eulerian and Lagrangian averages

The slowness of the particle drift from its initial position allows us to express the correlations in terms of the Eulerian correlation functions of the velocity. We shall apply Eq. (1.2) to the case where $\mathbf{v}(t, \mathbf{x})$ is the two-dimensional velocity field governing the motion of the floaters in a (quasi-)stationary ensemble of weakly nonlinear surface waves sustained by some forcing, see [114]. We first use the amplitude smallness to express the Lagrangian correlation function in Eq. (1.2) in terms of the velocity correlation functions given in the Eulerian frame. We follow [104] who considered Eq. (1.2) in the case of arbitrary low-amplitude waves. For a dispersion relation $\Omega_{\mathbf{k}}$, considering packets with both the wave number and the width of order k , the correlation time of w can be estimated as $\Omega_{\mathbf{k}}^{-1}$ and the correlation length as k^{-1} . The particle deviation from the initial position, $\mathbf{X}(t, \mathbf{x}) - \mathbf{x}$, during the period, $t \simeq \Omega_{\mathbf{k}}^{-1}$, is $\epsilon = kv/\Omega_{\mathbf{k}} \ll 1$ times smaller than k^{-1} which allows to expand Eq. (1.2) near \mathbf{x} . Performing the expansion to order ϵ^4 we find

$$\lambda \approx \lambda_2 + \lambda_3 + \lambda_4, \quad (1.3)$$

$$\lambda_2 \equiv \int_0^\infty dt \langle w(0)w(t) \rangle, \quad \lambda_3 \equiv \int_0^\infty dt \int_0^t dt_1 \left\langle w(0) \frac{\partial w(t)}{\partial x^\alpha} v^\alpha(t_1) \right\rangle, \quad (1.4)$$

$$\lambda_4 \equiv \int_0^\infty dt \int_0^t dt_1 \int_0^{t_1} dt_2 \left\langle w(0) v_\beta(t_2) \left(\frac{\partial w(t)}{\partial x_\alpha} \frac{\partial v_\alpha(t_1)}{\partial x_\beta} + \frac{\partial^2 w(t)}{\partial x_\alpha \partial x_\beta} v_\alpha(t_1) \right) \right\rangle. \quad (1.5)$$

Here we suppressed the spatial coordinate \mathbf{x} , over which the averaging is performed. The expansion above was introduced in [104]. Note that all contributions λ_i are of fourth or higher order in wave amplitude. We further evaluate this expression by a lengthy, but straightforward calculation, which is reproduced in section 1.5 and appendices C and E.

To calculate of λ we use a basic statistical property of the wave turbulence: its approximate Gaussianity. To leading order in the small wave amplitude, the correlation functions of appearing in the above expression for λ were calculated using Wick's theorem for Gaussian statistics. In Appendix B we elaborate on Gaussianity of wave turbulence.

1.5 The clustering rate λ for weakly-interacting waves

We start the consideration of (1.3) from the simplest case when the flow is solely due to weakly nonlinear waves. The normal coordinates of such waves satisfy the equation $\partial_t a_{\mathbf{k}} = -i\delta\mathcal{H}/\delta a_{\mathbf{k}}^*$ while the velocity Fourier component is assumed to be given by $\mathbf{v}_{\mathbf{k}} = \mathbf{A}_{\mathbf{k}}(a_{\mathbf{k}} - a_{-\mathbf{k}}^*)$. Here \mathcal{H} is the wave Hamiltonian, which can be expanded in wave amplitudes as follows [114]: $\mathcal{H} = \int d\mathbf{k} \Omega_{\mathbf{k}} |a_{\mathbf{k}}|^2 a_{\mathbf{k}}^* + \frac{1}{2} \int d\mathbf{k}_{123} (\mathbf{V}_{123} a_1 a_2^* a_3^* + \text{c.c.}) + \dots$. We do not write explicitly here other (third and fourth-order) terms since they will not contribute λ up to $\sim \epsilon^4$. We use throughout the shorthand notations $\mathbf{V}_{123} = V_{123} \delta(\mathbf{k}_1 - \mathbf{k}_2 - \mathbf{k}_3)$ and $V_{123} = V(\mathbf{k}_1, \mathbf{k}_2, \mathbf{k}_3)$, $\Omega(\pm \mathbf{k}_i) = \Omega_{\pm i}$ and $\mathbf{A}(\mathbf{k}_i) = \mathbf{A}_i$. One derives the clustering rate up to ϵ^4 using a standard perturbation theory for weakly interacting waves (see [114] and Appendix C). The first term in (1.3) is the time integral (the zero-frequency value) of the second moment. At the order ϵ^2 , the second moment in the frequency representation is proportional to the delta function: $\langle a^*(\mathbf{k}, \omega) a(\mathbf{k}', \omega') \rangle = (2\pi)^{d+2} n(\mathbf{k}) \delta(\omega - \Omega_{\mathbf{k}}) \delta(\mathbf{k} - \mathbf{k}') \delta(\omega - \omega')$. A finite width over ω and a finite value at $\omega = 0$ appear either due to finite linear attenuation (the case considered in [44]) or due to nonlinearity in the second order of perturbation theory (which gives ϵ^4 and is considered here). The second term in (1.3) is the triple moment which appears in the first order of the perturbation theory and the last term contains the fourth moment which is to be taken at the zeroth order (i.e. as a product of two second moments). Straightforward calculations³ then give for weakly nonlinear waves the ϵ^4 contribution:

$$\lambda = \text{Re} \int \frac{d\mathbf{k}_2 d\mathbf{k}_3}{(2\pi)^{2d}} \delta(\Omega_2 - \Omega_3) n(\mathbf{k}_2) n(\mathbf{k}_3) \left\{ \int \frac{d\mathbf{k}_1}{(2\pi)^d} \right. \\ \times \left[\left(\frac{\mathbf{V}_{213}^*}{\Omega_1} - \frac{\mathbf{V}_{3-12}}{\Omega_{-1}} \right) \left((2\pi)^{3d+1} |\mathbf{A}_1 \cdot \mathbf{k}_1|^2 \frac{V_{213}}{\Omega_1} \right. \right. \quad (1.6)$$

$$\left. \left. - \frac{(2\pi)^{2d}}{\Omega_2} (\mathbf{A}_1^* \cdot \mathbf{k}_1) (\mathbf{A}_2 \cdot \mathbf{k}_2) (\mathbf{A}_3^* \cdot (\mathbf{k}_2 + \mathbf{k}_1)) \right) \right] + \quad (1.7)$$

$$\left. + \frac{\pi}{\Omega_2^2} |(\mathbf{A}_3 \cdot \mathbf{k}_3) (\mathbf{A}_2^* \cdot \mathbf{k}_3) - (\mathbf{A}_3 \cdot \mathbf{k}_2) (\mathbf{A}_2^* \cdot \mathbf{k}_2)|^2 \right\}. \quad (1.8)$$

³ Note that one can also define Feynman rules and use diagrams in order to calculate λ . This is an equivalent approach and for completeness purposes it is given in Appendix C.

The common factor $\delta(\Omega_2 - \Omega_3)n(\mathbf{k}_2)n(\mathbf{k}_3)$ tells that here we have the contribution of two pairs of waves with the same frequencies. All three terms are generally nonzero (and positive) when the dispersion law is non-monotonic or non-isotropic, so that $\Omega_2 = \Omega_3$ does not require $k_2 = k_3$. In most interesting cases, however, Ω_k is a monotonous function of the modulus k so that $k_2 = k_3$. Let us show first that wave interaction does not contribute to λ in this case. Indeed, the first two terms, (1.6,1.7), that came out of the first two terms of (1.3), are proportional to the difference, $\mathbf{V}_{213}^* - \mathbf{V}_{3-12}$, between the amplitude of decay into a wave with \mathbf{k}_1 and confluence with a wave with $-\mathbf{k}_1$. Interaction coefficients for $k_2 = k_3$ have rotational symmetry and are thus functions of wave numbers so that $V_{213} - V_{3-12} = V_{213} - V_{312} = V_{212} - V_{212} = 0$. The last term (1.8) comes from the last two terms of (1.3) and does not contain the interaction coefficient V . This term is due to nonlinear relation between Eulerian and Lagrangian variables rather than due to wave interaction. We can compare (1.8) with the growth rate of the squared density for non-interacting waves, see (12) in [4] written there in terms of the energy spectrum, $E^{\alpha\beta}(\mathbf{k}, \omega) = 2\pi A^\alpha(\mathbf{k})A^{*\beta}(\mathbf{k})[n(\mathbf{k})\delta(\omega - \Omega_{\mathbf{k}}) + n(-\mathbf{k})\delta(\omega + \Omega_{-\mathbf{k}})]$. The comparison shows this part of our logarithmic growth rate being exactly half the growth rate for the second moment as it should be for a short-correlated flow [45]. Indeed, the process, of creation of density inhomogeneities, is effectively short-correlated since the time it takes ($1/\Omega_k\epsilon^4$ or longer) exceeds the correlation time of velocity divergence in the Lagrangian frame, $1/\Omega_k$. For monotonous $\Omega(k)$, (1.8) is nonzero only if the polarization vector $\mathbf{A}_{\mathbf{k}}$ is neither parallel nor perpendicular to \mathbf{k} , in other words if the polarization vectors contains both solenoidal and potential components. This is not the case for most waves in continuous media. We therefore conclude that for most common situations (in particular, for sound or for surface waves) the entropy production rate is zero in the order ϵ^4 . We find it remarkable that the flow of random potential waves is only weakly compressible (i.e. the senior Lyapunov exponent is much larger than the sum of the exponents).

1.6 The clustering of matter in surface waves

Note that for surface waves, the canonical variables are elevation $\eta(\mathbf{r}, t)$ and the potential $\phi(\mathbf{r}, z = \eta, t)$ which are related to the surface velocity by a nonlinear relation $\mathbf{v} = \nabla\phi(\mathbf{r}, \eta, t)$.

Expanding it in the powers of η , in the following section we show that this extra nonlinearity does not contribute λ in the order ϵ^4 .

1.6.1 The velocity field of the floaters

To use the Eq. (1.3) to find λ to order ϵ^4 , we established the expression for the surface flow \mathbf{v} to order ϵ^3 (see Appendix 1.6.1). The velocity field that governs the evolution of the floaters coordinates $\mathbf{r} = (x, y)$ in the horizontal plane, has the following form

$$\mathbf{v}(\mathbf{r}, t) = \left(\frac{\partial \phi(\mathbf{r}, z, t)}{\partial x} [z = \eta(\mathbf{r}, t)], \frac{\partial \phi(\mathbf{r}, z, t)}{\partial y} [z = \eta(\mathbf{r}, t)] \right), \quad (1.9)$$

where $\eta(\mathbf{r}, t)$ is the surface elevation and $\phi(\mathbf{r}, z, t)$ is the velocity potential, $\mathbf{v} = \nabla \phi$. In [112, 113] Zakharov showed that the system of weakly interacting surface waves is a Hamiltonian system with canonically conjugate coordinates $\eta(\mathbf{r}, t)$ and $\psi(\mathbf{r}, t) \equiv \phi(\mathbf{r}, \eta(\mathbf{r}, t), t)$. The calculation of the surface flow of the floaters to order ϵ^3 , needed for calculation of λ to order ϵ^4 , is given in [103]. The result is

$$\begin{aligned} \mathbf{v} = & i \int \frac{d\mathbf{k}_1}{(2\pi)^2} \mathbf{k}_1 \exp [i\mathbf{k}_1 \cdot \mathbf{r}] \psi_1 - i \int \frac{d\mathbf{k}_{12}}{(2\pi)^4} \exp [i(\mathbf{k}_1 + \mathbf{k}_2) \cdot \mathbf{r}] \overline{|k_1|} \mathbf{k}_2 \psi_1 \eta_2 \\ & - \frac{i}{2} \int \frac{d\mathbf{k}_{123}}{(2\pi)^6} e^{i(\mathbf{k}_1 + \mathbf{k}_2 + \mathbf{k}_3) \cdot \mathbf{r}} \psi_1 \eta_2 \eta_3 \left(|k_1|^2 \mathbf{k}_2 + |k_1|^2 \mathbf{k}_3 - 2\sqrt{k_1^2 + k_2^2} \overline{|k_1|} \mathbf{k}_3 \right), \end{aligned} \quad (1.10)$$

where h is the fluid depth and we introduced the shorthand notations $\eta_i(t) = \eta(\mathbf{k}_i, t)$, $\psi_i(t) = \psi(\mathbf{k}_i, t)$, $d\mathbf{k}_{ij\dots} = d\mathbf{k}_i d\mathbf{k}_j d\mathbf{k}_l \dots$ and $\overline{|k|} = |k| \tanh(|k|h)$. In the approximation of the infinitely deep fluid, $h \rightarrow \infty$, the above formula corresponds to formula (1.8) from [113]. Note that the velocity field on the surface $\mathbf{v}(\mathbf{r}, t)$ is neither potential, nor solenoidal.

Gaussianity of the wave turbulence⁴ is most succinctly expressed in terms of the normal coordinates $a(\mathbf{k}, t)$ defined by:

$$\eta(\mathbf{k}, t) = \sqrt{\frac{|k|}{2\Omega_{\mathbf{k}}}} [a(\mathbf{k}, t) + a^*(-\mathbf{k}, t)], \quad \psi(\mathbf{k}, t) = -i\sqrt{\frac{\Omega_{\mathbf{k}}}{2|k|}} [a(\mathbf{k}, t) - a^*(-\mathbf{k}, t)], \quad (1.11)$$

⁴ See Appendix B.

where $\Omega_{\mathbf{k}}$ is the dispersion relation: $\Omega_{\mathbf{k}}^2 = |\mathbf{k}|(g + (\sigma/\rho)|\mathbf{k}|^2) \tanh[|\mathbf{k}|h]$, where g is the gravitational acceleration, σ is the surface tension and ρ is the density of the fluid. Then in the Gaussian approximation the pair correlation functions are given by

$$\langle a^*(\mathbf{k}, t)a(\mathbf{k}', 0) \rangle = (2\pi)^2 \delta(\mathbf{k} - \mathbf{k}') n(\mathbf{k}) \exp[i\Omega_{\mathbf{k}} t], \quad \langle a(\mathbf{k}, t)a(\mathbf{k}', 0) \rangle = 0, \quad (1.12)$$

$$\langle \psi(\mathbf{k}, t)\psi(\mathbf{k}', 0) \rangle = \frac{\Omega_{\mathbf{k}}(2\pi)^2 \delta(\mathbf{k} + \mathbf{k}')}{2k} [n(\mathbf{k}) \exp(-i\Omega_{\mathbf{k}} t) + n(-\mathbf{k}) \exp(i\Omega_{-\mathbf{k}} t)],$$

$$\langle \eta(\mathbf{k}, t)\eta(\mathbf{k}', 0) \rangle = \frac{k(2\pi)^2 \delta(\mathbf{k} + \mathbf{k}')}{2\Omega_{\mathbf{k}}} [n(\mathbf{k}) \exp(-i\Omega_{\mathbf{k}} t) + n(-\mathbf{k}) \exp(i\Omega_{-\mathbf{k}} t)],$$

$$\langle \psi(\mathbf{k}, t)\eta(\mathbf{k}', 0) \rangle = \frac{(2\pi)^2 \delta(\mathbf{k} + \mathbf{k}')}{2i} [n(\mathbf{k}) \exp(-i\Omega_{\mathbf{k}} t) - n(-\mathbf{k}) \exp(i\Omega_{-\mathbf{k}} t)]. \quad (1.13)$$

We now return to the expression for the sum of the Lyapunov exponents (1.3) and calculate λ in Appendix E.

1.6.2 Results on clustering in surface waves

We have shown that the sum of the Lyapunov exponents for surface wave turbulence vanishes in the fourth order in wave amplitude. Using the approximate Gaussianity of the statistics, it is easy to see that the leading order term in λ is of the sixth order in wave-amplitude, or higher ($\lambda \lesssim \Omega_{\mathbf{k}} \epsilon^6$). For waves with a typical period of the order of seconds and not too small $\epsilon = 0.1$, we find that the time-scale $1/\Omega_{\mathbf{k}} \epsilon^6$ is of the order of weeks. Thus, even if there is no degeneracy in the sixth order and $\lambda \sim \Omega_{\mathbf{k}} \epsilon^6$, the formation of the inhomogeneities would occur at the time-scale of weeks and larger. It is unlikely that a low-amplitude wave turbulence would persist for such time. Thus, we expect the turbulence of small-amplitude surface waves to have a negligible effect on the formation of the floaters inhomogeneities in realistic situations. Let us stress that this weak compressibility of surface waves holds in the sense of the long-time action of the flow on the particles, while the characteristic value of the ratio of the surface flow divergence to the curl is of order one. We argued in [103] that since the wave interactions and the nonlinearity of the velocity-amplitude relation add to λ_1 additional terms of the fourth order in the wave amplitude and higher it is highly implausible that these terms produce exact cancelation of λ_1 in the fourth order. If so, we have the following order of magnitude estimates: $\lambda_1 \propto \Omega_{\mathbf{k}} \epsilon^4$ and $\lambda \propto \Omega_{\mathbf{k}} \epsilon^6$. It follows that surface wave turbulence is also weakly compressible

in the sense of the ratio $\lambda/\lambda_1 \ll 1$, which is of the second order in the wave amplitude. The Kaplan-Yorke dimension of the particles attractor on the surface is close to the space dimension: $D_{KY} \approx 2 - \lambda/\lambda_1 \approx 2$. For dimensionless exponents $\tilde{\lambda}_1 \equiv \lambda_1/\Omega_{\mathbf{k}}$ and $\tilde{\lambda} \equiv \lambda/\Omega_{\mathbf{k}}$ we find the order of magnitude relation $\tilde{\lambda} \sim \tilde{\lambda}_1^{3/2}$ holding at small wave amplitudes. The above estimates are supported by numerical simulations performed by [101] in a similar problem with *standing* surface waves. It was shown there that both $\lambda \ll \lambda_1$ and $2 - D_{KY} \ll 1$ hold. Moreover, the numerical values of the dimensionless exponents $\tilde{\lambda}$, $\tilde{\lambda}_1$ found there, can be easily seen to be in agreement with the relation $\tilde{\lambda} \sim \tilde{\lambda}_1^{3/2}$. The box-counting dimension of the particles attractor on the surface was found very close to D_{KY} , which we expect to hold for wave turbulence as well. The detailed calculations of the exact expressions for λ_1 and λ are subjects for future work.

1.7 Conclusions on clustering with surface waves

We believe that our conclusion on the weak clustering in surface waves with a small amplitude is an important step in identifying possible reasons for clusters of floaters observed on liquid surfaces ubiquitously. Our results suggest that other mechanisms need to be explored, such as the wave breaking and Langmuir circulation, see e.g. [99], the interplay of waves and currents (see the next section and [104]) and others.

1.8 Interplay of waves and currents

We now consider the clustering rate in the presence of solenoidal currents and potential waves, the situation most relevant for oceanological applications [79, 99]. The solenoidal flow \mathbf{u} of currents is weakly perturbed by potential waves moving with velocity field \mathbf{v} . To derive λ in the lowest (second) order in $\epsilon = kv/\Omega_k$, we neglect the contribution of \mathbf{v} into \mathbf{X} in Eq. (1.2) and assume $\partial_t \mathbf{X}(t, \mathbf{x}) \approx \mathbf{u}[t, \mathbf{X}(t, \mathbf{x})]$. In this order, $w = \nabla \cdot \mathbf{v}$ is Gaussian and one may integrate by parts: $\langle w(0, \mathbf{x})w(t, \mathbf{X}(t, \mathbf{x})) \rangle = \int dt' d\mathbf{x}' \Phi(t', \mathbf{x}' - \mathbf{x}) \langle \delta w[t, \mathbf{X}(t, \mathbf{x})] / \delta w(t', \mathbf{x}') \rangle$. Here $\Phi(t' - t, \mathbf{x}' - \mathbf{x}) = \langle w(t, \mathbf{x})w(t', \mathbf{x}') \rangle$ is the Eulerian correlation function and

$$\lambda \approx \int_0^\infty dt \langle \Phi[t, \mathbf{J}(t)] \rangle, \quad \mathbf{J}(t) \equiv \mathbf{X}(t, \mathbf{x}) - \mathbf{x}. \quad (1.14)$$

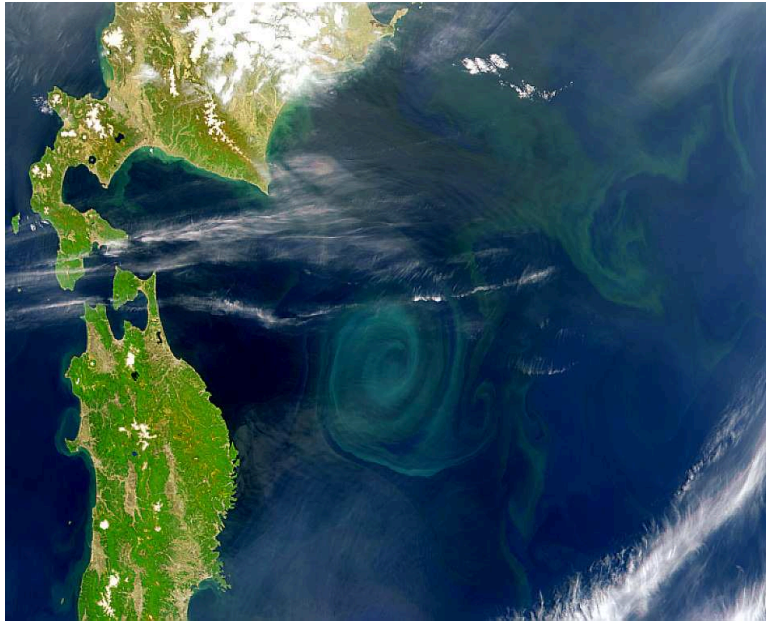


Figure 1.3: Satellite image of a swirl near Japan with a plankton bloom in it. Eddies commonly break off of the Kuroshio Current near Japan and go swirling about on their own for weeks or months, trapping plankton inside.

Waves and currents are considered statistically independent in this order. Using the spectrum, $k^\alpha k^\beta E_{\mathbf{k}}^{\alpha\beta} \equiv k^2 E_{\mathbf{k}}$, we can express $\Phi(t, \mathbf{r}) = (2\pi)^{-d} \int k^2 E_{\mathbf{k}} \cos(\mathbf{k} \cdot \mathbf{r} - \Omega_{\mathbf{k}} t) d\mathbf{k}$ and rewrite (1.14) as a weighted spectral integral:

$$\lambda = (2\pi)^{-d} \int k^2 E_{\mathbf{k}} \mu(\mathbf{k}) d\mathbf{k}, \quad (1.15)$$

$$\mu(\mathbf{k}) = \int_0^\infty \langle \cos[\mathbf{k} \cdot \mathbf{J}(t) - \Omega_{\mathbf{k}} t] \rangle dt. \quad (1.16)$$

The spectral weight $\mu(k)$ is the Lagrangian correlation time of the k -harmonic of w and is expressed via the characteristic function of the particle drift $\mathbf{J}(t)$. Without currents Eqs. (1.15,1.16) reproduce the first term of Eq. (1.3) since only the zero-frequency wave contributes. Already a steady uniform current $\bar{\mathbf{u}}$ contributes the clustering rate in the order ϵ^2 if there are waves whose Doppler-shifted frequency is zero in the current reference frame: $\lambda = (2\pi)^{-d} \int k^2 E_{\mathbf{k}} \delta(\Omega_{\mathbf{k}} - \mathbf{k} \cdot \bar{\mathbf{u}}) d\mathbf{k}$. Similar Cherenkov resonance has been noticed before for diffusivity [3]. Let us stress that this result is based on the assumption that waves are independent of currents; in particular, that there is no Doppler shift of the wave frequency. For instance, that takes place when there is only a surface mean current. If, on the contrary, the

current is homogeneous across the depth brought into motion by a wave (of the order of a wave length) for gravity waves or the whole water depth for inertio-gravity waves⁵) then Eq. (1.16) needs replacing $\Omega_{\mathbf{k}} \rightarrow \Omega_{\mathbf{k}} + \mathbf{k} \cdot \bar{\mathbf{u}}$, and the effect of the mean current is zero due to Galilean invariance.

Further on, we consider the fluctuating part of current velocity characterized by the rms velocity $u_0^2 \equiv \langle u^2 \rangle$ and the correlation time $\tau \equiv \int \langle u_\alpha(0, \mathbf{x}) u_\alpha[t, \mathbf{X}(t, \mathbf{x})] \rangle dt / u_0^2$. Accordingly, there are two dimensionless parameters that describe spatial and temporal relationships between wave and current parameters respectively: $L \equiv ku_0\tau$ is the ratio between the distance passed by the fluid particle during τ and the wavelength, and $T \equiv \Omega_{\mathbf{k}}\tau$ is the ratio between the correlation time of currents and wave period. The characteristic function $\langle \exp[i\mathbf{k} \cdot \mathbf{J}(t)] \rangle$ in general depends on the details of the currents statistics, but it has universal behavior both at $t \ll \tau$ and $t \gg \tau$ where general calculations are possible. On the plane of the dimensionless parameters L, T we distinguish three regions of different asymptotic behavior, see Figure (1.4).

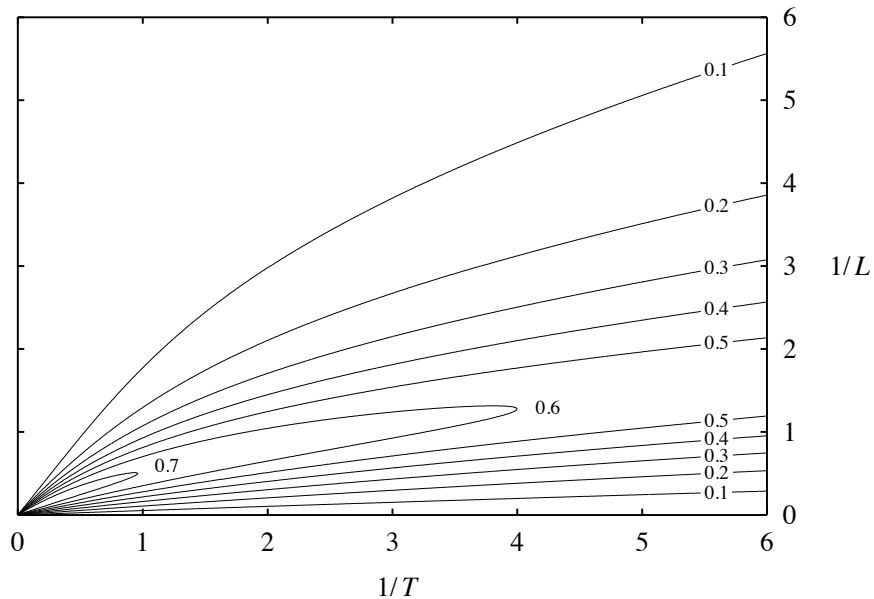


Figure 1.4: The isolines of the dimensionless clustering rate $\mu(k)\Omega_{\mathbf{k}}$ given by (1.20), here $L = ku_0\tau$, $T = \Omega_{\mathbf{k}}\tau$.

⁵ Inertio-gravity (also known as internal-gravity) waves are propagating under the influence of both buoyancy and Coriolis forces.

1.8.1 The ballistic limit

Consider first the ballistic limit when the integral Eq. (1.16) is determined by the times $t \ll \tau$. In this case the drift velocity does not change much and $\mathbf{J}(t) \approx \mathbf{u}(0, \mathbf{x})t$. Again, only those waves contribute that are in a Cherenkov resonance with the current (whose phase velocity coincides with the local projection of the current velocity): $\mu = \pi \langle \delta(\Omega_{\mathbf{k}} - \mathbf{k} \cdot \mathbf{u}) \rangle$. In this limit, the weight μ is determined by the single-time probability distribution of the current velocity which we denote $\mathcal{P}(\mathbf{u})$. In particular, for the isotropic Gaussian $\mathcal{P}(u) \propto \exp(-u^2/2u_0^2)$, we get

$$\mu(k) = (\pi d/2)^{1/2} (ku_0)^{-1} \exp[-(\sqrt{d}\Omega_k/\sqrt{2}ku_0)^2], \quad (1.17)$$

The ballistic approximation and (1.17) hold when $k^2 u_0^2 \tau^2 / d$ is much larger than both unity and $\Omega_k \tau$.

1.8.2 The diffusive limit

The second universal limit is that of slow clustering which proceeds for the time exceeding the correlation time of currents. At $t \gg \tau$, we use the diffusion approximation, $\langle \exp[i\mathbf{k} \cdot \mathbf{J}(t)] \rangle = \exp[-k^2 u_0^2 \tau t / d]$, in (E.15):

$$\mu(k) = \tau \frac{d(ku_0\tau)^2}{(ku_0\tau)^4 + (d\Omega_k\tau)^2}. \quad (1.18)$$

The above formula and the diffusive approximation hold when both $k^2 u_0^2 \tau^2 / d$ and $\Omega_k \tau$ are small. Formulas (1.15,1.18) can be compared with the expression for the clustering rate for waves with a linear damping, $\lambda \simeq \int k^2 E_k \gamma_k (\Omega_k^2 + \gamma_k^2)^{-1} d\mathbf{k}$ [44]. We see that in this limit the diffusive motion of fluid particles due to currents is equivalent in its effect to a damping of waves with $\gamma_k = k^2 u_0^2 \tau / d$, where $u_0^2 \tau / d$ is the eddy diffusivity.

1.8.3 Limit of fast-oscillating waves

The third asymptotic regime takes place for fast-oscillating waves when $\Omega_k \tau$ exceeds both unity and $k^2 u_0^2 \tau^2 / d$. An integral of the fast oscillating exponent with a slow function,

$\int_0^\infty \cos(\Omega_k t) f(t) dt$, decays as Ω_k^{-2n-2} , where $2n+1$ is the lowest order of the non-vanishing derivative of $f(t) = \langle \exp[i\mathbf{k} \cdot \mathbf{J}(t)] \rangle$ at $t=0$. When all odd derivatives at zero are zero, the integral decays exponentially. We see that the answer depends on the details of the statistics of currents.

If $\mathbf{u}[t, \mathbf{X}(t, \mathbf{x})]$ is Gaussian and isotropic with

$$\langle u^\alpha(0, \mathbf{x}) u^\beta(t, \mathbf{X}(t, \mathbf{x})) \rangle = (u_0^2/d) \delta^{\alpha\beta} \exp(-|t|/\tau), \quad \text{then} \quad (1.19)$$

$$\mu(k) = \tau \int_0^\infty ds \cos(Ts) \exp\left[\frac{L^2}{d} (1 - s - e^{-s})\right]. \quad (1.20)$$

It gives both limits Eqs. (1.17,1.18) and

$$\mu(k) = (ku_0)^2 / \tau \Omega_k^4 d, \quad (1.21)$$

at large Ω_k since the lowest non-vanishing derivative is $f'''(0)$. Isolines of Eq. (1.20) are shown in Figure 1 for arbitrary parameters. Remind that the whole description based on Eq. (1.14) is valid when $v \ll u$.

If one interpolates between the ballistic and diffusive regimes (i.e. between $J^2 \propto t^2$ and $J^2 \propto t$) with the help of the function $\sqrt{1 + (t/\tau)^2} - 1$, which is smooth at $t=0$, then the weight factor can be calculated analytically

$$\mu(k) = \frac{\tau L^2}{d} \exp\left(\frac{L^2}{d}\right) \frac{K_1\left(\sqrt{\frac{L^4}{d^2} + T^2}\right)}{\sqrt{\frac{L^4}{d^2} + T^2}}. \quad (1.22)$$

Here $K_1(x)$ is a Bessel function of an imaginary argument having the following asymptotics: $K_1(x) = \sqrt{\pi/2x} \exp(-x)[1 + \mathcal{O}(1/x)]$ for $x \gg 1$ and $K_1(x) \simeq 1/x + \mathcal{O}(x \ln(x))$ for $x \ll 1$. We see that (1.22) reproduces (1.17, 1.18) in the regions $L^2/d \gg 1$, $L^2/d \gg T$ and $L^2/d \ll 1$, $T \ll 1$ respectively. At the fast-oscillation limit one gets an exponentially small contribution

$$\mu(k) = \tau \sqrt{\frac{\pi(ku_0)^4 \tau}{2d^2 \Omega_k^3}} e^{-\Omega_k \tau}. \quad (1.23)$$

That concludes the analysis of the weight $\mu(k)$ and we can now turn to (1.15) to get the

clustering rate λ .

When the wave spectrum is not particularly wide (with the width comparable to k) we get

$$\lambda \simeq (kv)^2 \mu(k) = \epsilon^2 \Omega_k^2 \mu(k) . \quad (1.24)$$

Let us now find out which wavenumbers contribute (1.15) when the spectrum is wide. We assume an isotropic power spectrum $E_{\mathbf{k}} \propto k^{b-d}$ between some k_{min} and k_{max} and the dispersion relations $\Omega_{\mathbf{k}} = Ck^a$ [114]. First, we consider the ballistic regime. For $(a > 1 \wedge b > 0) \vee (a < 1 \wedge b < 0)$ the wavenumber $k_* = [bu_0^2/dC^2(a-1)]^{1/(2a-2)}$ determines λ . For $(b \leq 0 \wedge a > 1) \vee (b < -1 \wedge a = 1)$ the clustering rate is determined by k_{min} , while for $(b \geq 0 \wedge a < 1) \vee (b \geq -1 \wedge a = 1)$ by k_{max} . Let us give physical examples using Kolmogorov spectra of waves. For capillary waves on a deep water, $\Omega_k \propto k^{3/2}$ and $E_k \propto k^{-11/4}$, and λ is determined by k_{min} i.e. by longest waves in the wave turbulent spectrum (assuming the ballistic approximation is valid for them). For gravity waves on a deep water, $\Omega_k \propto k^{1/2}$, and for both Kolmogorov solutions, $E_k \propto k^{-20/6}$ and $E_k \propto k^{-7/2}$, the clustering rate is determined by waves around k_* . The clustering rate in the difusive regime is determined by k_{max} if $b \geq \max[2a - 4, 0]$ and by k_{min} if $b < \max[2a - 4, 0]$.

1.9 Results on clustering with waves and currents

The asymptotic behavior estimates, given in Eqs. (1.17,1.18,1.21,1.23), show that $\lambda/(\epsilon^2 \Omega_k) \simeq \Omega_k \mu(k)$ is a dimensionless function which has a maximum of order unity either in the ballistic regime where the phase velocity of waves is comparable to the current velocity or in the diffusive regime where the eddy diffusivity $u_0^2 \tau$ is comparable to $\Omega_{\mathbf{k}} k^{-2}$ (in the third asymptotic regime $\lambda/(\epsilon^2 \Omega_k)$ is always small). In those cases, $\lambda/\Omega_k \simeq \epsilon^2$, i.e. the degree of clustering during a period is the squared wave nonlinearity (typically ϵ is between 0.1 and 0.01). Such clustering is pretty fast (minutes for meter-sized gravity waves and a week for fifty-kilometer-sized inertio-gravity waves). Therefore, it is likely that the interplay between waves and currents is the source of inhomogeneities of floater distribution in many environmental situations.

Clustering leads to fractal distribution of floaters over the surface. When compressible component of the velocity is small, the Lyapunov exponents are due to the current flow, $\lambda_1 \sim \lambda_2 \sim \tau^{-1}$. Then, the fractal dimension of the density distribution can be expressed by the

Kaplan-Yorke formula $1 + \lambda_1/|\lambda_2| = 2 - \lambda/|\lambda_2| \approx 2 - \lambda\tau$. The fractal part reaches maximum in the ballistic regime when $\Omega_k \simeq ku_0$, then $\lambda\tau \simeq \epsilon^2\Omega_k\tau = \epsilon^2k\ell$ grows with $\ell = u_0\tau$ and reaches order unity when $k\ell \simeq \epsilon^{-2}$. Therefore, the distribution is most fractal when waves are weak and short while currents are long and strong. For example, meter-sized gravity waves on a water surface will produce most inhomogeneous distribution of floaters when there are currents with velocities in meters per second and scales in hundreds of meters. We see that the current-to-wave ratio of scales, $k\ell$, compensates for a small wave nonlinearity, ϵ^2 , so that even weak waves with the help of solenoidal currents can produce highly inhomogeneous fractal distribution of matter.

1.10 Remark on entropy production rate in dynamical systems

Apart from fluid mechanics, one can think about the evolution of a dynamical system as a flow in the phase space and treat density as a measure. Solenoidal (incompressible) flow corresponds to Hamiltonian dynamics and to a constant (equilibrium) measure. Compressibility corresponds to pumping and damping, i.e. to non-equilibrium. Indeed, the notion of singular (fractal) measures first appeared in non-equilibrium statistical physics [21, 37, 93] and then was applied in fluid mechanics [6, 13, 45, 95, 96]. Therefore, the formulas (1.14–E.15, 1.18–1.23) also describe the entropy production rate in dynamical systems under the action of perturbations periodic in space and in time.

2. Particles in a flow with time correlations

This chapter is about suspensions of dust, droplets, bubbles or other small impurities in fluids. Particles suspended in flows have finite sizes and their mass density usually different from the density of the carrier fluid, hence inertia causes particles to lag behind the flow. Among specialists they are referred to as *inertial particles*. Such particles have vastly different dynamics from point like tracers. First surprise with inertial particle came in 1987, when M. R. Maxey showed that no matter how weak the inertial effects are, they can not be neglected. Inertia of particles renders the effective flow to be compressible. Namely the dynamics of weakly inertial particles in an incompressible flow can be approximated by the dynamics of point like traces in a weakly compressible flow [72]. Mathematically, inertia is a singular perturbation since it adds a higher-order derivative (d^2/dt^2) to the equation. Yet another interesting observation is that in the same small portion of the fluid one can find inertial particles moving with substantially different velocities, which makes the problem of dynamics of inertial particles of kinetic, rather than hydrodynamic nature [11, 12, 46].

At long times inertial particles concentrate on singular sets evolving with the fluid motion, leading to the apparition of a strong spatial inhomogeneity dubbed *preferential concentration*. The spontaneous formation of clusters of particles suspended in chaotic flows may originate from two different physical processes: compressibility of the fluid flow and particle inertia. Surprisingly enough it has been shown that in compressible flows, where fluid trajectories coalesce, large enough inertia can induce a transition from the strong clustering regime (aggregation) into a weak clustering one, where particle trajectories remain chaotic, and the senior Lyapunov exponent is positive [34, 73, 74, 108]. Previously analytic results on this *aggregation-mixing transition* have been obtained under the assumption that the underlying flow is uncorrelated in time [33]. In [47] we tried to answer how time correlations can influence the aggregation-



Figure 2.1: Rain drops in clouds are examples of inertial particles driven by flow of air. Photograph show clouds in Israel, close to the Jordan river.

mixing transition. We introduced a one-dimensional model for the Lagrangian dynamics of inertial particles in a flow, where the fluid velocity gradients follow telegraph noise statistics. In parallel, with our work, the same time-correlated model flow was used also to describe the dynamics of point-like tracers in one and two spatial dimensions [43]. The inspiration behind our work was to investigate if the dynamics of inertial particles in time-correlated flows is qualitatively different, compared to the dynamics of these particles in time uncorrelated flows.

2.1 The model

Particles that we consider are so small, that the flow around them is viscous. Motion of each particle is described by a Newton equation, which includes the gravitational and the viscous (Stokes) force: $\dot{v}_i(t) = \tau^{-1} (u_i[t, r_i(t)] - v_i(t)) + g$, where $\tau = (2/9)(\rho_0 a^2 / \eta)$ is the *Stokes time*, a is the particle radius, ρ_0, ρ are the particle and fluid densities respectively, η is the dynamical flow viscosity and g is the gravitational acceleration. The fluid velocity $u(t, r)$ is a given random function of time and space. The separation of a pair of particles $R(t) \equiv r_1(t) - r_2(t)$ with relative

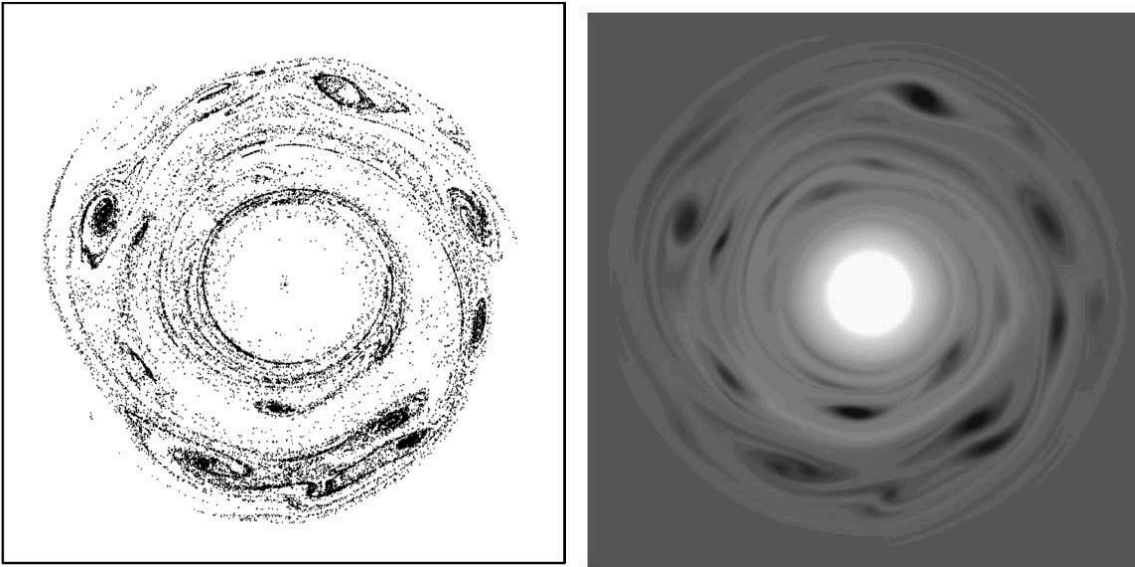


Figure 2.2: For the problem of planetary formation one seeks a mechanism to gather small dust particles together into aggregates. Dust particles are also examples of inertial particles. Authors in [22] introduce a scenario in which turbulence mediates this process by aggregating dust into anticyclonic regions. Distribution of dust in the disk (**left**) and the vorticity field (**right**) after about $t \sim 15$ (at $r = \pi/6$ a typical rotation time is $T \simeq 1.15$. It is determined by Kepler's law of motion). Figures are taken from [22].

velocity $V(t) \equiv v_1(t) - v_2(t)$ is governed by the following system of equations

$$\begin{aligned} \dot{R}(t) &= V(t), \\ \dot{V}(t) &= \frac{1}{\tau} (U[t, R(t)] - V(t)), \end{aligned} \quad (2.1)$$

where $U[t, R(t)] \equiv u_1[t, r_1(t)] - u_2[t, r_1(t)]$. At small separations one can assume $U[t, R(t)] = s(t)R$, where $s(t)$ is local velocity gradient (taken in the Lagrangian frame). Note, that so far we have two timescales in our problem: the Stokes time τ and the inverse velocity gradient $1/s$ (where s labels some characteristic value of $s(t)$; below we will take this characteristic value to be the r.m.s. value of $s(t)$). Their ratio is an important dimensionless parameter of the system: the *Stokes number*, $St \equiv s\tau$.

The equations (2.1) behave very differently for positive and negative velocity gradients. Positive gradients $|s|$ expand the system towards the asymptote $V = \xi R$, where $\xi = (-1 + \sqrt{1 + 4St})/(2\tau)$. In such gradients a pair of particles separates exponentially with a rate smaller than the rate of fluid trajectories $\xi < s$. On the other hand at negative velocity gradients, $-|s|$,

the separation of particles contracts. Depending on the relative intensity of fluid gradients and inertial drag two scenarios of contraction are observed. At small Stokes numbers $St < 1/4$ the system evolves toward the asymptote $V = \zeta R$, where $\zeta = (-1 + \sqrt{1 - 4St})/(2\tau)$. Particles slow down less efficiently than the fluid, and hence their separation goes to zero with a faster exponential rate $|\zeta| > s$. While at large Stokes numbers $St > 1/4$ the system has two complex conjugate eigenvalues $\zeta = (-1 \pm i\sqrt{4St - 1})/(2\tau)$ and the solution decays exponentially with a clockwise spiral motion on the (R, V) plane. Particles now collide (cross the $R = 0$ axis) with a nonzero relative velocity, which gives rise to shocks [46]. The critical value of Stokes number at which shocks start to appear, distinguishes between small and large Stokes number regimes: $St^* = 1/4$. Presence of such critical Stokes number is a characteristic of flows where fluid velocity gradient values are bounded. Conversely, if the statistics of the fluid velocity gradient is unbounded, shocks can appear at arbitrarily St , but they are exponentially suppressed in the limit $St \rightarrow 0$ [33, 46].

2.1.1 Telegraph noise

We assume that the velocity gradient has telegraph noise statistics, i.e. $s(t)$ is a two state Markov process ($s_1 = |s|$, $s_2 = -|s|$), with correlation time ν^{-1} ($\nu = \nu_1 + \nu_2$). The transition rate ν_i describes the transition $j \rightarrow i$, e.g. ν_2/ν is the fraction of time that the particle pair spends in the regions of compression. Since in potential flows particles spend more times in regions of local compression than in expanding regions, we set $\Delta\nu \equiv \nu_2 - \nu_1 > 0$. The mean value of $s(t)$ noise is $s_0 \equiv \langle s(t) \rangle = -s\Delta\nu/\nu$, while the noise fluctuations are exponentially correlated $\langle s(t)s(t') \rangle = 4s^2(\nu_1\nu_2/\nu^2) \exp(-\nu|t-t'|)$. An important observation is that $s^2(t) = s^2$ is a constant, this will prove to be crucial for the solvability of our model. Time correlations introduce a third time scale in our problem - the velocity gradient correlation time ν^{-1} . Hence, there is another dimensionless parameter of interest: the *Kubo number* $Ku \equiv s/\nu$.

The introduced model is analytically tractable. One can write systems of ordinary differential equation on the evolution of various correlation functions of the form $\langle \alpha^k(t)\phi[t, \alpha(\tau)] \rangle$, where $k = 1, 2, \dots; 0 < \tau \leq t$; $t = 0$ is the moment of imposing initial conditions and ϕ is a function of t and an arbitrary functional of $\alpha(\tau)$. Next for a stationary random process whose first

moment is zero and the second moment is an exponentially decaying function of the relative time there is a way to split the correlation functions by using the *formulae of differentiation*. Note that $\alpha(t)$ fulfills these requirements: $\langle \alpha(t) \rangle = 0$ and $\langle \alpha(t_1)\alpha(t_2) \rangle \propto \exp[-\nu|t_1 - t_2|]$. Thus in the case we are considering the formulae of differentiation hold and they are

$$\frac{d}{dt}\langle \alpha^k(t)\phi[t, \alpha(\tau)] \rangle = -\nu\langle \alpha^k(t)\phi[t, \alpha(\tau)] \rangle + \langle \alpha^k(t)\dot{\phi}[t, \alpha(\tau)] \rangle + \nu\langle \alpha^k(t) \rangle \langle \phi[t, \alpha(\tau)] \rangle, \quad (2.2)$$

$$\langle \alpha^k(t)\alpha(t_1)\dots\alpha(t_n) \rangle = -\nu\langle \alpha^k(t)\alpha(t_1)\dots\alpha(t_n) \rangle + \nu\langle \alpha^k(t) \rangle \langle \alpha(t_1)\dots\alpha(t_n) \rangle, \quad (2.3)$$

here $n = 1, 2, \dots$. These formulae were introduced in 1978 by V. E. Shapiro and V. M. Loginov in [90]. In our model, for a large class of functionals $\phi[t, \alpha(\tau)]$ one obtains a closed system of ODEs, due to the peculiar feature of the telegraph noise statistics: $s^2(t) = s^2$ is a constant.

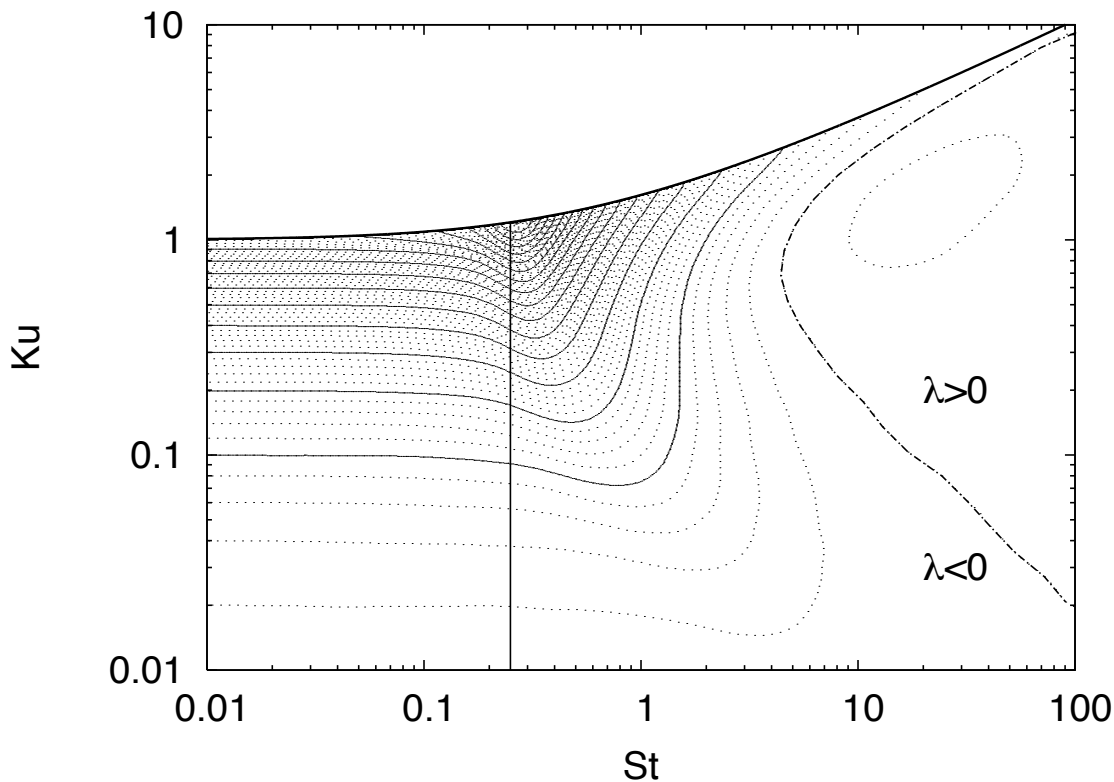


Figure 2.3: The isolines of the Lyapunov exponent λ on the plane of Stokes ($St \equiv s\tau$) and Kubo ($Ku \equiv s\nu^{-1}$). The isolines are spaced every $0.02s$ (dotted and solid lines). The boundary of the chaotic region ($\lambda > 0$) is represented by the dot-dashed line. The physically relevant region in (St, Ku) parameter space is below the solid line (see subsection 2.1). The solid line represents the upper bound for the Kubo number achievable in the system $Ku \leq Ku^* = 2St/(\sqrt{1 + 4St} - 1)$.

As already mentioned, in potential flows both fluid and inertial particles tend to spend

more time in regions of local compression than in expanding regions, this sets $\Delta\nu > 0$. The assumptions of statistical homogeneity and isotropy of the flow specify the actual value of $\Delta\nu$. The mean position of a particle is solely determined by its initial position (i.e. the distance R is statistically conserved, $\langle R \rangle = \text{const}$), due to these symmetries. Using the formulae of differentiation one easily obtains the evolution equations for moments: $\langle R \rangle$, $\langle V \rangle$, $\langle \alpha R \rangle$ and $\langle \alpha V \rangle$. They form a closed system of equations and allow for a constant solution for $\langle R \rangle$, only when $\Delta\nu = s/(1 + \nu\tau)$. From this condition on $\Delta\nu$ we observe that inertia reduces the trapping of particles in compressing regions. This effect is encoded in the behavior of the parameter $\Delta\nu$, which is a decreasing function of Stokes time τ , and vanishes in the limit $\tau \rightarrow \infty$. The positivity of ν_1 requires $\Delta\nu < \nu$, and gives an upper bound for the Kubo number achievable in the system

$$\text{Ku} \leq \text{Ku}^* = \frac{2\text{St}}{\sqrt{1 + 4\text{St}} - 1}. \quad (2.4)$$

In the limit of fluid tracers, $\tau \rightarrow 0$, the constraint becomes $\text{Ku} < 1$. The accessible region in (St, Ku) parameter space is shown in Figure (2.3) below the solid line.

2.2 Results

In the sections below we study the statistics of the particle-velocity gradient, the Lyapunov exponent, the Lyapunov moments and the limits of short- and long-correlated flows. Also, where appropriate we discuss the comparison with the fluid-tracer case.

2.2.1 The statistics of the particle-velocity gradient

From the system of equations (2.1) one can obtain the equation for the particle-velocity gradient $\sigma(t) = V(t)/R(t)$

$$\dot{\sigma}(t) = -\sigma^2(t) - \tau^{-1}[\sigma(t) - s(t)]. \quad (2.5)$$

Before proceeding forward, as a side remark note that in the one-dimensional case the substitution $R = \Psi \exp[-t/2\tau]$ turns this equation into the Schrödinger equation, $\ddot{\Psi} - s\Psi/\tau = \Psi/(4\tau^2)$,

where time has the role of space¹.

Next we use the formulae of differentiation (2.2,2.3) and obtain a system of equations for the averaged over noise stationary Probability Distribution Function (PDF) of $x \equiv \sigma + 1/(2\tau)$, $p(x) \equiv \int d\alpha \mathcal{P}(x, \alpha)/\tau$, where we denote $\mathcal{P}(x, \alpha)$ as the joint stationary PDF of x and α . The equations on $p(x)$ are

$$\left[\left(\frac{1}{4\tau^2} - x^2 + \frac{s_0}{\tau} \right) p \right]_x + q_x = 0, \quad (2.6)$$

$$\left[\left(\frac{1}{4\tau^2} - x^2 - \frac{s_0}{\tau} \right) q \right]_x + \left(\frac{s^2 - s_0^2}{\tau^2} \right) p_x + \nu q = 0, \quad (2.7)$$

where $q(x) \equiv \int d\alpha \mathcal{P}(x, \alpha)\alpha/\tau$. The first equation yields $q = -(C + (1/4\tau^2 - x^2 + s_0/\tau)p)$, and here C should be understood as the mean flux of x . Substituting q in the second equation we get the equation on $p(x)$

$$\left[\frac{s^2}{\tau^2} - \left(\frac{1}{4\tau^2} - x^2 \right)^2 \right] p_x + \left[(4x - \nu) \left(\frac{1}{4\tau^2} - x^2 \right) - \nu \frac{s_0}{\tau} \right] p + C(2x - \nu) = 0. \quad (2.8)$$

At large $|x|$ the PDF behaves like $p(x) \sim C/x^2$ ($C > 0$) which gives the probability of strong particle velocity gradients, and is therefore related to the probability of shocks. For small-Stokes-number ($St < St^*$) the PDF is bounded, while for large-Stokes-number ($St > St^*$) it is unbounded. We discuss the form of the PDF in some detail in the subsections below. The schematic in Figure 2.4 summarizes the different regions in the parameter space (St, Ku) where the transitions occur in the PDF of x .

The small Stokes number limit

At small Stokes numbers, $St < St^*$ and zero flux ($C = 0$) there is a unique positive integrable solution of Eq. (2.8) has the following form

$$p(x) = C_1 \frac{(w - x)^{m-1} (x - \tilde{w})^{\tilde{m}-1}}{(w + x)^{m+1} (x + \tilde{w})^{\tilde{m}+1}} \quad \text{for } x \in (\tilde{w}, w), \quad (2.9)$$

¹ The telegraph model for the Schrödinger equation was used by M. M. Benderskii and L. A. Pastur to evaluate the density of states [16].

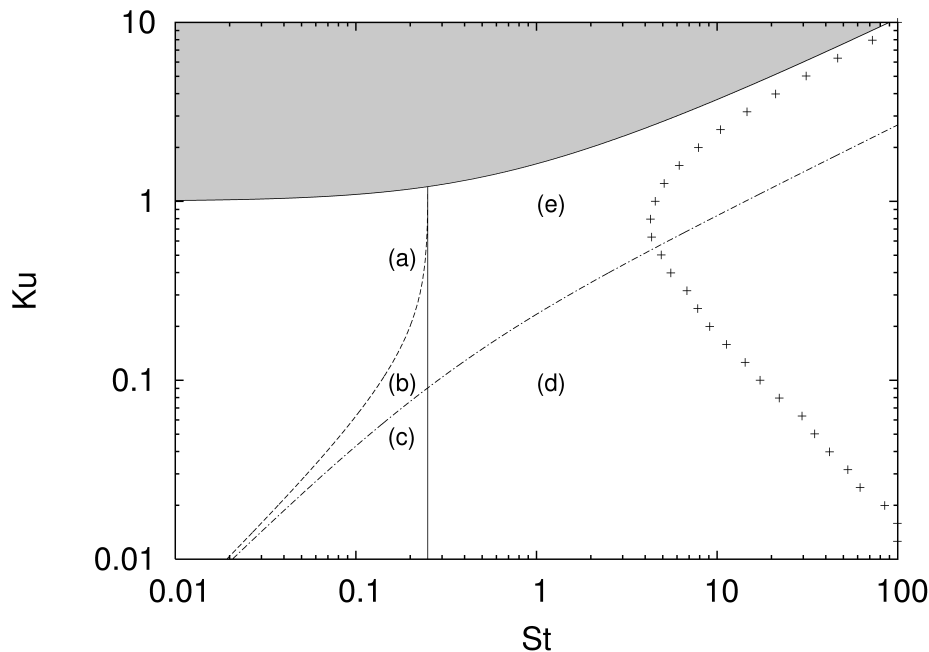


Figure 2.4: *Parameter space (St, Ku) . Shape transitions in the PDF of the particle velocity gradient x occur at $St = St^* = 1/4$ (vertical solid line), $\tilde{m} = 1$ (dashed line) and $m = 1$ (dash-dotted line). Labels refers to the PDFs shown in Figures 2.5 and 2.6. The gray area is not physically relevant. Crosses represent the boundary of the chaotic region*

here

$$\begin{aligned} w &= \sqrt{1 + 4St}/2\tau, & m &= (\nu + \Delta\nu)/4w, \\ \tilde{w} &= \sqrt{1 - 4St}/2\tau, & \tilde{m} &= (\nu - \Delta\nu)/4\tilde{w}. \end{aligned} \quad (2.10)$$

The solution is localized in the compact interval (\tilde{w}, w) , outside of this interval $p = 0$. Its shape is determined by the values of m and \tilde{m} . For $\tilde{m} < 1$ (low frequency) the PDF is peaked around the two border values. For $m < 1 < \tilde{m}$ (intermediate frequency) it vanishes at \tilde{w} , and finally when $m > 1$ (high frequency) it vanishes both at \tilde{w} and w (see Figure 2.5). Indeed, when $St < St^*$, the solution of the linear system for (R, V) oscillates between two asymptotes $V = (w - 1/2\tau)R$ and $V = (\tilde{w} - 1/2\tau)R$ according to the sign of the noise. If the noise frequency is low the system has enough time to get close to the two asymptotes and the PDF is peaked around them. Conversely, when the sign of the noise switches frequently, the system does not have enough time to reach the asymptotes and oscillates rapidly around the mean value.

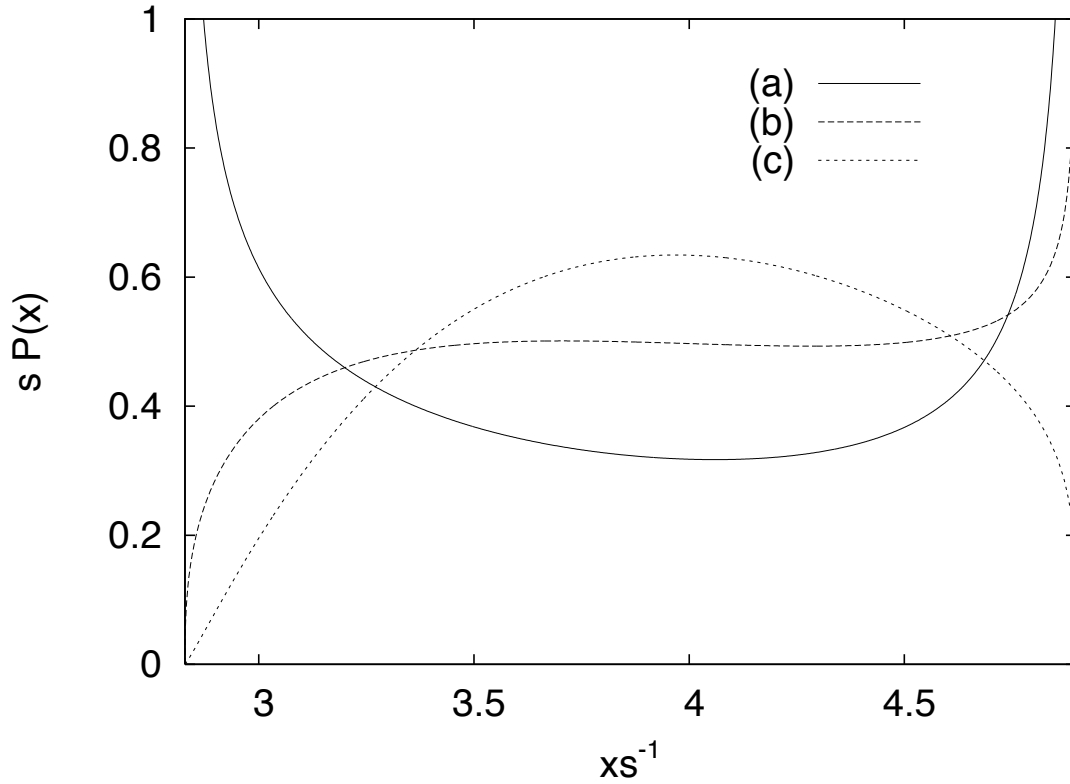


Figure 2.5: PDF of $x \equiv \sigma + 1/(2\tau)$, where σ is the particle-velocity gradient and τ is the Stokes time in the small Stokes regime ($St = 1/8$) for different values of Kubo number: $Ku = 1/8$ (a), $Ku = 1/16$ (b) and $Ku = 1/24$ (c).

The large Stokes number limit

At $St > St^*$ the solution of (2.8) consists of two different parts

$$p(x) = Cp_1(x) + C_2p_2(x) . \quad (2.11)$$

The first one is the solution of (2.8) with $C = 1$,

$$p_1 = \frac{|w-x|^{m-1}}{|w+x|^{m+1}(x^2+\tilde{w}^2)} e^{n(\arctan(x/\tilde{w}))} \int_{-w}^x dy \frac{|w+y|^{m+1}(\nu-2y)}{|y-w|^{m-1}(w^2-y^2)} e^{-n(\arctan(y/\tilde{w}))} , \quad (2.12)$$

while the second one is the right tail of the solution of the homogeneous (flux-less) equation:

$$p_2 = \frac{|w-x|^{m-1}}{|w+x|^{m+1}(x^2+\tilde{w}^2)} e^{n(\arctan(x/\tilde{w}))} I_{w,\infty}(x) . \quad (2.13)$$

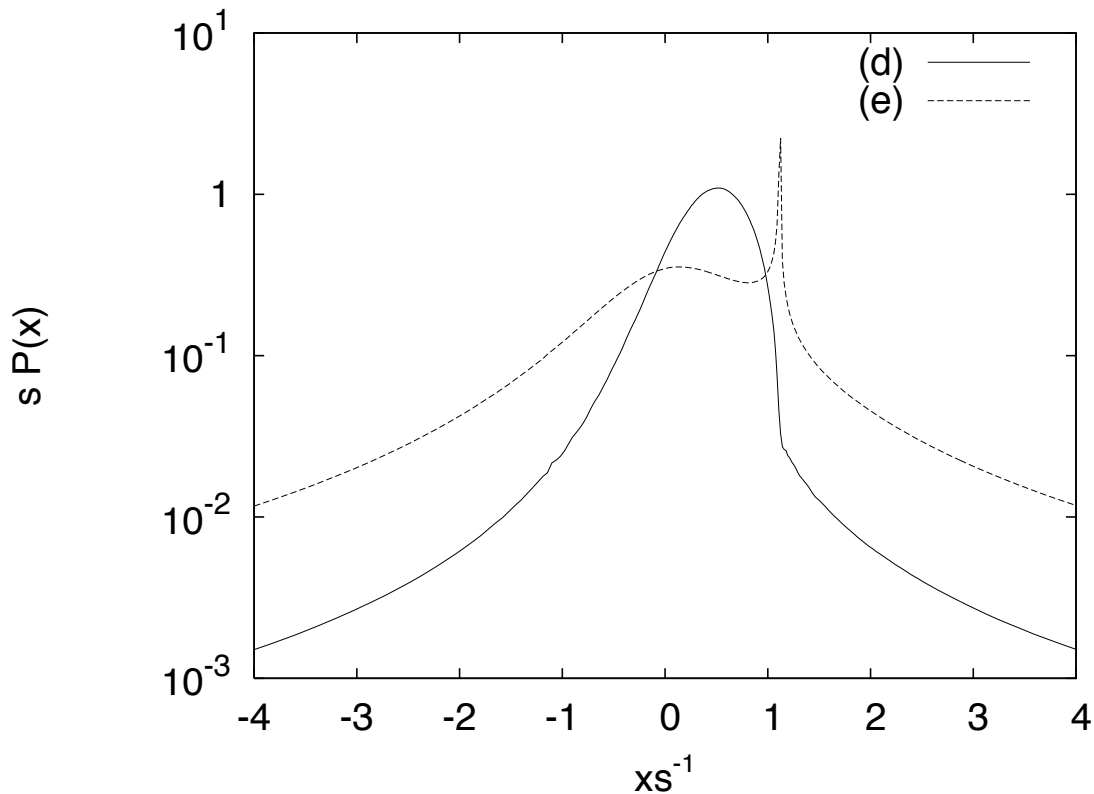


Figure 2.6: PDF of $x \equiv \sigma + 1/(2\tau)$, where σ is the particle velocity gradient and τ is the Stokes time, in the large Stokes regime ($St = 1$) for different values of Kubo number: $Ku = 0.1$ (d) and $Ku = 1$ (e).

Here $I_{w,\infty}(x)$ is the characteristic function (indicator) of the interval (w, ∞) , and

$$\begin{aligned} w &= \sqrt{4St + 1}/2\tau, & m &= (\nu + \Delta\nu)/4w, \\ \tilde{w} &= \sqrt{4St - 1}/2\tau, & n &= (\nu - \Delta\nu)/2\tilde{w}. \end{aligned} \quad (2.14)$$

Conditions for determining C and C_2 are: $\int p(x)dx = 1$ and $\int q(x)dx = 0$. These conditions guarantee the continuity of the PDF in the limit $St \rightarrow St^*$ (see Appendix G). The PDF obtained in the regime $St > St^*$ is extended over all real x , with power-law tails $p \sim C/x^2$ for large $|x|$ that are due to shocks, which occur for large negative values of $s(t)$. For short-correlated noise ($m > 1$), the PDF is characterized by an asymmetric core localized between $-w$ and w . When $m < 1$ a singular peak arises at $x = w$ (see Figure 2.6). This behavior is easily understood in term of solution of the linear system for (R, V) . When $s(t) = +|s|$ the solution converges toward the asymptote $V = \xi R = (w - 1/2\tau)R$. This produces the peak at $x = w$, provided that

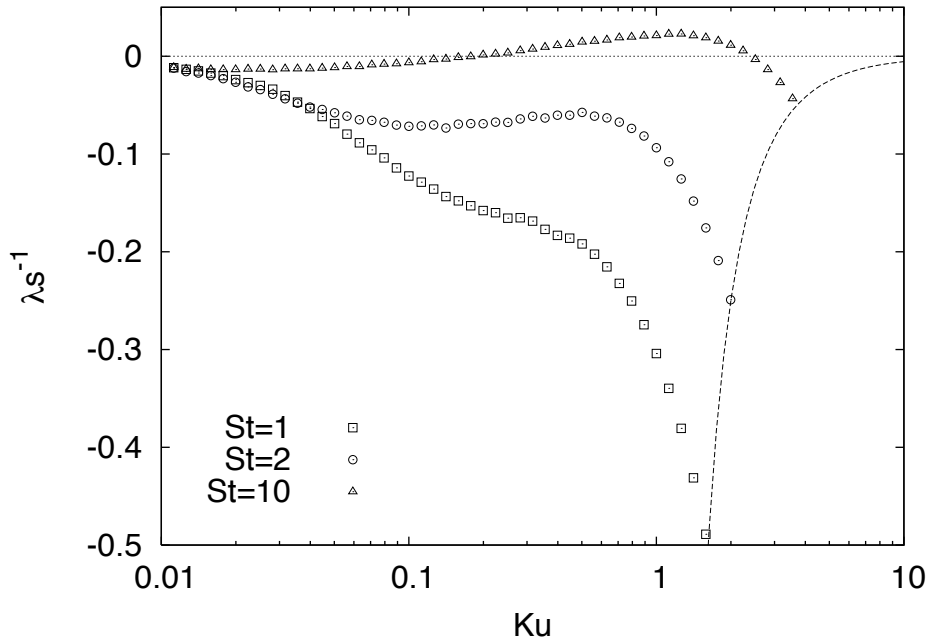


Figure 2.7: The Lyapunov exponent λ as a function of the Kubo number. An interval of positive Lyapunov exponents appears for $St \gtrsim 4.3$. The dashed line represents the asymptotic behavior for $Ku = Ku^*$.

the correlation time of the noise is long enough ($m < 1$) to get close to the asymptote. The large-Stokes number regime is hence characterized by an infinite series of shocks alternated to "quiet" phases in which the particle-velocity gradient relaxes toward ξ .

2.2.2 The Lyapunov exponent

The Lyapunov exponent of particle trajectories can be obtained from Eq. (2.5 as an ensemble average $\lambda \equiv \langle x(t) \rangle - \tau/2$ over different realizations of noise. For $St < St^*$ the mean value $\langle x(t) \rangle$ can be written in terms of hypergeometric functions of two variables (see [47]). The behavior of the Lyapunov exponent as a function of Stokes and Kubo number is shown in Figure 2.3. Lyapunov exponent is negative for small Stokes, and decreases approximately as $\lambda s^{-1} \sim -Ku$ at increasing Ku numbers. In the limit $St \rightarrow 0$, the exponent recovers the actual value for fluid tracers [43]: $\lambda_0 \equiv \lim_{\tau \rightarrow 0} \lambda = -s^2/\nu$. Notice that fluid tracers are always in the aggregation regime within this model, as signaled by the negative value of λ_0 . A sharp negative minimum $\lambda = -2s$ is found for $St = 1/4$ at $Ku = (\sqrt{2} + 1)/2$. It corresponds to the maximum aggregation of particles. As the correlation time of the flow decreases, the minimum

becomes less pronounced, and it moves to larger Stokes numbers. A region of positive Lyapunov exponents is present in the parameter-space for $St \gtrsim 4.3$. The isoline of vanishing Lyapunov exponent, which border this region, represents the transition from the strong clustering regime ($\lambda < 0$) to the chaotic regime ($\lambda > 0$). Indeed, Figure 2.7 shows that, as Stokes number increases, the interval of Kubo numbers appears where the Lyapunov exponent grows, and eventually becomes positive. This can be understood as follows: to achieve an effective mixing the correlation time of the fluid gradients must be long enough to provide substantial stretching of particle trajectories, but not too long, to avoid particle segregation in compressing regions. Therefore, the chaotic region is confined in bounded window of Ku numbers, where the lower bound is determined by stretching efficiency and particle trapping sets the upper bound.

2.2.3 Lyapunov moments

We also considered the behavior of the Lyapunov moments γ_n , defined as $\langle R^n \rangle \sim \exp(\gamma_n t)$. The evolution of $\langle R^n \rangle$, for n positive integer, is determined by a closed system of $2(n+1)$ equations. Details of the calculations are given in Appendix H. There is no simple explicit expression for γ_n in general. Taking the limit of vanishing inertia, $St \rightarrow 0$, one recovers the Lyapunov moments of fluid tracers [43],

$$\gamma_n = \sqrt{\left(\frac{\nu}{2}\right)^2 + s^2(n^2 - n)} - \frac{\nu}{2}. \quad (2.15)$$

The asymptotically linear behavior of γ_n for large n is the hallmark of the presence of an upper bound for velocity gradients.

2.2.4 Short-correlated flows

Next we examine the limit of short-correlated flows. In order to recover the δ -correlated noise fluctuations $\langle s(t)s(t') \rangle = 2D\delta(t-t')$, the limit $\nu \rightarrow \infty$ must be taken keeping constant $s^2/\nu = D$. Meaning as the Kubo number $Ku = s/\nu$ tends to zero the Stokes number $St = s\tau$ should grow, so that the product $KuSt = s^2\tau/\nu = D\tau$, remains constant. In this sense, the short correlated limit for inertial particles correspond always to the large-inertia case. In the delta-

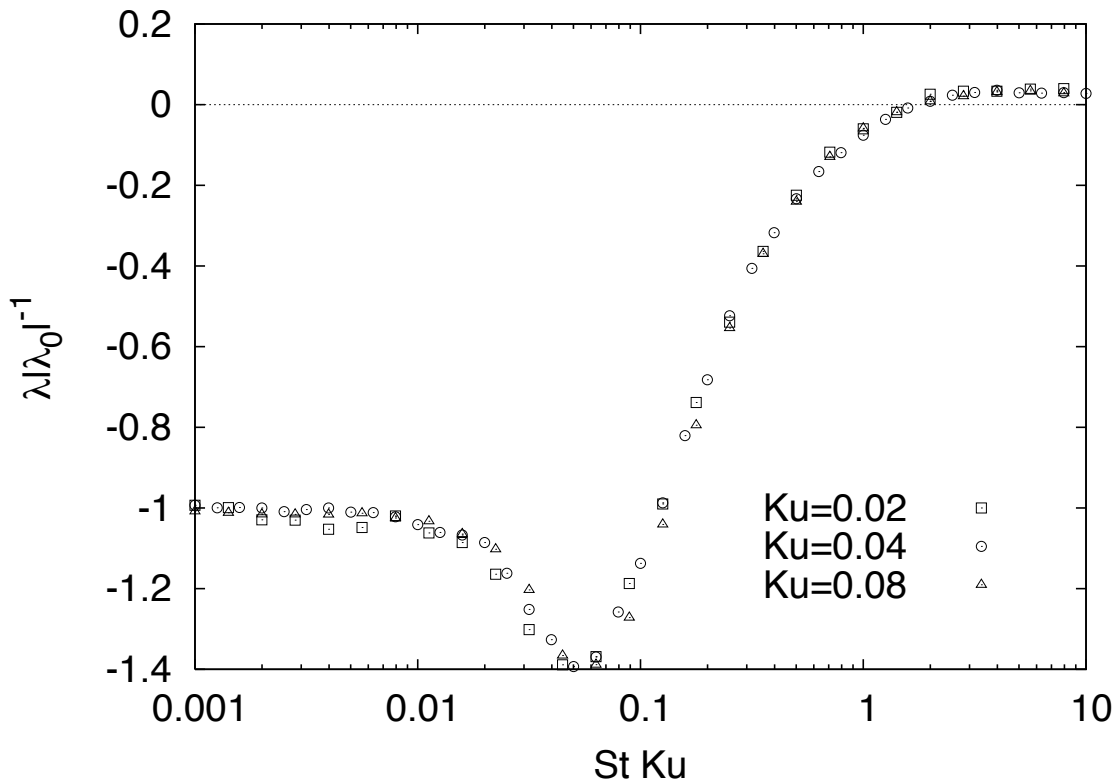


Figure 2.8: Lyapunov exponent $\lambda \equiv \langle x(t) \rangle - \tau/2$ in short-correlated flows.

correlated limit the relevant time-scale associated to fluid velocity gradients is given by the Lyapunov exponent of fluid tracers $\lambda_0 = -s^2/\nu = -D$. This is confirmed by the collapse of particle Lyapunov exponents in the short-correlated limit once their intensity and Stokes times are re-scaled with $|\lambda_0|$ (see Figure 2.8). A noticeable minimum is observed for $|\lambda_0|\tau = \text{KuSt} \simeq 0.05$ and a transition to chaos, i.e. from negative to positive λ , occurs for $\text{KuSt} \gtrsim 1.6$. These features are in qualitative agreement with previous analytic and theoretical results obtained in the framework of δ -correlated flows [33, 108]. Notice that in those studies Gaussian statistics is assumed for velocity gradients, at variance with our model in which only the two values $\pm s$ are allowed. Therefore quantitative details such as the exact position of the minimum can be different.

We remark that in the short-correlated asymptotics, the fluid-tracers limit becomes sin-

gular. Indeed one has

$$\lim_{\nu \rightarrow \infty} s_0 = \lim_{\nu \rightarrow \infty} -\frac{s^2}{\nu(1 + \nu\tau)} = \begin{cases} -D & \tau = 0 \\ 0 & \tau > 0 \end{cases}, \quad (2.16)$$

which signals that fluid tracers are still preferentially attracted by regions of ongoing compression, while inertial particles with arbitrary finite τ are not. Notice that in the limit $\nu \rightarrow \infty$ fluid velocity gradients become unbound because $s \rightarrow \infty$, and for fluid tracers we recover the quadratic behavior of Lyapunov moments $\gamma_n = D(n^2 - n)$.

2.2.5 Long-correlated flows

Time correlation of fluid gradient is bounded by the maximal Kubo number, see Eq. (2.4). When $Ku = Ku^*$ the transition rate ν_1 from $-s$ to s vanishes, while the transition rate ν_2 from s to $-s$ reaches its maximum $\nu^* = (\sqrt{1 + 4St} - 1)/(2\tau)$. Particles initially seeded in expanding regions are gradually captured by contracting ones, where they remain trapped forever. Therefore the population of expanding regions decreases exponentially as

$$P(t) \sim \exp(-\nu^*t). \quad (2.17)$$

Moments of particle separations will consequently evolve asymptotically according to

$$\langle |R|^n \rangle \sim e^{n\xi t} P(t) + (1 - P(t)) e^{nRe(\zeta)t} f(Im(\zeta)t), \quad (2.18)$$

where $\zeta = (-1 \pm i\sqrt{4St - 1})$ and $f(t)$ is a periodic function, with a period 2π . Notice that $\nu^* = \xi$ and therefore for $n = 1$ the decreasing fraction of particle in expanding regions is exactly balanced by the exponential growth of their separation. From (2.17,2.18) the Lyapunov moments of $\langle |R|^n \rangle$, $\tilde{\gamma}_n$, are

$$\begin{aligned} \tilde{\gamma}_n &= \xi(n - 1) \quad \text{for } n \geq (\xi - Re(\zeta))^{-1}, \\ \tilde{\gamma}_n &= Re(\zeta)n \quad \text{for } n \leq (\xi - Re(\zeta))^{-1}. \end{aligned} \quad (2.19)$$

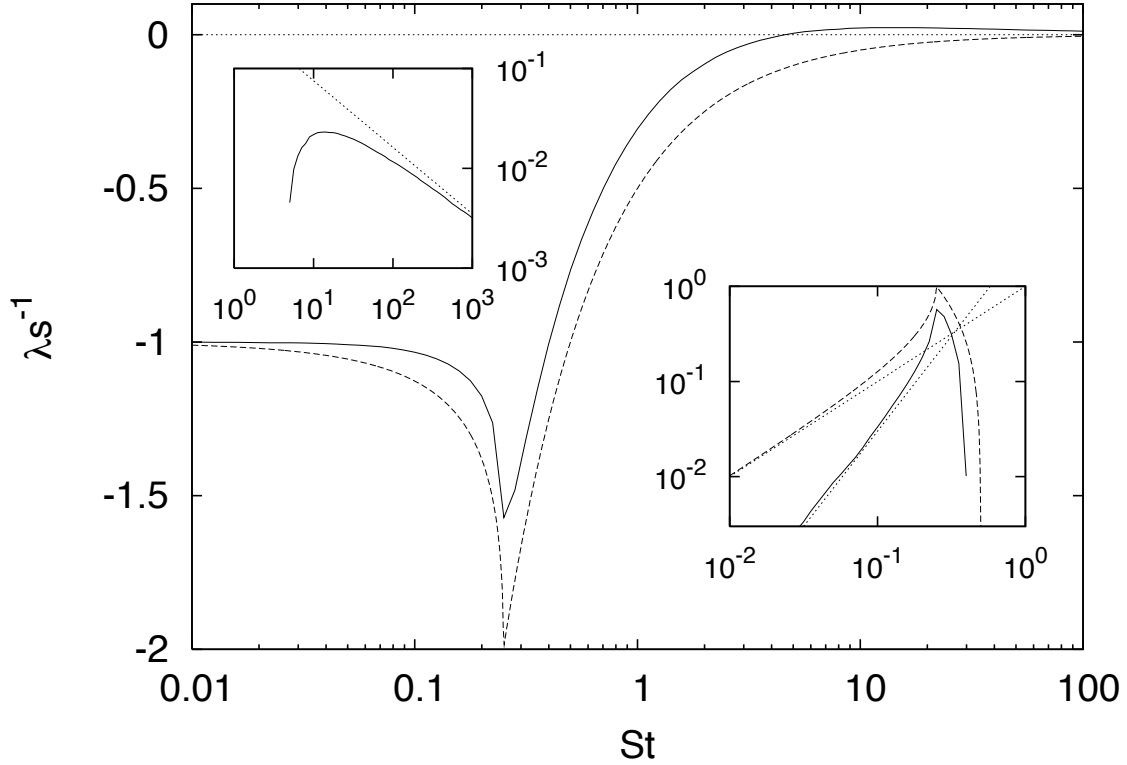


Figure 2.9: Lyapunov exponent λ for $Ku = 1$ (solid line) and on the line $Ku = Ku^*$ (dashed line), corresponding to the longest correlation of velocity gradients achievable within the model. **Upper inset:** asymptotic behavior for large Stokes number $\lambda s^{-1} \sim St^{-2/3}$ (dotted line), ($Ku = 1$). **Lower inset:** asymptotic behavior for small Stokes number $|\lambda - \lambda_0|s^{-1} \sim St^\zeta$ (dotted line).

In the limit of fluid tracers one obtains $\tilde{\gamma}_n = s(n - 1)$ for $n \geq 1/2$ and $\tilde{\gamma}_n = -sn$ for $n \leq 1/2$, in agreement with Eq. (H.5). Finally, the Lyapunov exponent along the critical line $Ku = Ku^*$ is $\lambda = (\partial\tilde{\gamma}_n/\partial)|_{n=0} = Re(\zeta)$. In Figure 2.9 we compare its behavior with that of the Lyapunov exponent along the line $Ku = 1$. For small Stokes number both of them recover the fluid-tracers limit $\lambda \rightarrow \lambda_0 = -s$, but with different power law behavior. On the line $Ku = Ku^*$ we have $|\lambda - \lambda_0|s^{-1} \sim St$, while for $Ku = 1$ we have $|\lambda - \lambda_0|s^{-1} \sim St^2$ (see lower inset of Figure 2.9). For large Stokes number Lyapunov vanishes as $\lambda s^{-1} \sim -St^{-1}$ on the line $Ku = Ku^*$ and as $\lambda s^{-1} \sim St^{-2/3}$ for $Ku = 1$ (see upper inset of Figure 2.9). In between these two asymptotics a sharp minimum appears for $St = St^*$.

The asymptotic decay $St^{-2/3}$, here shown for long-correlated flows, has been already predicted and observed also for δ -correlated flows [15, 49]. The agreement between these results confirms that in the large-Stokes number limit the role of time correlation becomes insignificant

and particles behave as if suspended in δ -correlated-in-time flows.

2.3 Conclusions

In spite of its simplicity our model reproduces the phenomenon of trapping of particles in compressing regions for time-correlated flows. The telegraph noise statistics represents a special case of time-correlated statistics, for which the Lagrangian dynamics of inertial particles is amenable to analytical treatment. We studied the effects of finite-time correlations of velocity gradients on the trajectories of inertial particles. Also, we obtained numerical results on the dependence of the Lyapunov exponent on Stokes and Kubo numbers (see Figure 2.3). We derived the Lyapunov moments and have discussed the asymptotics of long- and short-correlated flows, as well as the fluid-tracers limit.

For large Stokes numbers, a regime characterized by the formation of shocks, we found a chaotic region in parameter space (St, Ku) , where the Lyapunov exponent becomes positive. From this finding we concluded that inertia is responsible for the transition from a strong clustering regime, originated by the compressible nature of the flow, to a chaotic regime. The latter is observed in a range of Kubo numbers such that the time correlation of fluid gradients is long enough to provide substantial stretching, but not too long to cause particles to remain trapped in a compressing region.

2.3.1 Further directions

Many of the complex phenomena which occur in real flows are beyond the scope of this model. In particular it would be very interesting to study the effects of preferential concentration (strong spatial inhomogeneity) in hyperbolic regions. The increase of chaoticity of inertial particle trajectories in turbulent flows is commonly believed to be the consequence of these effects [14]. For such a study a two-dimensional extension of the model is needed. However a two-dimensional case is still an unsolved problem even in time uncorrelated flows. Namely this problem is formally equivalent to another unsolved problem in physics - dynamics of spins in a random magnetic field². Another possible direction is to characterize the structures which are

² Mapping to the spin problem: One writes the Newton's equation for the particle separation and makes a

observed in particle distributions at all scales within the turbulent inertial range [50]. Such an analysis requires an entirely different approach, since the Lyapunov statistics suitably describes only the clustering of inertial particles at the dissipative scales of the turbulent flow.

substitution of the form $\mathbf{R} = \mathbf{S} \exp[-it/(2\tau)]$. In this way one is left with a Schrödinger equation, where time is space and two components of the vector are spins.

Part II

Two-dimensional turbulence

3. Passive scalar contours

Turbulent advection is rife: it appears in many natural and engineering settings, which range from atmospheric phenomena, combustion, stretching and amplification of magnetic fields on galactic and terrestrial scales, biology (large fluctuations make the local gradient concentrations, of e.g. odor or nutrients, futile for navigation) etc. Usually the advected "substance" has an effect on the turbulent flow itself, by generating local forces. However in some instances this feedback effect is negligibly small. It is these cases we will concentrate on here. In general a transported field can have arbitrary structure (scalar, vector or tensor), however we confine our analysis to *passive scalar* fields - scalar fields that are passively transported by the flow. A passive scalar substance could be a pollutant, smoke dispersing in the air, a fluorescent dye mixing in a turbulent jet, a temperature field (if the buoyancy forces are small compared to inertial stresses), a salinity field etc. On Figure (3.1) we show some examples of passive scalar from natural settings and on Figure (3.2) are examples from experiment and numerics.



Figure 3.1: Instances of passive scalar turbulence observed in nature: (**left**) cigarette smoke (Photo of Humphrey Bogart by Yousuf Karsh, 1946 ("Yousuf Karsh collection" at the Library and Archives Canada).), (**middle**) blue dye in water (©iStockphoto.com/claylib) and (**right**) jets long after they were released from an airplane (French "Mirages" celebrating 150 years of the city of Nice, 2010.)

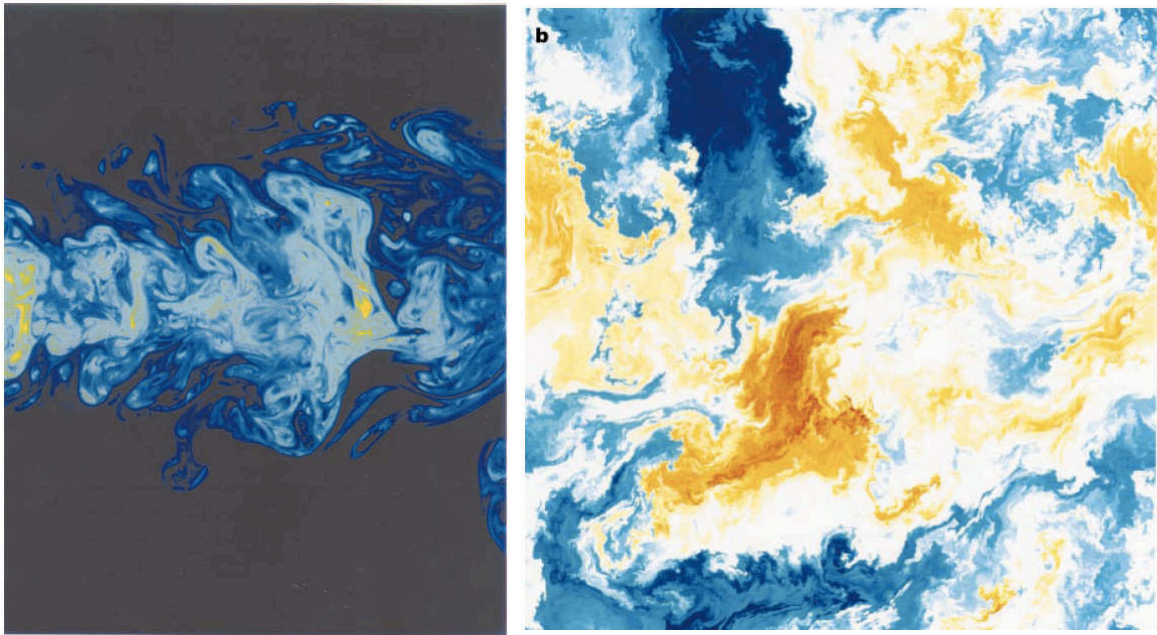


Figure 3.2: Instances of passive scalar in experiment and simulations. *(left)* Fluorescent dye in a turbulent jet of Reynolds number $Re = 4000$ [97]; *(right)* numerical simulation of passive scalar advection in two dimensions for a rough Kraichnan velocity on a 8192 square grid [27].

Passive scalar substance can exhibit complex dynamic behavior that shows many phenomenological parallels with the behavior of the turbulent velocity field. Yet the statistical properties of this so-called passive scalar turbulence are decoupled from those of the underlying velocity field. Few years ago passive scalar turbulence has yielded to mathematical analysis¹. A close link was discovered between the multipoint statistics of the advected fields and the collective behavior of the separating Lagrangian (fluid) particles. Essential for this progress has been the observation that the anomalous scaling properties and the coherent structures in the scalar field occur even for a scalar advected by a random Gaussian velocity field [60, 61, 63]. Namely the non-trivial statistical aspects of the scalar originate from the mixing process itself, rather than being inherited from the carrier flow. The turbulent flow transports and disperses the scalar. The spatial non-uniformity of the velocity field causes the lines of constant scalar concentration to stretch and fold; as a result, variations of the scalar concentration reach progressively smaller scales. This process amplifies the local concentration gradients until molecular diffusivity finally takes over, causing local variations of the scalar to dissipate.

¹ For a survey of passive scalar literature see references in reviews [45, 91, 102].

The evolution of the passive scalar $\theta(t, \mathbf{r})$ is governed by the advection-diffusion equation

$$\partial_t \theta(t, \mathbf{r}) + (\mathbf{v}(t, \mathbf{r}) \cdot \nabla) \theta(t, \mathbf{r}) = \kappa \nabla^2 \theta(t, \mathbf{r}) + \varphi(t, \mathbf{r}), \quad (3.1)$$

where $\mathbf{v}(t, \mathbf{r})$ is the velocity field, κ is the molecular diffusivity and $\varphi(\mathbf{r}, t)$ describe the sources. Two distinct situations can be considered: the smooth or the rough velocity case. In smooth velocity fields, in the absence of forcing and dissipation, the advection equation can be easily solved in terms of the Lagrangian flow. To calculate the value of θ at a given time one has to trace the field evolution equations backwards along the Lagrangian trajectories. The tracer θ is conserved along the Lagrangian trajectories: $\theta(t, \mathbf{r}) = \theta(\mathbf{R}(0; \mathbf{r}, t), 0)$, where $\mathbf{R}(\cdot; \mathbf{r}, t)$ denotes the Lagrangian trajectory passing at time t through point \mathbf{r} . Actually for scalar dynamics, the space integral of any function of $\theta(t, \mathbf{r})$ is conserved in the absence of sources and diffusion.

Most of the results on the passive scalar statistics are on averaged quantities - moments and multi-point correlation functions of the passive scalar field. Here we aim to consider non-local objects, such as individual contours of the passive scalar field. It is therefore that we choose the simplest possible case, a passive scalar advected by *Batchelor-Kraichnan* velocities, where a lot of analytical results are known for on the scalar's statistics. We choose the forcing to be white in time and Gaussian and assume the velocity to be smooth, i.e. to be in the so-called *Batchelor regime* [8]. This is a reasonable assumption for scales much smaller than the viscous scale $\eta \equiv (\nu^3/\epsilon)^{1/4}$, where ν is the kinematic viscosity of the flow and ϵ is the energy dissipation rate. In this case the velocity field enters into the advection equations only through the time-dependent strain matrix $\mathbf{v}(t, \mathbf{r}) = \partial_t \mathbf{R}(t) + \hat{\sigma}(t)(\mathbf{r} - \mathbf{R}(t))$, where $\hat{\sigma}(t)$ is taken along the same trajectory. On these scales a two-dimensional incompressible flow is characterized with a Lyapunov exponent that λ_1 ($\lambda_2 = -\lambda_1$) that stretches the blobs in some direction depending on the velocity realization. We also assume that the flow is *Kraichnan* [60], which stands for velocity ensemble being Gaussian, δ -correlated in time and its correlations being scale invariant. Hence the incompressible Kraichnan velocity ensemble in the Batchelor regime

is then fully specified by the two-point correlations of the strain matrix $\hat{\sigma}$

$$\hat{\sigma} = \begin{pmatrix} a & b+c \\ b-c & -a \end{pmatrix}, \quad (3.2)$$

where a , b and c are mutually independent, Gaussian random functions of time, with zero mean and variance: $\langle a(t)a(t') \rangle = \langle b(t)b(t') \rangle = \langle c(t)c(t') \rangle / 2 = D^2 \delta(t-t')$. Incompressibility is guaranteed by $\text{tr} \hat{\sigma} = 0$. We also choose $\langle \det \hat{\sigma} \rangle = 0$ since we wish the potential and solenoidal parts have equal strength on average. The velocity field has nonzero gradients therefore it stretches the blob in one direction and compresses it in the other direction. These compressions and elongations appear exponential in time. The diffusion stops reducing the dimension of the blob, when its width becomes of the order of the diffusion scale $r_d \propto \sqrt{\kappa/\lambda_1}$. Here the Prandtl number $\text{Pr} \equiv \nu/\kappa$ is large².

Besides, the diffusion scale r_d and the viscous scale η , we have one more characteristic scale in our problem, it is the forcing scale l . In order to be able to describe the stretching and the compressions in detail, we choose to have a wide *convective interval*: $r_d \ll l$. However, since one and the same mechanism compresses and stretches a blob, it is necessary to resolve well also the interval of scales above the forcing scale $l \ll \eta$. The large resolutions render the numerical modeling of this problem to be technically demanding.

Since the velocity field is smooth and just elongates the blob in one direction and shrinks it in the perpendicular direction, we expect the fractal dimension of the blob's perimeter to be equal to unity for $r < l$. We believe that it is the interplay of the forcing and the velocity field that can lead to a nontrivial fractal dimension at scales r much larger than the forcing scale ($l \ll r \ll \eta$).

3.1 Heuristic arguments for fractal dimension $D_0 = 3/2$

Let us present some heuristic arguments on the fractal dimension of passive scalar contour lines. As it was noted in the last section, we expect a nontrivial fractal dimension only for

² In heat transfer problems, the Prandtl number controls the relative thickness of the momentum and thermal boundary layers. When Pr is small, it means that the heat diffuses very quickly compared to the velocity (momentum). The mass transfer analog of the Prandtl number is the Schmidt number.

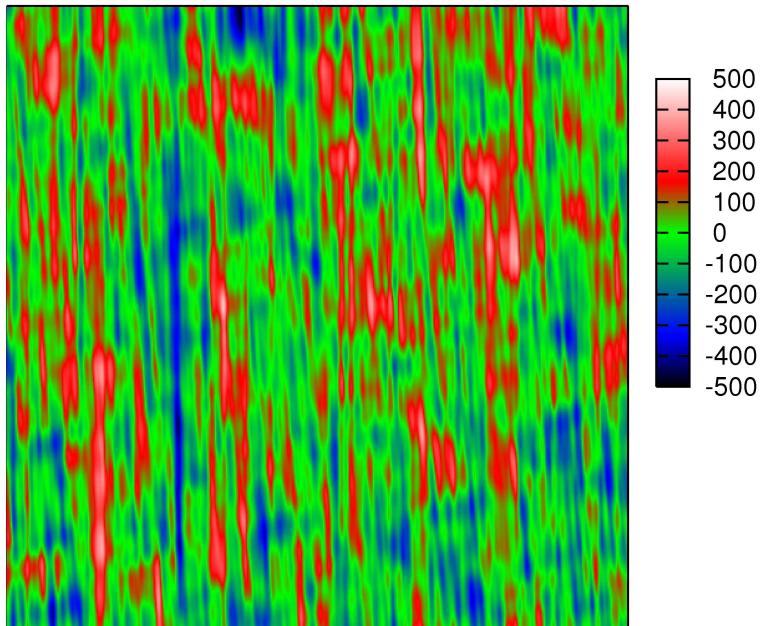


Figure 3.3: Snapshot of a part of the passive scalar field. The square has $75l \times 75l$, where l is the initial blob size (forcing scale). Note the vertical stripes of scalar, this is due to stretching along the velocity gradient.

long contours. By long here we mean contours with perimeters which are much longer than the forcing scale $P \gg l$. The longest contours one finds at the *Corsin integral* level $\int d\mathbf{r}\theta(\mathbf{r}, t) = 0$.

The smooth isolines produced by pumping are stretched and compressed so that wherever one looks at the passive scalar field, there is usually just a set of parallel lines. And at scales above the diffusion scale, r_d , the complete level set is dense [29]. However we are interested in the fractal dimension of a single line. Most of lines which are inside an area proportional to πl^2 are straight and aligned along the expansion direction. Some of lines inside this area of size l have turning points or "fjords" (see Figure 3.4). The creation of fjords by the joint action of velocity and pumping is sketched on Figure 3.5. When an isoline is longer than forcing scale l the action of pumping can shift and displace parts of the line differently. Since the velocity and the forcing are uncorrelated, it is natural to assume that turnings happen randomly. In that case at some scale L , which is larger than the forcing scale l , the number of turning points scales as $L^{1/2}$, thus for smooth velocity fields we have that the perimeter of a contour scales as $P \propto L^{3/2}$, which corresponds to fractal dimension $D_0 = 3/2$.

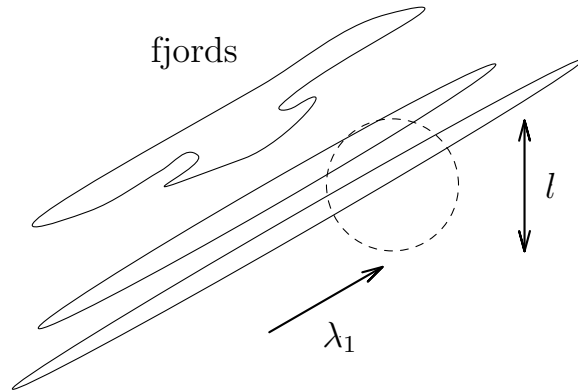


Figure 3.4: Isolines of the passive scalar are represented with the solid line. They are elongated along the first Lyapunov exponent λ_1 . Long ones are dominated by fjords. The dashed circle just shows the initial size of one blob, l .

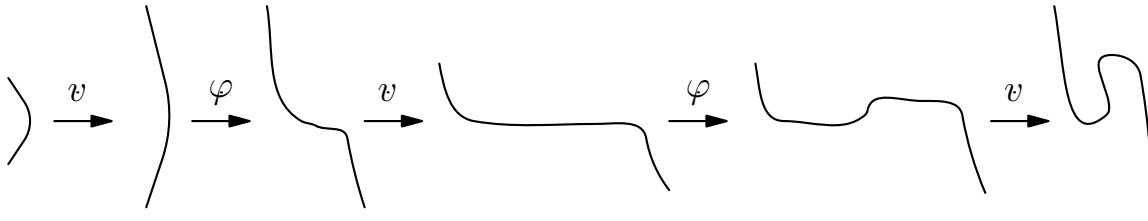


Figure 3.5: The creation of fjords on a part of an isoline by successive stretching and compression by velocity v and shifting by forcing φ .

3.2 The numerical algorithm

3.2.1 Generating the passive scalar field

We developed a new computational method to generate the passive scalar field as a collection of blobs of scalar. Our method mimics impinging drops of ink on a piece of paper. It is based on the fact that the advection-diffusion equation (3.1) is linear. To get a snapshot of the passive scalar field at a particular time, we sum over all of the blobs of scalar that hit the surface, at random times and positions in the past. We assume that the passive scalar field is a collection of a large number of blobs, in order to ensure the Gaussian statistics of the resulting field.

Each blob initially had a spherical shape

$$\theta(t_0, \mathbf{r}_0) = A \exp \left[-\frac{(\mathbf{r}_0 - \mathbf{r}_c)^2}{2l^2} \right], \quad (3.3)$$

where t_0 is the time that the blob of amplitude A had dropped on the surface at position \mathbf{r}_c .

The shape of such a blob at a later time t can be found by the method of characteristics

$$\theta(t, \mathbf{r}_0) = \frac{Al^2}{\sqrt{\det \hat{I}(t, t_0)}} \exp \left\{ -\frac{1}{2} \left[\hat{W}(t, t_0) \mathbf{r}_0 - \mathbf{r}_c \right] \hat{I}^{-1}(t, t_0) \left[\hat{W}(t, t_0) \mathbf{r}_0 - \mathbf{r}_c \right] \right\}, \quad (3.4)$$

$$\hat{I}(t, t_0) = \hat{W}(t, t_0) \hat{W}(t, t_0)^T + \kappa \int_0^t dt' \hat{W}(t, t_0) \hat{W}(t', t_0)^{-1} \left[\hat{W}(t, t_0) \hat{W}^{-1}(t', t_0) \right]^T, \quad (3.5)$$

here $\hat{W}(t, t_0)$ is the evolution operator, $\mathbf{r}(t) = \hat{W}(t, t_0) \mathbf{r}(t_0)$, and $\hat{I}(t, t_0)$ is the tensor of inertia. Notice that to specify a blob at a time t it is enough to know six values: the symmetric matrix $\hat{I}(t, t_0)$, \mathbf{r}_c and t_0 .

These blobs are advected by a Kraichnan random velocity field. The direction of elongation depends on the velocity realization. Since there is spatial asymmetry in the problem, we use it to optimize the computations. We precalculate the velocity field evolution and obtain the elongation direction, then we align the vertical axis along this direction. Next we start impinging blobs. At each time step we record in to a data file blobs that fell on the plane at that time. We have seen, in the previous paragraph, that each blob is fully characterized by six values. Once we have created enough blobs to ensure the Gaussianity of the passive scalar field we start summing over them. The outcome is a snapshot of the passive scalar field.

3.2.2 Analysing the contours

To obtain the isolines of the passive scalar field we modified the Hoshen-Kopelman algorithm (HK algorithm) [54]. This algorithm is mainly used to label percolation clusters. Its innovatory idea is that not a single label, but a set of labels determines the same cluster. For example as the algorithm scans through the matrix two clusters with different labels might merge into a single one. In this case the HK algorithm rather than returning and "repainting" the joint cluster with a unique label, it just adds both labels to a set of labels that denote this new single cluster. In each set of labels, one is the so-called proper label of the cluster, but the cluster itself is never "repainted" with its proper label. HK algorithm needs one passing through the matrix in order to determine the clusters and as such is extremely efficient when working with large matrices. We modified the HK algorithm to label contours instead of clusters (CHK algorithm) and to calculate arbitrary contour integrals on the fly. Like HK, the CHK algorithm is also a

one passage algorithm.

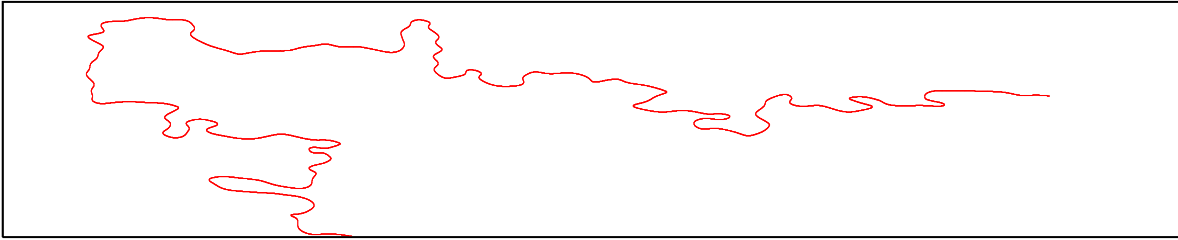


Figure 3.6: A typical long passive scalar contour. This particular one has perimeter $P \simeq 270l$, where l is the forcing scale. Here in order visualize the fjords better, we enlarged twice the vertical axis.

We measure the fractal dimension by box-counting. To calculate the *box-counting dimension* for a fractal, one imagines that the fractal lies on an evenly-spaced grid, and counts how many boxes are required to cover it. If $N(\epsilon)$ is the number of boxes of edge length ϵ needed to cover the fractal, the box-counting dimension is defined as the following limit:

$$D_0 = -\lim_{\epsilon \rightarrow 0} [\ln N(\epsilon) / \ln(\epsilon)]. \quad (3.6)$$

3.3 Results

We made several velocity realizations of 20000^2 resolution and some of 60000^2 . These snapshots represent $600l \times 600l$. The ratio of the forcing to the dissipation scale was $l/r_d = 100$. The large simulations, 60000^2 , resolve up to the diffusion scale, while in the smaller simulations one pixel is $3r_d$. Our preliminary results show that the fractal dimension at scales much larger than the forcing scale is the same in both types of simulations. This numerically justifies neglecting diffusion in our heuristic arguments, for the fractal dimension. In Figure 3.6 we show a typical long contour and on Figure 3.7 we show the box counting dimension obtained from a single velocity realization, of resolution 20000^2 , where we averaged over 80 curves. We clearly observe two distinct box counting fractal dimensions. First one is valid below forcing scale and has the value of $D_0 = 0.9 \pm 0.3$, while on scales larger than the forcing scale, we get $D_0 = 1.3 \pm 0.2$. Future steps include a more extensive analysis of the data available and getting the generalized box-counting dimension [105].

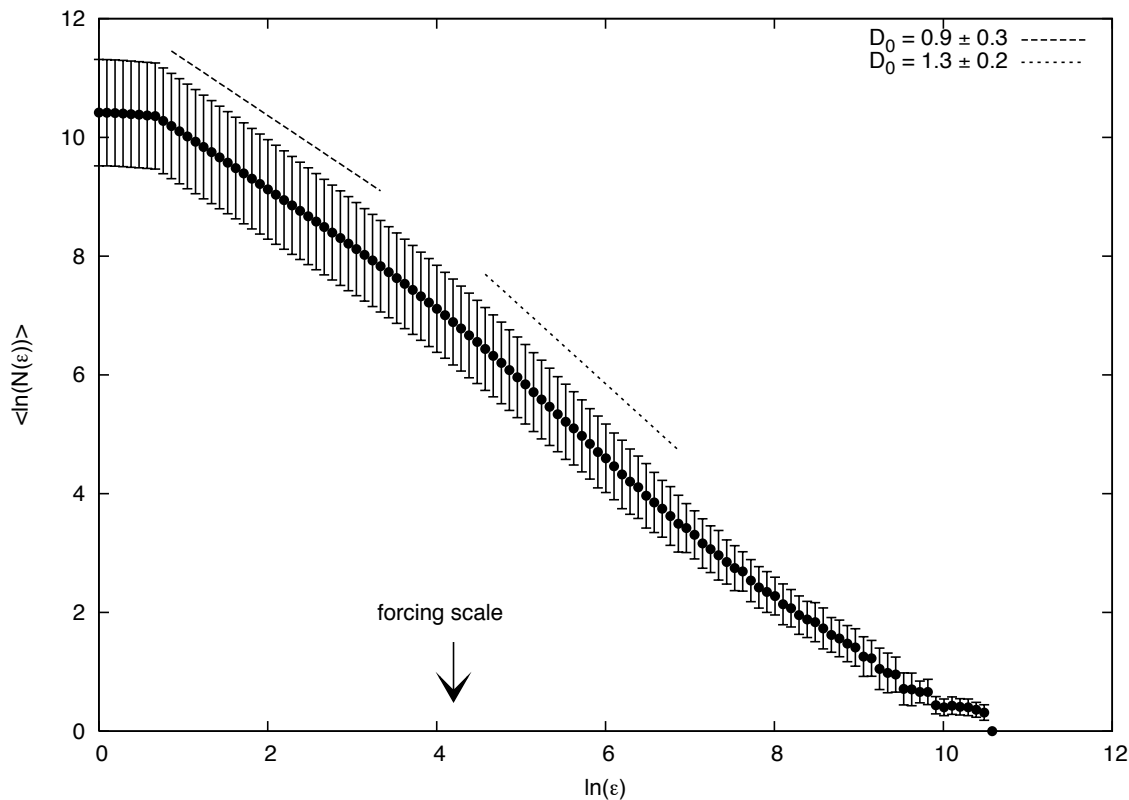


Figure 3.7: The fractal dimension of passive scalar isolines, at $\theta = 0$ level obtained by box counting. The dashed line has the slope $D_0 = 0.9 \pm 0.3$, the line's projection on the horizontal axis is the interval of sub-forcing scales, which was used to make this fit. While, the dotted line has the slope $D_0 = 1.3 \pm 0.2$ slope and this line's horizontal projection represents the interval of scales above the forcing scale (that was used to get the value of the slope). Here averaged over 80 contours from a single velocity realization. All the contours we averaged over had perimeters larger than $360l$, where l is the forcing scale. The error bars represent the deviation from $\langle \ln(N(\epsilon)) \rangle$, where $N(\epsilon)$ is the number of boxes of size ϵ needed to cover the curve.

4. 2D turbulence of point vortices

This chapter is about an idealized two-dimensional turbulent flow. In nature manifestations of such flows are the large-scale motions in the atmosphere, shallow layers of a fluid, soap film etc. In 2D taking the curl of the Navier-Stokes equations yields an equation involving only vorticity $\boldsymbol{\omega}(\mathbf{r}, t) \equiv \nabla \times \mathbf{v}(\mathbf{r}, t)$

$$\partial_t \boldsymbol{\omega} + (\mathbf{v} \cdot \nabla) \boldsymbol{\omega} = \nabla \times \mathbf{f} + \nu \Delta \boldsymbol{\omega}. \quad (4.1)$$

In the absence of forcing and dissipation, the two arguably most important invariants are the integrated squared vorticity, so-called *enstrophy*, $\Omega \equiv \int \omega^2 d\mathbf{r}$ and the kinetic energy (integrated squared velocity). The existence of two quadratic and positive invariants dictates that the steady state of turbulence must have two cascades. The intuition from 3D flows is that the energy cascades towards small scales, however in 2D when one excites turbulence at a large scale by injecting energy and enstrophy at finite rates, the energy does not cascade toward large scales. The reason is that the exact relation $\langle \epsilon \rangle = \nu \langle \omega^2 \rangle$, that holds for homogeneous turbulence, tells us that a nonzero energy dissipation implies infinite enstrophy dissipation in the inviscid limit. Thus, energy flows upscale (inverse cascade) while enstrophy cascades downscale (direct cascade). The direction of the cascade was concluded from the non-equilibrium development of L. Onsager's equilibrium treatment of a system of point vortices (1949), in which the joint conservation of energy and enstrophy lead to the notion of *negative temperatures*. The temperature is negative when the available phase-space volume *decreases* with increasing energy. The phenomenon arises at sufficiently high energy because the nonvanishing enstrophy requires the energy to be redistributed only among modes with low wavenumbers. R. H. Kraichnan discovered the velocity spectrum in the inverse cascade for two-dimensional

incompressible turbulence [59].

We set out first to repeat the results of E. D. Siggia and H. Aref [92], who got the inverse energy cascade in a system of point vortices by introducing some small scale forcing. The later goal in mind was to study the statistics of this flow in detail. However so far we have not been able to reproduce the results of [92]. All we see is the equilibrium energy spectra.

4.1 Point vortices

The Euler equation can be cast in Hamiltonian form. A particularly simple formulation emerges when the vorticity field is approximated by a large number of point vortices of individual circulation Γ_i : $\omega(\mathbf{r}, t) = \sum_{i=1}^N \Gamma_i \delta(\mathbf{r} - \mathbf{r}_i(t))$. The canonically conjugate Hamiltonian variables are the simply: $\Gamma_i x_i$ and $\Gamma_i y_i$. In the absence of boundaries the Hamiltonian is the energy of interaction of the vortices: $\mathcal{H} = (-1/4) \sum_{i < j; i, j=1}^N \Gamma_i \Gamma_j \ln |\mathbf{z}_i - \mathbf{z}_j|$, where $z_j = x_j + iy_j$. This system represents potentially a rich playground for analytical calculations on two-dimensional flows. The equilibrium case is a matter of classical textbooks. Here we look at a system of point vortices subjected to external forcing, which drives the system out of equilibrium.

As a starting point we wanted to repeat the numerical results of E. G. Siggia and H. Aref [92] and obtain the inverse energy cascade. To model the inverse cascade of energy in 2D they have used point vortices and devised a physically plausible forcing technique to inject energy. Vortex methods have been successfully used to simulate a number of nearly inviscid flows when the vorticity distribution is nonuniformly distributed. When used in conjunction with a lattice, to facilitate inversion of Poisson's equation (the *cloud-in-cell* algorithm [28, 92]), their numerical efficiency is competitive with finite difference or spectral methods. For the statistically homogeneous, isotropic flow simulated here, one might hope that, in spite the effects of the lattice, a vortex simulation would better express the local conservation of circulation (Kelvin's theorem). A second reason for applying vortex methods is that they do not require viscosity, i.e. the inverse cascade of energy ($\pi \langle k |v_k|^2 \rangle \propto k^{-5/3}$) extends all the way to the highest wavenumber resolved. In the following section we describe our numerical efforts.

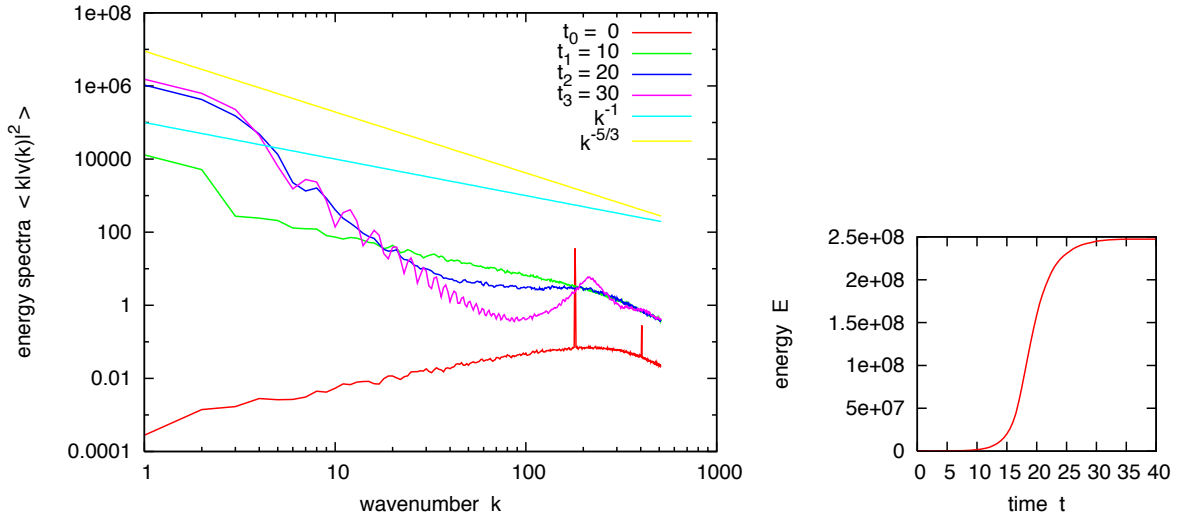


Figure 4.1: (left) Energy spectra $E(k) = \langle k|v(k)|^2 \rangle$ and (right) energy $E = (1/2) \sum_{\alpha\beta} \omega_{\alpha\beta} \psi_{\alpha\beta}$ (α and β are the site coordinates on the torus) at various moments of time. The parameters of the simulation were $\beta\Gamma = 0.04$, $\Gamma = 1.0$, $k_f = 256$, $dt = 5.0 \times 10^{-5}$. There were 256^2 vortices on a grid of 1024×1024 points. The total vorticity was zero.

4.1.1 Cloud-in-cell algorithm

We will investigate the properties of point vortices on a torus. The stream function of the flow, $\psi(\mathbf{r}, t) \equiv \nabla \times \mathbf{v}(\mathbf{r}, t)$, obeys the Poisson equation $\Delta\psi(\mathbf{r}, t) = -\omega(\mathbf{r}, t)$, where $\omega(\mathbf{r}, t) = \sum_{i=1}^N \Gamma_i \delta(\mathbf{r} - \mathbf{r}_i)$, is the vorticity and $\Gamma_i = \pm\Gamma$ is the circulation of each vortex. The point vortices move according to

$$\dot{\mathbf{r}}_i = -\hat{\mathbf{z}} \times \nabla\psi'(\mathbf{r}_i) + \beta\Gamma_i \nabla\psi'_f(\mathbf{r}, t), \quad (4.2)$$

here ψ' is the stream function due to all vortices except the one at \mathbf{r}_i and the last term represents the forcing: β is a scale factor, and ψ'_f is the stream function ψ' , filtered to remove all wavenumbers less than some set threshold value k_f . The reason for this filtering is to fulfill the constraint that the energy transfer from small to large scales is not modified by uniform sweeping. In the absence of forcing, the Eq. (4.2) represents the advection of vortices along instantaneous stream lines. The force represents a small incremental velocity up or down the local stream function depending on the sign of Γ_i . Due to forcing, for $\beta > 0$, same sign vortices slightly attract. If we spread randomly point-vortices on the torus and let them evolve, after some time they will form a dipole, and they tend to remain in this dipole configuration in most

cases for arbitrarily long times.

4.2 Concluding remarks

E. G. Siggia and H. Aref claim that there is a transient state, for which the energy spectra has the same scaling as in the 2D inverse cascade of energy ($\pi\langle k|v_k|^2\rangle \propto k^{-5/3}$). We tried to repeat their results [92] with a wide range of parameters. All we have observed is heating of the system and equilibrium like spectra $E(k) \propto k^{-1}$. Our runs were larger than [92] and do not recover $k^{-5/3}$ scaling. At this point it is unclear, whether $k^{-5/3}$ was not observed, because of the numerical method employed ("cloud-in-the-cell") or two-dimensional turbulence can not be fully modeled with point vortices.

Nevertheless, this inconsistency with [92] poses an intriguing question, as to what extent the point vortex model a suitable model of two-dimensional turbulence. For example we know that such a system is dynamically conformally invariant, while the real two-dimensional turbulence is not (only certain aspects of it have been conjectured to be conformally invariant [17, 81]).

Part III

Non-equilibrium mixing accelerates computations

5. Efficient Sampling with Irreversible Monte Carlo Algorithms

Recent decades have been marked by fruitful interaction between physics and computer science, with one of the most striking examples of such interaction going back to forties when physicists proposed a Markov Chain Monte Carlo (MCMC) algorithm [75, 76]. MCMC evaluates large sums, or integrals, approximately, in a sense imitating how nature would do efficient sampling itself. Development of this idea has become wide spread and proliferated a broad variety of disciplines. (See [55, 64, 65] for a sample set of reviews in physics and computer science.) If one formally follows the letter of the original MCMC suggestion one ought to ensure that the Detailed Balance (DB) condition is satisfied. This condition reflects microscopic reversibility of the underlying equilibrium dynamics. A reader, impressed with indisputable success of the reversible MCMC techniques, may still wonder if the equilibrium dynamics is the most efficient strategy for sampling and evaluating the integrals? In [100] we argue that typically the answer is NO. Let us try to illustrate the ideas on a simple everyday life example. Consider mixing sugar in a cup of coffee, which is similar to sampling, as long as the sugar particles have to explore the entire interior of the cup. DB dynamics corresponds to diffusion taking an enormous mixing time. This is certainly not the best way to mix. Moreover, our everyday experience suggests a better solution – enhance mixing with a spoon. Spoon steering generates an out-of-equilibrium external flow which significantly accelerates mixing, while achieving the same final result – uniform distribution of sugar concentration over the cup. In this letter we show constructively, with a practical algorithm suggested, that a similar strategy can be used to decrease mixing time of known reversible MCMC algorithms.

There are two main obstacles which prevent fast mixing by traditional MCMC methods.

First, the effective energy landscape can have high barriers, separating the energy minima. In this case mixing time is dominated by rare processes of passing the barriers. Second, slow mixing can originate from the high entropy of the states basin (too many comparably important states) providing major contribution to the system partition function. In the later case mixing time is determined by the number of steps it takes for reversible (diffusive) random walk to explore all the relevant states.

MCMC algorithms are best described on discrete example. Consider a graph with vertices $i = 1, \dots, \mathcal{N}$ each labeling a state of the system and edges ($i \rightarrow j$) corresponding to “allowed” transitions between the states. For instance, an N -dimensional hypercube corresponds to a system of N spins (with $\mathcal{N} = 2^N$ states) with single-spin flips allowed. An MCMC algorithm can be described in terms of the transition matrix T_{ij} representing the probability of a single MCMC step from state j to state i . Probability of finding the system in state i at time t , P_i^t , evolves according to the following Master Equation (ME): $P_i^{t+1} = \sum_j T_{ij} P_j^t$. Stationary solution of ME, $P_i^t = \pi_i$, satisfies the Balance Condition (BC):

$$\sum_j (T_{ij}\pi_j - T_{ji}\pi_i) = 0. \quad (5.1)$$

$Q_{ij} = T_{ij}\pi_j$ from the lhs of Eq. (5.1) can be interpreted as the stationary probability flux from state i to state j . Obviously, stationarity of the probability flow reads conditions incoming and outgoing fluxes at any state to sum up to zero. Note also, that Eq. (5.1) is nothing but the incompressibility condition of the stationary probability flow.

The DB used in traditional MCMC algorithms is a more stringent condition, as it requires the piecewise balance of terms in the sum (5.1): for any pair of states with allowed transitions one requires, $T_{ij}\pi_j = T_{ji}\pi_i$. The main reason for DB is so often used in practice originates from its tremendous simplicity. Otherwise, DB-consistent schemes constitute only a small subset of all other MCMC schemes convergent to the same stationary distribution π . From the hydrodynamic point of view reversible MCMC corresponds to irrotational probability flows, while irreversibility relates to nonzero rotational part, e.g. correspondent to vortices contained in the flow. Putting it formally, in the irreversible case antisymmetric part of the ergodic flow matrix is nonzero and it actually allows the following cycle decomposition, $Q_{ij} - Q_{ji} =$

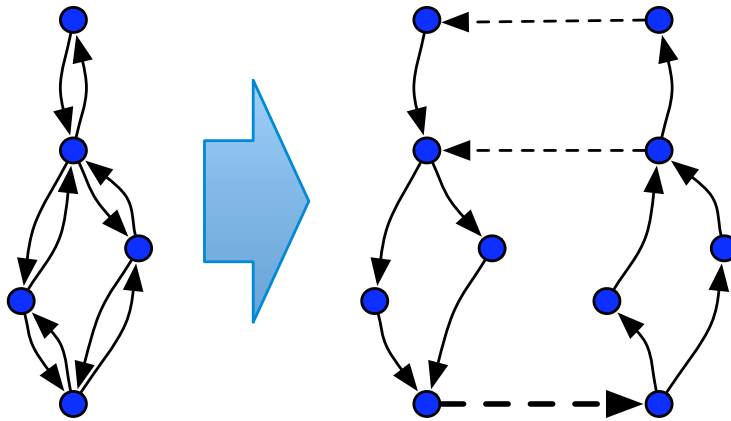


Figure 5.1: Schematic representation of the replication deformation. Dashed lines represent replica switching transitions, which compensate for compressibility of the probability flows associated with solid lines.

$\sum_{\alpha} J_{\alpha}(C_{ij}^{\alpha} - C_{ji}^{\alpha})$, where index α enumerates cycles on the graph of states with the adjacency matrices C_{ij}^{α} . Then, J_{α} stands for the magnitude of the probability flux flowing over cycle α .

5.1 The irreversible MCMC algorithm

Aiming to achieve practical and flexible implementation we focus on building irreversible MCMC algorithms via controlled deformation of an existent reversible MCMC. To be more specific, we adopt and develop replication/lifting trick discussed in [26, 35]. The main idea behind our strategy is as follows. Instead of planting into the system an irreversible probability flux, correspondent to an “incompressible” BC, we add a mixing desirable “compressible” flux, and compensate for its compressibility by building an additional replica with reversed flux and allowing some inter-replica transitions. To enforce BC one tunes the replica switching probabilities computed “on the fly” (and locally). The replication idea is illustrated in Figure 5.1. Acknowledging generality of the setting, we focus here on explaining one relatively simple implementation of this idea. Generalization and modifications of the procedure will be analyzed and discussed elsewhere.

Consider reversible MCMC algorithm characterized by the transition matrix T_{ij} which (a) obeys the DB condition, and (b) converges to the equilibrium distribution π_i . Assume that each state has duplicates in two replicas, marked by \pm . Following some local rule (an

example will be provided below) one introduces a split between states within each of the replicas, $T_{ij} = T_{ij}^{(+)} + T_{ij}^{(-)}$, such that all $T_{ij}^{(\pm)}$ are positive and satisfy, $\forall i \neq j$, $T_{ij}^{(+)}\pi_j = T_{ji}^{(-)}\pi_i$, to be called the skew DB condition. The total transition matrix,

$$\hat{\mathcal{T}} = \begin{pmatrix} \hat{T}^{(+)} & \hat{\Lambda}^{(+,-)} \\ \hat{\Lambda}^{(-,+)} & \hat{T}^{(-)} \end{pmatrix}, \quad (5.2)$$

also contains nonzero and positive (as probabilities) inter-replica terms, $\Lambda_{ii}^{(\pm,\mp)}$, allowing transitions only between two replicas of the same state. One tunes the inter-replica terms to ensure convergence to the given steady distribution, π_i . This is achieved by choosing $\Lambda_{ii}^{(\pm,\mp)} = \max\left\{0, \sum_j T_{ij}^{(\pm)} - T_{ij}^{(\mp)}\right\} \leq 0$, and the diagonal terms $T_{ii}^{(\pm)}$ are fixed according to the stochasticity condition: $T_{ii}^{(\pm)} = 1 - \sum_{j,j \neq i} T_{ji}^{(\pm)} - \Lambda_{ii}^{(\mp,\pm)}$. This description completes our construction of an irreversible MCMC algorithm from a given reversible one. Note that this construction is not unique, and in general multiple choices of $\Lambda_{ii}^{(\pm,\mp)}$ are possible. The proposed scheme is illustrated below on example of a simple spin system, with the Metropolis-Hastings (MH)-Glauber algorithm chosen as the respective reversible prototype.

MH [51] is the most popular reversible MCMC algorithm. MH-transition from a current state i is defined in two steps. (A) A new state j is selected randomly. (B) The proposed state is accepted with probability $p_{acc} = \min(1, \pi_j/\pi_i)$ or rejected with the probability $1 - p_{acc}$ respectively. Selecting the proposed state i.i.d. randomly from all possible single spin flips corresponds to the Glauber dynamics popular in simulations of spin systems. Let us now explain how to build an irreversible MCMC algorithm for spin systems based on the reversible MH-Glauber algorithm. One considers separation in two replicas according to the sign value, $+$ or $-$, of the spin to be flipped. Then, our irreversible MH-Glauber scheme works as follows. Spin α is selected i.i.d. randomly from the pool of all other spins of the system having $+$ or $-$ values, depending on the sign of the replica where the system stays. The selected spin is flipped with the probability $p_{acc} = \min(1, \pi_j/\pi_i)$, in which case the system stays in the same replica. If the flip is not accepted the state is switched to its counterpart of the other replica with probability $\Lambda_{ii}^{(\mp,\pm)}/(1 - \sum_j T_{ji}^{(\pm)})$. (These transitions are indicated as dash lines in Figure 5.1.) Note, that in the case of the Glauber dynamics both $\Lambda_{ii}^{(\mp,\pm)}$ and $\sum_j T_{ji}^{(\pm)}$ are

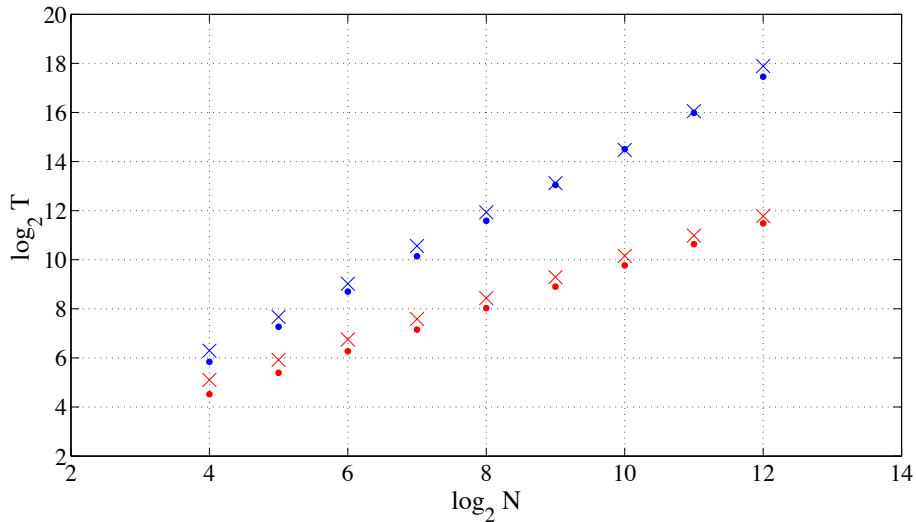


Figure 5.2: Correlation time of the total spin de-correlation in the spin-cluster model. Dots correspond to the direct diagonalization of the transition matrices. Crosses are correlation times found from respective MCMC simulations. Blue and red colors correspond to reversible and irreversible algorithms respectively. Best fitting slopes are given by $T_{rev} \sim N^{1.43}$ and $T_{irr} \sim N^{0.85}$.

local quantities depending only on the current state of the system, and calculating transition probabilities constitutes an insignificant computational overhead.

5.2 Testbed - a ferromagnetic spin-chain

We choose N -spins ferromagnetic cluster (equal strength interaction between all the spins) as a testbed and discuss sampling from respective stationary distribution, $\pi_{s_1 \dots s_N} \sim \exp \left[(-J/2N) \sum_{k,k'} s_k s_{k'} \right]$. Note, that a state of the simple system is completely characterized by its global spin, $S = \sum_k s_k$, and respective probability distribution, $P(S) \sim \frac{N!}{N_+!N_-!} \exp [-JS^2/(2N)]$, where $N_{\pm} = (N \pm S)/2$ is the number of positive/negative spins. Considered in the thermodynamic limit, $N \rightarrow \infty$, the system undergoes a phase transition at $J = 1$. Away from the transition, in the paramagnetic phase $J < 1$, $P(S)$ is centered around $S = 0$ and the width of the distribution is estimated by $\delta S \sim \sqrt{N/J}$, which changes to $\delta S \sim N^{3/4}$ at the critical point $J = 1$. One important consequence of the distribution broadening is a slowdown observed at the critical point for reversible MH-Glauber sampling. Then characteristic correlation time of S (measured in the number of Markov chain steps) is esti-

mated like $T_{rev} \sim (\delta S)^2$, and the computational overhead associated with the critical slowdown is $\sim \sqrt{N}$. We brought this simple model to illustrate the advantage of using irreversibility. As shown below, the irreversible modification of the MH-Glauber algorithm applied to the spin cluster problem achieves complete removal of the critical slowdown. To estimate the correlation time in the irreversible case we first note that, while switching from one replica to another the system will always come through the $S = 0$ state. (This follows directly from the observation that $\Lambda_{ii}^{(+,-)} = 0$ for the states with $S > 0$ and $\Lambda_{ii}^{(-,+)} = 0$ for the states with $S < 0$.) The Markovian nature of the algorithm implies that all the trajectories connecting two consequent $S = 0$ -swipes are statistically independent, and therefore the correlation time is roughly equal to the typical number of steps in each of these trajectories. Recalling that inside a replica (i.e. in between two consecutive swipes) the dynamics of S is strictly monotonous, one estimates $T_{irr} \sim \delta S$. This estimate suggests a significant acceleration: $T_{irr} \sim \sqrt{T_{rev}} \ll T_{rev}$. Note, that one expects to observe significant acceleration even outside of the critical domain, for both larger and smaller values of J .

5.2.1 Results

We verified the correlation time estimation via numerical tests. Implementing reversible and irreversible versions of the MH-Glauber algorithm we, first, analyzed decay of the pair correlation function, $\langle S(0)S(t) \rangle$, with time. Respective correlation time was reconstructed by fitting the large time asymptotics with the exponential function, $\exp(-t/T_{rev})$, and exponential-oscillatory function, $\exp(-t/T_{irr}) \cos(\omega t - \varphi)$, in the reversible and irreversible cases respectively. Second, for both MH and IMH algorithms we constructed transition matrix corresponding to the random walk in S , calculated spectral gap, Δ , related to the correlation time as, $T = 1/\text{Re}\Delta$. In both tests we analyzed critical point $J = 1$ and used different values of N ranging from 16 to 4096. Simulation results are shown in Figure 5.2. The results found for two settings are consistent with each other. Numerical values ($T_{rev} \sim N^{1.43}$ and $T_{irr} \sim N^{0.85}$) are also in a reasonable agreement with respective theoretical predictions ($T_{rev} \sim N^{3/2}$ and $T_{irr} \sim N^{3/4}$) while a slight discrepancy can be attributed to finite size effects. Note, that in the irreversible case correlation time of the global spin correlation function (number of respective MC steps)

grows with the number of spins, N , but does it slower than linearly. In other words, mixing becomes so efficient that equilibration of the global spin correlations is observed even before all spin of the systems are flipped. One concludes, that performance of the irreversible scheme is at least as favourable as the one of the cluster algorithms [98, 109] tested on the spin cluster model [80, 84]. (We note, however, that direct comparison of the two algorithms is not straightforward, as the cluster algorithm flips many spins at once and therefore its convergence is normally stated in renormalized units.)

5.3 Relation of proposed irreversible MCMC to previous studies

Here we would like to discuss relations of the proposed algorithm, irreversible MCMC, to previous studies. Although potential power of algorithms with broken DB has been realized for already a while, only handful of irreversible examples have been proposed so far. One of the examples is the sequential updating algorithm [85] designed to simulate two-dimensional Ising system. In essence, the algorithm consists of a number of subsystems (replicas) with internal dynamics, each characterized by its own transition matrix. In a great contrast with our algorithm, the system switches between replicas in a predefined deterministic fashion. Similar idea of breaking DB by switching irreversibly but periodically between reversible portions was implemented in the successive over-relaxation algorithm of [1]. Another noteworthy sampling algorithm with DB broken is Hybrid Monte Carlo of [53], where Hamiltonian dynamics is used to accelerate sampling. Once again the story here relates to replicas, each parameterized by distinct momentum, with switches between the replicas controlled deterministically by the underlying Hamiltonian. It is also appropriate to cite relevant efforts originated in statistics [35], mathematics [26] and computer science [56]. Several simple examples of irreversible algorithms were discussed and analyzed in [35]. [26] showed that improvement in mixing, provided by a multi-replica lifting, does not allow reduction stronger than the one observed in the diffusive-to-ballistic scenario, $T \rightarrow \sqrt{T}$, where T is the mixing time of the underlying reversible algorithm. The grain of salt here is that the acceleration was achieved via a replication of an extremely high, $\sim k^2$, degree where k is the number of states. [56] showed that complementary distributed network ideas allows to reduce this replication scaling a bit.

We also find it useful to discuss reversible algorithms showing certain similarity to the algorithm and ideas of the Letter. First of all, it is important to mention again cluster algorithms [40, 98, 109] which were most successful in biting the odds of the critical slowdown in the regular systems of the Ising type. The trick here is to explore duality of the model, which allows two alternative representations related to each other via a state-non-local transformation. The cluster algorithm switches between two dual representations, thus realizing long jumps in the phase space. Note that such jumps would be forbidden by phase-space local dynamics in either of the two representations. Best algorithms of the cluster type achieves truly impressive rate of convergence. The downside is in the fact that the cluster algorithms are model specific and rather difficult in implementation because of extreme phase space non-locality of the steps. Worm algorithm of [82] allows essential reduction in the critical slowdown via mapping to a high-temperature-inspired loop representation and making local moves there. The last but not the least, we mention the simulated annealing algorithm of [57] built on a temperature-graded replication consistent with DB. One attractive direction for future research is to explore if (and under which conditions) additional irreversibility can improve already good mixing performance provided within each of these reversible algorithms.

5.4 Conclusions

Here we described how to upgrade a reversible MC into an irreversible MC converging to the same distribution faster. To prove the concept we designed a spin-problem specific irreversible algorithm, and tested it on the mean-field spin-cluster model. We showed on this example that the irreversible modification can lead to dramatic acceleration of MC mixing. Our results suggest that the irreversible MC algorithms are especially beneficial for acceleration of mixing in systems containing multiple soft and zero modes, however inaccessible for standard (reversible) schemes. This situation occurs typically in systems experiencing critical slowdown in the vicinity of a phase transition, and it is also an inherent property of systems possessing internal symmetries of high degree. Entropic degeneracy is the main factor limiting the convergence of regular MCMC algorithm in these problems. To conclude, we are convinced that ideas discussed might be useful in studies of phase transitions, soft matter dynamics, protein

structures and granular media [100].

Bibliography

- [1] Adler, S. L. (1981). An overrelaxation method for the monte carlo evaluation of the partition function for multiquadratic actions. *Phys. Rev. D*, **23**, 2901–2904.
- [2] Balk, A. M. (2001). Anomalous diffusion of a tracer advected by wave turbulence. *Phys. Lett. A*, **279**, 370–378.
- [3] Balk, A. M. (2006). Wave turbulent diffusion due to the doppler shift. *J. Stat. Mech.*, **08**, P08018.
- [4] Balk, A. M., Falkovich, G., and Stepanov, M. G. (2004). Growth of density inhomogeneities in a flow of wave turbulence. *Phys. Rev. Lett.*, **92**, 244504.
- [5] Balkovsky, E., Falkovich, G., Lebedev, V., and Shapiro, I. Y. (1995). Large-scale properties of wave turbulence. *Phys. Rev. E*, **52**, 4537–4540.
- [6] Balkovsky, E., Falkovich, G., and Fouxon, A. (2001). Intermittent distribution of inertial particles in turbulent flows. *Phys. Rev. Lett.*, **86**, 2790–2793.
- [7] Bandi, M. M., Goldberg, W. I., and jr Cressman, G. R. (2006). Measurement of entropy production rate in compressible turbulence. *Europhys. Lett.*, **76**, 595–601.
- [8] Batchelor, G. K. (1959). Small-scale variation of convected quantities like temperature in turbulent fluid part 1. general discussion and the case of small conductivity. *J. Fluid. Mech.*, **5**, 113–133.
- [9] Batchelor, G. K. (2002). *An Introduction to Fluid Dynamics*. Cambridge University, Cambridge.

- [10] Bauer, M. and Bernard, D. (2006). 2d growth processes: Sle and loewner chains. *Phys. Rept.*, **432**, 115–221.
- [11] Bec, J. (2003). Fractal clustering of inertial particles in random flows. *Phys. Fluids.*, **15**, L81.
- [12] Bec, J. (2005). Multifractal concentrations of inertial particles in smooth random flows. *J. Fluid Mech.*, **528**(255–277).
- [13] Bec, J., Gawedzki, K., and Horvai, P. (2004). Multifractal clustering in compressible flows. *Phys. Rev. Lett.*, **92**, 224501.
- [14] Bec, J., Biferale, L., Boffeta, G., Cencini, M., Musacchio, S., and Toschi, F. (2006). Lyapunov exponents of heavy particles in turbulence. *Phys. Fluids*, **18**, 091702.
- [15] Bec, J., Cencini, M., and Hillerbrand, R. (2007). Heavy particles in incompressible flows: the large stokes asymptotics. *Physica D*, **222**, 11–22.
- [16] Benderskii, M. M. and Pastur, L. A. (1970). On the spectrum of the one-dimensional schrödinger equation with a random potential. *Sov. Phys. JETP* 30, 158, **82(124)**(2(6)), 273–184.
- [17] Bernard, D., Boffeta, G., Celani, A., and Falkovich, G. (2006). Conformal invariance in two-dimensional turbulence. *Nature Phys.*, **2**, 124–128.
- [18] Bernard, D., Boffeta, G., Celani, A., and Falkovich, G. (2007). Inverse turbulent cascades and conformally invariant curves. *Phys. Rev. Lett.*, **98**, 024501.
- [19] Boffetta, G., Davoudi, J., Eckhardt, B., and Schumacher, J. (2004). Lagrangian tracers on a surface flow: The role of time correlations. *Phys. Rev. Lett.*, **93**, 134501.
- [20] Boffetta, G., Davoudi, J., and Lillo, F. D. (2006). Multifractal clustering of passive tracers on a surface flow. *Europhys. Lett.*, **74**, 62–68.
- [21] Bowen, R. and Ruelle, D. (1975). The ergodic theory of axiom a flows. *Invent. Math.*, **29**, 181–202.

BIBLIOGRAPHY

- [22] Bracco, A., Chavanis, P. H., and Provenzale, A. (1999). Particle aggregation in turbulent keplerian flow. *Phys. Fluids*, **11**, 2280–2287.
- [23] Cardy, J. (2005). Sle for theoretical physicists. *Annals of Physics*, **81–118**, 318.
- [24] Cardy, J. (2006). Turbulence: The power of two dimensions. *Nature Physics*, **2**, 67–68.
- [25] Chelton, D. B. and Eddy, W. F. (1993). *Statistics and Physical Oceanography*. National Academy Press.
- [26] Chen, F., Lovasz, L., and Pak, I. (1999). Lifting markov chains to speed up mixing. *Proceedings of the ACM symposium on Theory of Computing*, pages 275–281.
- [27] Chen, S. and Kraichnan, R. H. (1998). Simulations of a randomly advected passive scalar field. *Phys. Fluids*, **10**, 2867–2884.
- [28] Christiansen, J. P. (1973). Vortex methods for flow simulation. *J. Comp. Phys.*, **13**, 363–379.
- [29] Constantin, P. and Proccacia, I. (1994). The geometry of turbulent advection: sharp estimates for the dimension of level sets. *Nonlinearity*, **7**, 1045–1054.
- [30] Cressman, J. R. and Goldberg, W. (2003). Compressible flow: Turbulence at the surface. *J. Stat. Phys.*, **113**, 875–883.
- [31] Cressman, J. R., Davoudi, J., Goldberg, W., and Schumacher, J. (2004). Eulerian and lagrangian studies in surface flow turbulence. *New J. Phys.*, **6**, 53.
- [32] Denissenko, P., Falkovich, G., and Lukaschuk, S. (2006). How waves affect the distribution of particles that float on a liquid surface. *Phys. Rev. Lett.*, **97**(244501).
- [33] Derevyanko, S. A., Falkovich, G., Turitsyn, K., and Turitsyn, S. (2007). Explosive growth of inhomogeneities in the distribution of droplets in a turbulent air. *J. Turbul.*, **8**, 1–18.
- [34] Deutsch, J. M. (1985). Aggregation-disorder transition induced by fluctuating random forces. *J. Phys. A*, **18**, 1449–1456.

- [35] Diaconis, P., Holmes, S., and Neal, R. M. (1997). Analysis of a non-reversible markov chain sampler. *Technical Report BU-1385-M*.
- [36] Dominicis, C. D. and Peliti, L. (1978). Field-theory renormalization and critical dynamics above t_c : Helium, antiferromagnets, and liquid-gas system. *Phys. Rev. B*, **18**, 353–376.
- [37] Dorfman, J. (1999). *Introduction to Chaos in Nonequilibrium Statistical Mechanics*. Cambridge University Press.
- [38] Dyachenko, A. I., Korotkevich, A. O., and Zakharov, V. E. (2003). Weak turbulence of gravity waves. *J. Exp. Theor. Phys. Lett.*, **77**, 546–550.
- [39] Eckhardt, B. and Schumacher, J. (2001). Turbulence and passive scalar transport in a free-slip surface. *Phys. Rev. E*, **64**, 016314.
- [40] Edwards, R. and Sokal, A. D. (1988). Generalization of the fortuin-kastelyan-swendsen-wang representation and monte-carlo algorithm. *Phys. Rev. D*, **38**, 2009–2012.
- [41] Falkovich, G. and Fouxon, A. (2003). Entropy production away from the equilibrium. *nlin.CD/ 0312033*.
- [42] Falkovich, G. and Fouxon, A. (2004). Entropy production and extraction in dynamical systems and turbulence. *New J. Phys.*, **6**.
- [43] Falkovich, G. and Martins-Afonso, M. (2007). Fluid-particle separation in a random flow described by the telegraph model. *Phys. Rev. E*, **76**, 026317.
- [44] Falkovich, G. and Shlomo, D. (2005). Evolution of a passive scalar spectrum in the flow of random waves. *Phys. Rev. E*, **71**, 067304.
- [45] Falkovich, G., Gawedzki, K., and Vergassola, M. (2001). Particles and fields in fluid turbulence. *Rev. Mod. Phys.*, **73**, 913–975.
- [46] Falkovich, G., Fouxon, A., and Stepanov, M. (2002). Acceleration of rain initiation by cloud turbulence. *Nature*, **419**, 151–154.

BIBLIOGRAPHY

- [47] Falkovich, G., Musacchio, S., Piterbarg, L., and Vucelja, M. (2007). Inertial particles driven by a telegraph noise. *Phys. Rev. E*, **76**, 026313.
- [48] Fjortoft, R. (1953). On the changes in the spectral distribution of kinetic energy for two-dimensional nondivergent flow. *Tellus*, **5**, 225–230.
- [49] Fouxon, I. and Horvai, P. (2008). Separation of heavy particles in turbulence. *Phys. Rev. Lett.*, **100**, 040601.
- [50] Frisch, H. L. and Lloyd, S. P. (1960). Electron levels in a one-dimensional random lattice. *Phys. Rev.*, **120**, 1175.
- [51] Hastings, W. K. (1970). Monte carlo sampling methods using markov chains and their applications. *Biometrika*, **57**, 97–109.
- [52] Herterich, K. and Hasselmann, K. (1982). The horizontal diffusion of tracers by surface waves. *J. Phys. Oceanogr.*, **12**, 704–11.
- [53] Horvath, I. and Kennedy, A. D. (1998). The local hybrid monte carlo algorithm for free field theory: Rexamining overrelaxation. *Nucl. Phys. B*, **510**, 367–400.
- [54] Hoshen, J. and Kopelman, R. (1976). Percolation and cluster distribution. i. cluster multiple labeling technique and critical concentration algorithm. *Phys. Rev. B*, **14**, 3438.
- [55] Jerrum, M. and Sinclair, A. (1996). *Approximation Algorithms for NP-hard Problems*. PWS Publishing, Boston.
- [56] Jung, K., Shah, D., and Shin, J. (2008). Lifted markov chains for fast linear computations.
- [57] Kirkpatrick, S., Gelatt, C. D., and Vecchi, M. P. (1983). Optimization by simulated annealing. *Science*, **220**, 671–680.
- [58] Kolmogorov, A. N. (1941). Dissipation of energy in locally isotropic turbulence. *Dokl. Akad. Nauk SSSR*, **32**, 16–18. reprinted in Proc. R. Soc. Lond. A 434.
- [59] Kraichnan, R. H. (1967). Inertial ranges in two-dimensional turbulence. *Phys. Fluids*, **10**, 1417–1423.

- [60] Kraichnan, R. H. (1968). Small-scale structure of a scalar field convected by turbulence. *Phys. Fluids*, **11**, 945–953.
- [61] Kraichnan, R. H. (1974). Convection of a passive scalar by a quasi-random straining field. *J. Fluid Mech.*, pages 737–762.
- [62] Kraichnan, R. H. (1975). Statistical dynamics of two-dimensional flow. *J. Fluid. Mech.*, **67**, 155–175.
- [63] Kraichnan, R. H. (1994). Anomalous scalling of a randomly advected passive scalar. *Phys. Rev. Lett.*, **72**, 1016–1019.
- [64] Krauth, W. (2006). *Statistical Mechanics: Algorithms and Computations*. Oxford University Press, Oxford.
- [65] Landau, D. P. and Binder, K. (2000). *A guide to Monte Carlo Simulations in Statistical Physics*. Cambridge University Press, Cambridge.
- [66] Landau, L. D. and Lifshitz, E. M. (1959). *Fluid Mechanics*. Pergamon Books Ltd.
- [67] Lawler, G. (1995). Conformally invariant processes in the plane. *Math. Survey Monogr.*, **114**, 1183.
- [68] Leith, C. E. (1968). Diffusion approximation for two-dimensional turbulence. *Phys. Fluids*, **11**, 671–673.
- [69] Longuet-Higgins, M. S. (1963). The effect of non-linearities on statistical distributions in the theory of sea waves. *J. Fluid Mech.*, **17**, 459–480.
- [70] Lvov, V. S., Lvov, Y., Newell, A. C., and Zakharov, V. (1997). Statistical description of acoustic turbulence. *Phys. Rev. E*, **56**, 390–405.
- [71] Martin, P. C., Siggia, E., and Rose, H. A. (1973). Statistical dynamics of classical systems. *Phys. Rev. A*, **8**, 423–437.
- [72] Maxey, M. R. (1987). The gravitational settling of aerosol particles in homogeneous turbulence and random flow fields. *J Fluid Mech.*, **174**, 441–465.

BIBLIOGRAPHY

- [73] Mehlig, B. and Wilkinson, M. (2004). Coagulation by random velocity fields as a kramers problem. *Phys. Rev. Lett.*, **92**, 250602.
- [74] Mehlig, B., Wilkinson, M., Duncan, K., Weber, T., and Ljunggren, M. (2005). Aggregation of inertial particles in random flows. *Phys. Rev. E*, **72**, 051104.
- [75] Metropolis, N. and Ulam, S. (1949). The monte carlo method. *J. Am. Stat. Assoc.*, **44**, 335–341.
- [76] Metropolis, N., Rosenbluth, A., Rosenbluth, M., Teller, A., and Teller, E. (1953). Equations of state calculations by fast computing machines. *J. of Chem. Phys.*, **21**, 1087–1092.
- [77] Nameson, A., Antonsen, T., and Ott, E. (1996). Power law wave number spectra of fractal particle distributions advected by flowing fluids. *Phys. Fluids*, **8**, 2426–2434.
- [78] Ott, E. (2002). *Chaos in Dynamical Systems*. Cambridge University Press, Cambridge.
- [79] Pedlosky, J. (1987). *Geophysical fluid dynamics*. Springer, New York.
- [80] Persky, N., Ben-Av, R., Kanter, I., and Domany, E. (1996). Mean-field behavior of cluster dynamics. *Phys. Rev. E*, **54**, 2351–2358.
- [81] Polyakov, A. M. (1996). The theory of turbulence of 2d. *Nucl. Phys.*, **396**, 367–387.
- [82] Prokof'ev, N. and Svistunov, B. (2001). Worm algorithms for classical statistical models. *Proceedings of the ACM symposium on Theory of Computing*, **87**, 160601.
- [83] R. Ramshankar, D. B. and Gollub, J. (1990). Transport by capillary waves. part i. particle trajectories. *Phys. Fluids A*, **2**, 1955–1965.
- [84] Ray, T. S., Tamao, P., and Klein, W. (1999). Mean-field study of the swendsen-wang dynamics. *Phys. Rev. A*, **39**, 5949–5953.
- [85] Ren, R. and Orkoulas, G. (2006). Acceleration of markov chain monte carlo simulations through sequential updating. *J. Chem. Phys.*, **124**, 064109.
- [86] Ruelle, D. (1996). Positivity of entropy production in nonequilibrium statistical mechanics. *J. Stat. Phys.*, **85**, 1–23.

- [87] Ruelle, D. (1997). Positivity of entropy production in the presence of a random thermostat. *J. Stat. Phys.*, **86**, 935–990.
- [88] Ruelle, D. (1999). Smooth dynamics and new theoretical ideas in nonequilibrium statistical mechanics. *J. Stat. Phys.*, **95**, 393–468.
- [89] Schroder, E., Andersen, J., Levinsen, M., Alstrom, P., and Goldberg, W. (1996). Relative particle motion in capillary waves. *Phys. Rev. Lett.*, **76**, 4717.
- [90] Shapiro, V. E. and Loginov, V. M. (1978). “formulae of differentiation” and their use for solving stochastic equations. *Physica*, **91A**, 563–574.
- [91] Shraiman, B. and Siggia, E. D. (2000). Scalar turbulence. *Nature*, **405**, 639–646.
- [92] Siggia, E. D. and Aref, H. (1981). Point-vortex simulation of the inverse energy cascade in two-dimensional turbulence. *Phys. Fluids*, **24**, 171–173.
- [93] Sinai, Y. G. (1972). Gibbs measures in ergodic theory. *Russian Math. Surveys*, **27**, 21–69.
- [94] Sommerer, J. C. (1996a). Experimental evidence for power-law wave number spectra of fractal tracer distributions in a complicated surface flow. *Phys. Fluids*, **8**, 2441–2446.
- [95] Sommerer, J. C. (1996b). Experimental evidence for power-law wave number spectra of fractal tracer distributions in a complicated surface flow. *Phys. Fluids*, **8**, 2441–2446.
- [96] Sommerer, J. C. and Ott, E. (1993). Particles floating on a moving fluid: A dynamically comprehensible physical fractal. *Science*, **259**, 335–339.
- [97] Sreenivasan, K. R. (1991). On local isotropy of passive scalars in turbulent shear flows. *Proc. R. Soc. Lond. A*, **434**, 165–182.
- [98] Swendsen, R. H. and Wang, J.-S. (1987). Nonuniversal critical dynamics in monte carlo simulations. *Phys. Rev. Lett.*, **58**, 86–88.
- [99] Thorpe, S. A. (2005). *The Turbulent Ocean*. Cambridge Univ. Press.
- [100] Turitsyn, K. S., Chertkov, M., and Vucelja, M. (2008). Irreversible monte carlo algorithms for efficient sampling. accepted in *Physica D*, arXiv:0809.0916v2.

BIBLIOGRAPHY

- [101] Umeki, M. (1992). Lagrangian motion of fluid particles induced by three-dimensional standing surface waves. *Phys. Fluids A*, **4**, 1968–1978.
- [102] Vergeles, S. S. (2006). Spatial dependence of correlation functions in the decay problem for a passive scalar in a large-scale velocity field. *J. Exp. Theor. Phys.*, **102**, 685–701.
- [103] Vucelja, M. and Fouxon, I. (2007). Weak compressibility of surface wave turbulence. *J. Fluid Mech.*, **593**, 281–296.
- [104] Vucelja, M., Falkovich, G., and Fouxon, I. (2007). Clustering of matter in waves and currents. *Phys. Rev. E*, **75**, 065301(R).
- [105] Vucelja, M., Turitsyn, K. S., and Falkovich, G. (2008). Passive scalar contours. *in preparation*.
- [106] Vucelja, M., Falkovich, G., and Shafarenko, A. (2010). Energy cascade of point vortices. unpublished.
- [107] Weichman, P. B. and Glazman, R. E. (420). Passive scalar transport by traveling wave fields. *J. Fluid Mech.*, pages 147–200.
- [108] Wilkinson, M. and Mehlig, B. (2003). Path coalescence transition and its applications. *Phys. Rev. E*, **68**, 040101(R).
- [109] Wolff, U. (1989). Lifting markov chains to speed up mixing. *Phys. Rev. Lett.*, **62**, 361–365.
- [110] Wyld, H. W. (1961). Formulation of the theory of turbulence in an incompressible fluid. *Ann. Phys.*, **14**, 143–165.
- [111] Yu, L., Ott, E., and Chen, Q. (1991). Fractal distribution of floaters on a fluid surface and the transition to chaos for random maps. *Physica D*, **53**, 102–124.
- [112] Zakharov, V. E. (1966). *Waves in nonlinear dispersive mediums*. Ph.D. thesis, *in Russian*, Institute for Nuclear Physics (Physics and Mathematics), Novosibirsk.
- [113] Zakharov, V. E. (1968). Stability of periodic waves of finite amplitude on the surface of a deep fluid (note a sign misprint in (1.8)). *J. Appl. Mech. Tech. Phys.*, **9**, 190–194.

- [114] Zakharov, V. E., L'vov, V., and Falkovich, G. (1992). *Kolmogorov spectra of turbulence*. Springer-Verlag, Berlin.

List of Publications

Bellow is the list of publications derived from the doctoral research.

- [6] M. Vucelja, G. Falkovich, A. Shafarenko,
Energy cascade of point vortices, unpublished (2008).
- [5] M. Vucelja, G. Falkovich, K. S. Turitsyn,
Passive scalar contours, in preparation.
- [4] K. S. Turitsyn, M. Chertkov and M. Vucelja,
Irreversible Monte Carlo Algorithms for Efficient Sampling, cond-mat/0809.0916, in press
in Physica D.
- [3] M. Vucelja and I. Fouxon,
Weak compressibility of surface wave turbulence, J. Fluid Mech., **593**, 281–296 (2007).
- [2] G. Falkovich, S. Musacchio, L. Piterbarg and M. Vucelja,
Inertial particles driven by telegraph noise, Phys. Rev. E, **76**, 026313 (2007).
- [1] M. Vucelja, G. Falkovich and I. Fouxon,
Clustering of matter in waves and currents, Phys. Rev. E, **75**, 065301(R) (2007).

Statement about independent collaboration

I declare that the thesis summarizes my independent research. A portion of the research was performed in collaboration with another investigators. I was the principal contributor in [103–106]. In the other two papers, [47, 100], the order of authors families is according to the contribution to the paper.

Appendix

A Derivation of the Green-Kubo formula for the clustering rate λ

The sum of Lyapunov exponents $(-\lambda)$ is expressible with the help of a time integral of the pair-correlation function of velocity divergence [41, 42]. So far it is the only combination of Lyapunov exponents known, to have such a short and operational expression. It is this expression, given in Eq. (1.2), that we used to derive our conclusions in [103, 104]. Hence let us sketch the proof of passing to Eq. (1.2) starting from the definition of the sum of Lyapunov exponents, Eq. (1.1). The original proof can be found in [41]. It should be noted that Eq. (1.2) is valid for statistically stationary velocity fields, however here we will discuss the case of a time independent velocity field, since the generalization to the statistically stationary case is rather straightforward.

Let us consider a smooth dynamical system defined by a steady velocity field $\mathbf{v}(\mathbf{x}) = d\mathbf{x}/dt$, where \mathbf{x} is the coordinate of the system. The velocity field defines the flow $\mathbf{X}(t, \mathbf{x})$ in space

$$\frac{\partial \mathbf{X}}{\partial t}(t, \mathbf{x}) = \mathbf{v}[\mathbf{X}(t, \mathbf{x})], \quad \text{where} \quad \mathbf{X}(0, \mathbf{x}) = \mathbf{x}, \quad (\text{A.1})$$

and an significant relation holds between them: $\mathbf{v}[\mathbf{X}(t, \mathbf{x})] = \hat{W}(t, \mathbf{x})\mathbf{v}(\mathbf{x})$, where $W_{ij}(t, \mathbf{x}) \equiv \partial X_i(t, \mathbf{x})/\partial x_j$. This relation allows, in particular, to describe the evolution of an arbitrary differentiable function $f[\mathbf{X}(t, \mathbf{x})]$ defined along a trajectory, namely

$$\frac{df}{dt} = (\mathbf{v}(\mathbf{x}) \cdot \nabla_{\mathbf{x}})f[\mathbf{X}(t, \mathbf{x})] = -w(\mathbf{x})f[\mathbf{X}(t, \mathbf{x})] + \nabla_{\mathbf{x}} \cdot [\mathbf{v}(\mathbf{x})f[\mathbf{X}(t, \mathbf{x})]]. \quad (\text{A.2})$$

We integrate this identity over space

$$\frac{d}{dt} \int \frac{d\mathbf{x}}{V} f[\mathbf{X}(t, \mathbf{x})] = - \int \frac{d\mathbf{x}}{V} w(\mathbf{x}) f[\mathbf{X}(t, \mathbf{x})] \equiv - \langle w(0) f(t) \rangle, \quad (\text{A.3})$$

$$\int \frac{d\mathbf{x}}{V} f(\mathbf{x}) - \int \frac{d\mathbf{x}}{V} f[\mathbf{X}(t, \mathbf{x})] = \int_0^t \langle w(0) f(t') \rangle dt'. \quad (\text{A.4})$$

Here we assume that the space integral of the last term in Eq. (A.2) vanishes because it can be written as an integral over the boundary. This is true in the periodic case or in the case where the normal component of velocity vanishes (it might be interesting to consider the cases where boundary is important as well). We shall see below that our main equality Eq. (1.2) is a particular case of Eq. (A.3). Integrating Eq. (A.4) over time we have

$$\int \frac{d\mathbf{x}}{V} f(\mathbf{x}) - \frac{1}{t} \int_0^t dt' \int \frac{d\mathbf{x}}{V} f[\mathbf{X}(t', \mathbf{x})] = \int_0^t \langle w(0) f(t') \rangle dt' - \frac{1}{t} \int_0^t t' \langle w(0) f(t') \rangle dt'. \quad (\text{A.5})$$

Next we consider what may happen with Eqs. (A.4) and (A.5), when $t \rightarrow \infty$. From Eq. (A.4) we observe that provided $\int_0^\infty \langle w(0) f(t) \rangle dt$ exists there must also exist a finite limit of the spatial average

$$\lim_{t \rightarrow \infty} \int \frac{d\mathbf{x}}{V} f[\mathbf{X}(t, \mathbf{x})] = \int \frac{d\mathbf{x}}{V} f(\mathbf{x}) - \int_0^\infty \langle w(0) f(t) \rangle dt. \quad (\text{A.6})$$

If we choose as the initial state of the continuity equation, a constant $n_0(\mathbf{x}) \equiv n(t=0, \mathbf{x}) = 1/V$, then Eq. (A.6) can be rewritten as

$$\lim_{t \rightarrow \infty} \int \frac{d\mathbf{x}}{V} f(\mathbf{x}) n(t, \mathbf{x}) = \int \frac{d\mathbf{x}}{V} f(\mathbf{x}) - \int_0^\infty \langle w(0) f(t) \rangle dt, \quad (\text{A.7})$$

which suggests that the finiteness of temporal correlations, i.e. the existence of the integrals $\int_0^\infty \langle w(0) f(t) \rangle dt$ for continuous f is equivalent to the existence of the limiting non-equilibrium state characterized by the probability measure $\mu_{\text{lim}} = \lim_{t \rightarrow \infty} n(\mathbf{x}, t)$. The difference of the non-equilibrium state measure μ_{lim} and equilibrium measure E satisfies

$$\mu_{\text{lim}}(f) - E(f) = - \int_0^\infty \langle w(0) f(t) \rangle dt, \quad \mu_{\text{lim}}(f) = \int f d\mu_{\text{lim}}, \quad E(f) \equiv \int \frac{d\mathbf{x}}{V} f(\mathbf{x}). \quad (\text{A.8})$$

As for the Eq. (A.5), it involves a weaker limit $\mu_{\text{av}} = \lim_{t \rightarrow \infty} t^{-1} \int_0^t n(\mathbf{x}, t') dt'$ (for details see [88]). The existence of this limit is equivalent to the convergence of the subtracted correlation integral

$$\mu_{\text{av}}(f) - E(f) = - \lim_{t \rightarrow \infty} \left[\int_0^t \langle w(0)f(t') \rangle dt' - \frac{1}{t} \int_0^t t' \langle w(0)f(t') \rangle dt' \right]. \quad (\text{A.9})$$

Thus we have $\mu_{\text{av}}(f) = \mu_{\text{lim}}(f)$, provided that $\int_0^\infty \langle w(0)f(t) \rangle dt$ exists.

A limit of the type used in μ_{av} appears when one considers the sum of Lyapunov exponents $\sum_{i=1}^d \lambda_i(\mathbf{x})$. That sum determines the growth rate of an infinitesimal volume initially located at \mathbf{x} . From Eq. (1.1) we observe that $\sum_{i=1}^d \lambda_i$ is represented as a time-average of a function on the phase space. This is a unique combination of Lyapunov exponents that is representable in such a form. Using Eq.(A.5) we have

$$\begin{aligned} \int \frac{d\mathbf{x}}{V} \sum_{i=1}^d \lambda_i(\mathbf{x}) &= - \lim_{t \rightarrow \infty} \left[\int_0^t \langle w(0)w(t') \rangle dt' - \frac{1}{t} \int_0^t t' \langle w(0)w(t') \rangle dt' \right] \\ &= - \int_0^\infty \langle w(0)w(t) \rangle dt, \end{aligned} \quad (\text{A.10})$$

where the last equality holds provided the integral exists. We used $E(w) = 0$ assuming that the integral over the boundary vanishes. The above formula holds for systems whose stationary measure is arbitrarily far from the equilibrium measure and nevertheless it has a remarkable resemblance to the Green-Kubo formula holding near equilibrium. It also suggests that $\int d\mathbf{x} \sum_{i=1}^d \lambda_i \leq 0$ always. Here we note that $\int d\mathbf{x} \sum_{i=1}^d \lambda_i < 0$ signifies that μ is singular. Therefore, the criteria of singularity of the non-equilibrium measure is $\int_0^\infty \langle w(0)w(t) \rangle dt > 0$.

The above relations are simplified for systems satisfying the SRB theorem that guarantees the equality between temporal average and average with respect to the limiting measure for any continuous function f , [21, 93]. For SRB-theorem systems $\sum_{i=1}^d \lambda_i(\mathbf{x})$ is constant almost everywhere, thus for such systems using Eq. (A.10) we obtain Eq. (1.2).

B Note on the Gaussianity of weak wave turbulence

It is commonly assumed and somewhat backed up empirically that the statistics of the weak wave turbulence at wavenumbers much greater than the pumping is close to Gaussian, for wide classes of pumping statistics. On the other hand when the forcing itself is Gaussian, the statistics of wave amplitudes will remain close to Gaussian as long as the nonlinearity is weak. It is an open problem in wave turbulence to find the precise conditions which guarantee the wave field is a Gaussian field. One starts by solving the linear equation for waves in the spectral interval of pumping and formulate the criteria on the forcing that guarantee that the cumulants remain small. For more information see e.g. [25, 69, 114] and the references within.

C The diagrammatic technique

Here we provide the diagrammatic technique derivations of the clustering rate of matter λ (given by Eq. (1.1)) by weakly-interacting waves. This technique was introduced by H.W. Wyld in the turbulence community [110] and in condensed matter it is known as the Martin-Siggia-Rose formalism [71]. Bellow we immediately proceed with calculations, since the problem and main definitions have been already introduced in Chapter 1.

It is more convenient to switch from the velocity potential at the surface ψ and elevation η to another pair of canonically conjugate coordinates, which we label a and a^* . In order to do this, let us first derive the dispersion law of small amplitude waves in deep fluids. Retaining only the linear terms in the equations of motion we have

$$\frac{\partial \eta}{\partial t} = \left. \frac{\partial \phi}{\partial z} \right|_{z=0}, \quad (\text{C.1})$$

$$\frac{\partial \psi}{\partial t} + g\eta - \alpha \nabla^2 \eta = 0, \quad (\text{C.2})$$

here we take $\partial \phi / \partial z|_{z=0}$, we get $\Omega(\mathbf{k}) = \sqrt{g|k| + \alpha|k|^3}$. Now we can introduce a and a^* as follows

$$a(\mathbf{k}, t) = \sqrt{\frac{\Omega(k)}{2|k|}} \eta(\mathbf{k}, t) + i \sqrt{\frac{|k|}{2\Omega(k)}} \psi(\mathbf{k}, t), \quad (\text{C.3})$$

then from the fact that $\eta(\mathbf{r}, t)$ and $\psi(\mathbf{r}, t)$ are real we get

$$\begin{aligned} a(\mathbf{k}, t) &= \sqrt{\frac{\Omega(k)}{2|k|}} \eta(\mathbf{k}, t) + i \sqrt{\frac{|k|}{2\Omega(k)}} \psi(\mathbf{k}, t), \\ a^*(-\mathbf{k}, t) &= \sqrt{\frac{\Omega(k)}{2|k|}} \eta(\mathbf{k}, t) - i \sqrt{\frac{|k|}{2\Omega(k)}} \psi(\mathbf{k}, t), \\ \eta(\mathbf{k}, t) &= B_k [a(\mathbf{k}, t) + a^*(-\mathbf{k}, t)], \quad B_k \equiv \sqrt{\frac{|k|}{2\Omega(k)}}, \end{aligned} \quad (\text{C.4})$$

$$\psi(\mathbf{k}, t) = A_k [a(\mathbf{k}, t) - a^*(-\mathbf{k}, t)], \quad A_k \equiv -i \sqrt{\frac{\Omega(k)}{2|k|}}. \quad (\text{C.5})$$

Let us express the sum of Lyapunov exponents via a and a^* , for this we calculate several

of auxiliary correlation functions. Bellow in (C.10-C.18) the subscript indices refer to q for variables ψ , η , a and H , F , J and K which we introduced as follows

$$\langle a_1 a_2 \rangle \equiv (2\pi)^{d+1} \delta(q_1 + q_2) H_1 \quad (\text{C.6})$$

$$\langle a_1^* a_2 \rangle \equiv (2\pi)^{d+1} \delta(q_1 - q_2) F_1 \quad (\text{C.7})$$

$$\langle a_1 a_2 a_3 \rangle \equiv (2\pi)^{d+1} \delta(q_1 + q_2 + q_3) J_{123} \quad (\text{C.8})$$

$$\langle a_1^* a_2 a_3 \rangle \equiv (2\pi)^{d+1} \delta(q_1 - q_2 - q_3) K_{123} \quad (\text{C.9})$$

Note that $F_q = F_q^*$ and $H_q = H_{-q}$ by definition. The auxiliary correlation functions are

$$\begin{aligned} \langle \psi_1 \psi_2 \rangle &= A_1 A_2 \langle (a_1 - a_{-1}^*) (a_2 - a_{-2}^*) \rangle = A_1 A_2 \langle a_1 a_2 - a_{-1}^* a_2 - a_1 a_{-2}^* + a_{-1}^* a_{-2}^* \rangle = \\ &= (2\pi)^{d+1} \delta_{q_1+2} A_1 A_{-1} (H_1 + H_{-1}^* - F_1 - F_{-1}) \\ &= (2\pi)^{d+1} \delta_{q_1+2} A_1 A_{-1} (2\text{Re}(H_1) - F_1 - F_{-1}), \end{aligned} \quad (\text{C.10})$$

$$\begin{aligned} \langle \psi_1 \eta_2 \psi_3 \rangle &= A_1 B_2 A_3 \langle (a_1 - a_{-1}^*) (a_2 + a_{-2}^*) (a_3 - a_{-3}^*) \rangle = \\ &= A_1 B_2 A_3 (\langle a_1 a_2 a_3 \rangle + \langle a_{-1}^* a_{-2}^* a_{-3}^* \rangle - \langle a_{-1}^* a_2 a_3 \rangle - \langle a_1 a_{-2}^* a_{-3}^* \rangle + \\ &+ \langle a_1 a_{-2}^* a_3 \rangle + \langle a_{-1}^* a_2 a_{-3}^* \rangle - \langle a_1 a_2 a_{-3}^* \rangle - \langle a_{-1}^* a_{-2}^* a_3 \rangle) = \\ &= A_1 B_2 A_3 (2\pi)^{d+1} \delta_{q_1+2+3} \times \\ &\times (J_{123} + J_{-1-2-3}^* - K_{-123} - K_{1-2-3}^* + K_{1-23} + K_{-12-3}^* - K_{12-3} - K_{-1-23}^*), \end{aligned} \quad (\text{C.11})$$

$$\begin{aligned} \langle \psi_1 \psi_2 \psi_3 \rangle &= A_1 A_2 A_3 \langle (a_1 - a_{-1}^*) (a_2 - a_{-2}^*) (a_3 - a_{-3}^*) \rangle = \\ &= A_1 A_2 A_3 (\langle a_1 a_2 a_3 \rangle - \langle a_{-1}^* a_{-2}^* a_{-3}^* \rangle - \langle a_{-1}^* a_2 a_3 \rangle + \langle a_1 a_{-2}^* a_{-3}^* \rangle \\ &- \langle a_1 a_{-2}^* a_3 \rangle + \langle a_{-1}^* a_2 a_{-3}^* \rangle - \langle a_1 a_2 a_{-3}^* \rangle + \langle a_{-1}^* a_{-2}^* a_3 \rangle) \\ &= A_1 A_2 A_3 (2\pi)^{d+1} \delta_{q_1+2+3} \times \\ &\times (J_{123} - J_{-1-2-3}^* - K_{-123} + K_{1-2-3}^* - K_{1-23} + K_{-12-3}^* - K_{12-3} + K_{-1-23}^*), \end{aligned} \quad (\text{C.12})$$

$$\langle \psi_1 \eta_2 \psi_3 \eta_4 \rangle = A_1 B_2 A_3 B_4 \langle (a_1 - a_{-1}^*)(a_2 + a_{-2}^*)(a_3 - a_{-3}^*)(a_4 + a_{-4}^*) \rangle = \quad (C.13)$$

$$\begin{aligned} &= A_1 B_2 A_3 B_4 (-\langle a_{-1}^* a_{-2}^* a_3 a_4 \rangle + \langle a_{-1}^* a_2 a_{-3}^* a_4 \rangle - \\ &- \langle a_1 a_{-2}^* a_{-3}^* a_4 \rangle - \langle a_{-1}^* a_2 a_3 a_{-4}^* \rangle + \langle a_1 a_{-2}^* a_3 a_{-4}^* \rangle - \langle a_1 a_2 a_{-3}^* a_{-4}^* \rangle) = \\ &= (2\pi)^{2d+2} A_1 B_2 A_3 B_4 [-(F_1 F_2 + F_{-1} F_{-2})(\delta q_{1+3} \delta q_{2+4} + \delta q_{1+4} \delta q_{2+3}) \\ &+ (F_{-1} F_{-3} + F_1 F_3)(\delta q_{1+2} \delta q_{3+4} + \delta q_{1+4} \delta q_{2+3}) - (F_{-1} F_{-4} + F_1 F_4)(\delta q_{1+2} \delta q_{3+4} + \delta q_{1+3} \delta q_{2+4})], \end{aligned} \quad (C.14)$$

$$\langle \psi_1 \eta_2 \psi_3 \psi_4 \rangle = A_1 B_2 A_3 A_4 \langle (a_1 - a_{-1}^*)(a_2 + a_{-2}^*)(a_3 - a_{-3}^*)(a_4 - a_{-4}^*) \rangle =$$

$$\begin{aligned} &= A_1 B_2 A_3 A_4 (-\langle a_{-1}^* a_{-2}^* a_3 a_4 \rangle + \langle a_{-1}^* a_2 a_{-3}^* a_4 \rangle - \langle a_1 a_{-2}^* a_{-3}^* a_4 \rangle \\ &+ \langle a_{-1}^* a_2 a_3 a_{-4}^* \rangle - \langle a_1 a_{-2}^* a_3 a_{-4}^* \rangle + \langle a_1 a_2 a_{-3}^* a_{-4}^* \rangle) \\ &= (2\pi)^{2d+2} A_1 B_2 A_3 A_4 [(F_1 F_2 - F_{-1} F_{-2})(\delta q_{1+3} \delta q_{2+4} + \delta q_{1+4} \delta q_{2+3}) \\ &+ (F_{-1} F_{-3} - F_1 F_3)(\delta q_{1+2} \delta q_{3+4} + \delta q_{1+4} \delta q_{2+3}) + (F_{-1} F_{-4} - F_1 F_4)(\delta q_{1+2} \delta q_{3+4} + \delta q_{1+3} \delta q_{2+4})], \end{aligned} \quad (C.15)$$

$$\langle \psi_1 \psi_2 \eta_3 \psi_4 \rangle = (2\pi)^{2d+2} A_1 A_2 B_3 A_4 [(F_1 F_3 - F_{-1} F_{-3})(\delta q_{1+2} \delta q_{3+4} + \delta q_{1+4} \delta q_{2+3}) \quad (C.16)$$

$$+ (F_{-1} F_{-2} - F_1 F_2)(\delta q_{1+3} \delta q_{2+4} + \delta q_{1+4} \delta q_{2+3}) + (F_{-1} F_{-4} - F_1 F_4)(\delta q_{1+3} \delta q_{2+4} + \delta q_{1+2} \delta q_{3+4})],$$

$$\langle \psi_1 \psi_2 \psi_3 \eta_4 \rangle = (2\pi)^{2d+2} A_1 A_2 A_3 B_4 [(F_1 F_4 - F_{-1} F_{-4})(\delta q_{1+3} \delta q_{2+4} + \delta q_{1+2} \delta q_{3+4}) \quad (C.17)$$

$$+ (F_{-1} F_{-3} - F_1 F_3)(\delta q_{1+4} \delta q_{2+3} + \delta q_{1+2} \delta q_{3+4}) + (F_{-1} F_{-2} - F_1 F_2)(\delta q_{1+4} \delta q_{2+3} + \delta q_{1+3} \delta q_{2+4})],$$

$$\langle \psi_1 \psi_2 \psi_3 \psi_4 \rangle = A_1 A_2 A_3 A_4 \langle (a_1 - a_{-1}^*)(a_2 - a_{-2}^*)(a_3 - a_{-3}^*)(a_4 - a_{-4}^*) \rangle =$$

$$\begin{aligned} &= A_1 A_2 A_3 A_4 (\langle a_{-1}^* a_{-2}^* a_3 a_4 \rangle + \langle a_{-1}^* a_2 a_{-3}^* a_4 \rangle + \langle a_1 a_{-2}^* a_{-3}^* a_4 \rangle \\ &+ \langle a_{-1}^* a_2 a_3 a_{-4}^* \rangle + \langle a_1 a_{-2}^* a_3 a_{-4}^* \rangle + \langle a_1 a_2 a_{-3}^* a_{-4}^* \rangle) \\ &= (2\pi)^{2d+2} A_1 A_2 A_3 A_4 [(F_1 F_2 + F_{-1} F_{-2})(\delta q_{1+3} \delta q_{2+4} + \delta q_{1+4} \delta q_{2+3}) \\ &+ (F_{-1} F_{-3} + F_1 F_3)(\delta q_{1+2} \delta q_{3+4} + \delta q_{1+4} \delta q_{2+3}) + (F_{-1} F_{-4} + F_1 F_4)(\delta q_{1+2} \delta q_{3+4} + \delta q_{1+3} \delta q_{2+4})]. \end{aligned} \quad (C.18)$$

Notice that we substituted the correlation function of four a fields with correlation functions

of pairs of a fields (Wick's theorem). This substitution is justified, since we need the these correlation functions in their lowest order. Likewise, we kept only the F correlation functions, i.e. only correlation function of $\langle a_i^* a_j^* a_k a_l \rangle$ type. This follows from $F_q \gg H_q$ in the zeroth order, which will be shown in subsection C.4.

Using (C.10-C.18) we express λ from (1.3) as a function of a and a^*

$$\begin{aligned}
\lambda &\simeq \int \frac{d\mathbf{k}_1}{(2\pi)^d} k_1^4 A_1 A_{-1} [\text{Re}(H(\mathbf{k}_1, 0)) - F(\mathbf{k}_1, 0)] \\
&- \int \frac{dq_{123}}{(2\pi)^{3d+3}} (2\pi)^{d+1} \delta q_{1+2+3} \left[|k_1| k_3^2 (\mathbf{k}_1 \cdot \mathbf{k}_2 + k_2^2) (2\pi) \delta(\omega_3) A_1 B_2 A_3 \times \right. \\
&\times (J_{123} + J_{-1-2-3}^* - K_{-123} - K_{1-2-3}^* + K_{1-23} + K_{-12-3}^* - K_{12-3} - K_{-1-23}^*) \\
&+ k_1^2 k_2^2 (\mathbf{k}_2 \cdot \mathbf{k}_3) \left(\frac{i\pi}{\omega_3} (\delta(\omega_1) - \delta(\omega_2)) + \frac{1}{\omega_1 \omega_2} \right) A_1 A_2 A_3 \times \\
&\left. \times (J_{123} - J_{-1-2-3}^* - K_{-123} + K_{1-2-3}^* - K_{1-23} + K_{-12-3}^* - K_{12-3} + K_{-1-23}^*) \right] \\
&+ \lim_{t \rightarrow \infty} \int \frac{dq_{1234}}{(2\pi)^{4d+4}} (2\pi)^{2d+2} \times \\
&\times \left\{ \frac{|k_1|}{2} (\mathbf{k}_1 \cdot \mathbf{k}_2 + k_2^2) |k_3| (\mathbf{k}_3 \cdot \mathbf{k}_4 + k_4^2) (2\pi) \delta(\omega_3 + \omega_4) \times \right. \\
&\times A_1 B_2 A_3 B_4 [- (F_1 F_2 + F_{-1} F_{-2}) (\delta q_{1+3} \delta q_{2+4} + \delta q_{1+4} \delta q_{2+3}) \\
&+ (F_{-1} F_{-3} + F_1 F_3) (\delta q_{1+2} \delta q_{3+4} + \delta q_{1+4} \delta q_{2+3}) - (F_{-1} F_{-4} + F_1 F_4) (\delta q_{1+2} \delta q_{3+4} + \delta q_{1+3} \delta q_{2+4})] \\
&+ |k_1| (\mathbf{k}_1 \cdot \mathbf{k}_2 + k_2^2) k_3^2 (\mathbf{k}_3 \cdot \mathbf{k}_4) \left[- \frac{e^{-i(\omega_3 + \omega_4)t} - 1}{(\omega_3 + \omega_4)\omega_4} + \frac{e^{-i\omega_3 t} - 1}{\omega_3 \omega_4} \right] \times \\
&\times A_1 B_2 A_3 A_4 [(F_1 F_2 - F_{-1} F_{-2}) (\delta q_{1+3} \delta q_{2+4} + \delta q_{1+4} \delta q_{2+3}) \\
&+ (F_{-1} F_{-3} - F_1 F_3) (\delta q_{1+2} \delta q_{3+4} + \delta q_{1+4} \delta q_{2+3}) + (F_{-1} F_{-4} - F_1 F_4) (\delta q_{1+2} \delta q_{3+4} + \delta q_{1+3} \delta q_{2+4})] \\
&+ k_1^2 |k_2| (\mathbf{k}_2 \cdot \mathbf{k}_3 + k_3^2) (\mathbf{k}_2 \cdot \mathbf{k}_4 + \mathbf{k}_3 \cdot \mathbf{k}_4) \left[- \frac{e^{-i(\omega_2 + \omega_3 + \omega_4)t} - 1}{(\omega_2 + \omega_3 + \omega_4)\omega_4} + \frac{e^{-i(\omega_2 + \omega_3)t} - 1}{(\omega_2 + \omega_3)\omega_4} \right] \times \\
&\times A_1 A_2 B_3 A_4 [(F_1 F_3 - F_{-1} F_{-3}) (\delta q_{1+2} \delta q_{3+4} + \delta q_{1+4} \delta q_{2+3}) \\
&+ (F_{-1} F_{-2} - F_1 F_2) (\delta q_{1+3} \delta q_{2+4} + \delta q_{1+4} \delta q_{2+3}) + (F_{-1} F_{-4} - F_1 F_4) (\delta q_{1+3} \delta q_{2+4} + \delta q_{1+2} \delta q_{3+4})] \\
&+ k_1^2 k_2^2 (\mathbf{k}_2 \cdot \mathbf{k}_4) |k_3| \left[- \frac{e^{-i(\omega_2 + \omega_3 + \omega_4)t} - 1}{(\omega_2 + \omega_3 + \omega_4)(\omega_3 + \omega_4)} + \frac{e^{-i\omega_2 t} - 1}{\omega_2 (\omega_3 + \omega_4)} \right] \times \\
&\times A_1 A_2 A_3 B_4 [(F_1 F_4 - F_{-1} F_{-4}) (\delta q_{1+3} \delta q_{2+4} + \delta q_{1+2} \delta q_{3+4}) \\
&+ (F_{-1} F_{-3} - F_1 F_3) (\delta q_{1+4} \delta q_{2+3} + \delta q_{1+2} \delta q_{3+4}) + (F_{-1} F_{-2} - F_1 F_2) (\delta q_{1+4} \delta q_{2+3} + \delta q_{1+3} \delta q_{2+4})]
\end{aligned} \tag{C.19}$$

$$\begin{aligned}
& + k_1^2 k_2^2 (\mathbf{k}_2 \cdot \mathbf{k}_3) (\mathbf{k}_2 + \mathbf{k}_3) \cdot \mathbf{k}_4 \left[\frac{e^{-i(\omega_2 + \omega_3 + \omega_4)t} - 1}{i(\omega_2 + \omega_3 + \omega_4)(\omega_3 + \omega_4)\omega_4} - \frac{e^{-i\omega_2 t} - 1}{i\omega_2(\omega_3 + \omega_4)\omega_4} \right. \\
& \left. - \frac{e^{-i(\omega_2 + \omega_3)t} - 1}{i(\omega_2 + \omega_3)\omega_3\omega_4} + \frac{e^{-i\omega_2 t} - 1}{i\omega_2\omega_3\omega_4} \right] A_1 A_2 A_3 A_4 [(F_1 F_2 + F_{-1} F_{-2})(\delta q_{1+3} \delta q_{2+4} + \delta q_{1+4} \delta q_{2+3}) \\
& + (F_{-1} F_{-3} + F_1 F_3)(\delta q_{1+2} \delta q_{3+4} + \delta q_{1+4} \delta q_{2+3}) + (F_{-1} F_{-4} + F_1 F_4)(\delta q_{1+2} \delta q_{3+4} + \delta q_{1+3} \delta q_{2+4})] + \\
& + \frac{1}{2} k_1^2 k_2^2 (\mathbf{k}_2 \cdot \mathbf{k}_3) (\mathbf{k}_2 \cdot \mathbf{k}_4) \left[\frac{e^{-i(\omega_2 + \omega_3 + \omega_4)t} - 1}{i(\omega_2 + \omega_3 + \omega_4)\omega_3\omega_4} - \frac{e^{-i(\omega_2 + \omega_4)t} - 1}{i(\omega_2 + \omega_4)\omega_3\omega_4} - \right. \\
& \left. - \frac{e^{-i(\omega_2 + \omega_3)t} - 1}{i(\omega_2 + \omega_3)\omega_3\omega_4} + \frac{e^{-i\omega_2 t} - 1}{i\omega_2\omega_3\omega_4} \right] A_1 A_2 A_3 A_4 [(F_1 F_2 + F_{-1} F_{-2})(\delta q_{1+3} \delta q_{2+4} + \delta q_{1+4} \delta q_{2+3}) \\
& + (F_{-1} F_{-3} + F_1 F_3)(\delta q_{1+2} \delta q_{3+4} + \delta q_{1+4} \delta q_{2+3}) + (F_{-1} F_{-4} + F_1 F_4)(\delta q_{1+2} \delta q_{3+4} + \delta q_{1+3} \delta q_{2+4})] \left. \right\}
\end{aligned}$$

C.1 Correlation functions of normal coordinates

A system of waves in terms of the introduced normal variables $a(\mathbf{k}, t)$ can be represented with the following equations

$$\frac{\partial a(\mathbf{k}, t)}{\partial t} = -i \frac{\delta \mathcal{H}(t)}{\delta a^*(\mathbf{k}, t)} - i f(\mathbf{k}, t) - \gamma_0(\mathbf{k}) a(\mathbf{k}, t) \quad (\text{C.20})$$

$$\begin{aligned}
\mathcal{H} = & \int d\mathbf{k} \Omega_{\mathbf{k}} a_{\mathbf{k}}^* a_{\mathbf{k}} + \int d\mathbf{k}_{123} \left(\frac{1}{2} V_{123} a_1 a_2^* a_3^* \delta \mathbf{k}_{1-2-3} + \frac{1}{6} U_{123} a_1^* a_2^* a_3^* \delta \mathbf{k}_{1+2+3} + \text{c.c.} \right) + \\
& + \int d\mathbf{k}_{1234} \left(\frac{1}{8} W_{1234} a_1^* a_2^* a_3 a_4 \delta \mathbf{k}_{1+2-3-4} + R_{1234}^* a_1 a_2 a_3 a_4 \delta \mathbf{k}_{1+2+3+4} \right. \\
& \left. + Q_{1234} a_1 a_2^* a_3^* a_4^* \delta \mathbf{k}_{1-2-3-4} + \text{c.c.} \right). \quad (\text{C.21})
\end{aligned}$$

Here $\mathcal{H}(t)$ is the wave Hamiltonian, $f(\mathbf{k}, t)$ is forcing and $\gamma_0(\mathbf{k})$ the bare (linear) damping. In the Hamiltonian we have written the non-interacting term and corrections that correspond to three-wave and four-wave mixing. Also we have introduced shorthand notations $\delta(\mathbf{k}_1 + \mathbf{k}_2 + \mathbf{k}_3) \rightarrow \delta \mathbf{k}_{1+2+3}$, $a_{\mathbf{k}_1} \rightarrow a_1$, $V(\mathbf{k}_1, \mathbf{k}_2, \mathbf{k}_3) \rightarrow V_{123}$ and $d\mathbf{k}_1 d\mathbf{k}_2 d\mathbf{k}_3 \rightarrow d\mathbf{k}_{123}$, $\int_{-\infty}^{\infty} \rightarrow \int$ and suppressed the dependence on time (only in the notation), which here enters as a parameter. Interaction coefficients have the following symmetries [114]: $V_{123} = V_{132}$, $U_{123} = U_{132} = U_{213}$, $Q_{1234} = Q_{1324} = Q_{1243}$, $R_{1234} = R_{2134} = R_{1243} = R_{3214} = R_{4231}$ and $W_{1234} = W_{2134} = W_{1243} = W_{3412}^*$. The last equality for W_{1234} follows, since Hamiltonian is real.

The wave equation, which we will solve perturbatively, in order to find $\langle aa \rangle$, $\langle a^* a \rangle$, $\langle aaa \rangle$

and $\langle a^*aa \rangle$ correlation functions, is

$$\frac{\partial a(\mathbf{k}, t)}{\partial t} = -i \frac{\delta \mathcal{H}}{\delta a^*(\mathbf{k}, t)} - if(\mathbf{k}, t) - \gamma_0 a(\mathbf{k}, t). \quad (\text{C.22})$$

Let us rescale the field $a \rightarrow \epsilon a$ and $f \rightarrow \epsilon f$, where $\epsilon \ll 1$ and the new variables a and f are now of the order of unity ¹. Now in the rescaled Hamiltonian the interaction coefficients V and U have smallness ϵ and the four-wave interaction coefficients have smallness ϵ^2 . For the time being we will only consider three-wave interaction, later we will consider also the four-wave interaction. Let us write one more time wave equation with the \mathcal{H}^3 hamiltonian explicitly

$$\begin{aligned} \partial_t a_k &= -i\Omega_k a_k - if_k - \gamma_{0k} a_k \\ &- i\epsilon \int d\mathbf{k}_{12} \left(V_{123} a_1 a_2^* \delta_{\mathbf{k}_{1-2-k}} + \frac{1}{2} V_{k12}^* a_1 a_2 \delta_{\mathbf{k}_{k-1-2}} + \frac{1}{2} U_{k12} a_1^* a_2^* \delta_{\mathbf{k}_{1+2+k}} \right). \end{aligned} \quad (\text{C.23})$$

To simplify the notation, we have omitted the time dependence of a and f and wrote the dependence of all quantities on \mathbf{k} as subscript k . If there will be the need to stress dependence on $-\mathbf{k}$ we will denote it as subscript $-k$ or write it explicitly. The generating functional of the above equation is

$$\begin{aligned} Z_f[l, l^*] &= \int \mathcal{D}a \mathcal{D}a^* \exp \left\{ \int dt (la + l^* a^*) \right\} \prod_{\mathbf{k}, t} \delta \left[\frac{\partial a}{\partial t} + i\Omega_k a - \gamma_{0k} a + i \frac{\delta \mathcal{H}_{\text{int}}}{\delta a^*} + if_k \right] \times \\ &\times \prod_{\mathbf{k}, t} \delta \left[\frac{\partial a^*}{\partial t} - i\Omega_k a^* - \gamma_{0k} a^* - i \left(\frac{\delta \mathcal{H}_{\text{int}}}{\delta a^*} \right)^* - if^* \right] \mathcal{J}[a, a^*], \end{aligned} \quad (\text{C.24})$$

here each a and l is a function of \mathbf{k} and t and $\mathcal{J}[a, a^*]$ is the Jacobian which will enter the normalization. Next, we introduce two new fields, $p(\mathbf{k}, t)$ and $p^*(\mathbf{k}, t)$ and set $(p)^* = p^*$

$$\begin{aligned} Z_f[l, l^*] &= \int \mathcal{D}a \mathcal{D}a^* \mathcal{D}p \mathcal{D}p^* \exp \left\{ \int dt (la + l^* a^*) \right\} \times \\ &\times \exp \left\{ i \int \frac{d\mathbf{k}}{(2\pi)^d} dt \left[\frac{\partial a}{\partial t} + i\Omega_k a - \gamma_{0k} a + i \frac{\delta \mathcal{H}_{\text{int}}}{\delta a^*} + if \right] p^* \right\} \times \end{aligned}$$

¹ We assume that the original f , has the same smallness as a , since otherwise a could not remain small during evolution.

$$\begin{aligned}
& \times \exp \left\{ -i \int \frac{d\mathbf{k}}{(2\pi)^d} dt \left[\frac{\partial a^*}{\partial t} - i\Omega_k a^* - \gamma_{0k} a^* - i \left(\frac{\delta \mathcal{H}_{\text{int}}}{\delta a^*} \right)^* - if \right] p \right\} \tilde{\mathcal{J}}[a, a^*] \\
& = \int \mathcal{D}a \mathcal{D}a^* \mathcal{D}p \mathcal{D}p^* \exp \left\{ \int dt (la + l^* a^*) \right\} \times \\
& \times \exp \left\{ \int \frac{d\mathbf{k}}{(2\pi)^d} dt \left[i \left(\frac{\partial a}{\partial t} + i\Omega_k a - \gamma_{0k} a \right) p^* - i \left(\frac{\partial a^*}{\partial t} - i\Omega_k a^* - \gamma_{0k} a^* \right) p \right] \right\} \quad (\text{C.25}) \\
& \times \exp \left\{ - \int \frac{d\mathbf{k}}{(2\pi)^d} dt \left[\frac{\delta \mathcal{H}_{\text{int}}}{\delta a^*} p^* + \left(\frac{\delta \mathcal{H}_{\text{int}}}{\delta a^*} \right)^* p \right] \right\} \exp \left\{ - \int \frac{d\mathbf{k}}{(2\pi)^d} dt [fp^* + f^*p] \right\} \tilde{\mathcal{J}}[a, a^*].
\end{aligned}$$

We average over forcing f

$$Z_f[l, l^*] = \int \mathcal{D}f \mathcal{D}f^* \mathcal{P}[f, f^*] \frac{Z_f[l, l^*]}{Z_f[l=0, l^*=0]} \quad (\text{C.26})$$

here $\mathcal{P}[f, f^*]$ is the probability distribution of forcing, which general is unknown. Note that $Z_f[l=0, l^*=0] = 1$, due to the Jacobian appearing in $Z_f[l, l^*]$. We obtain an interaction vertex of p and p^* , which we do not know explicitly, unless we specify $\mathcal{P}[f, f^*]$. Hence we will assume that we know one of the basic objects of this field theory: the pair correlation function, i.e. wave spectra (it will be introduced later as $n(\mathbf{k})$) in the lowest order. Our results on the sum of Lyapunov exponents are to be interpreted, as functionals of this spectra. We obtain for the generating functional

$$\begin{aligned}
Z[l, l^*] & = \int \mathcal{D}a \mathcal{D}a^* \mathcal{D}p \mathcal{D}p^* \exp \left\{ \int dt (la + l^* a^*) \right\} \times \\
& \times \exp \left\{ \int \frac{d\mathbf{k}}{(2\pi)^d} dt \left[i \left(\frac{\partial a}{\partial t} + i\Omega_k a - \gamma_{0k} a \right) p^* - i \left(\frac{\partial a^*}{\partial t} - i\Omega_k a^* - \gamma_{0k} a^* \right) p \right] \right\} \quad (\text{C.27}) \\
& \times \exp \left\{ - \int \frac{d\mathbf{k}}{(2\pi)^d} dt \left[\frac{\delta \mathcal{H}_{\text{int}}}{\delta a^*} p^* + \left(\frac{\delta \mathcal{H}_{\text{int}}}{\delta a^*} \right)^* p \right] \right\} \left\langle \exp \left\{ - \int \frac{d\mathbf{k} dt}{(2\pi)^d} [fp^* + f^*p] \right\} \right\rangle_f \tilde{\mathcal{J}}[a, a^*],
\end{aligned}$$

here the $\tilde{\mathcal{J}}[a, a^*]$ is the new normalization (c.f. [36]). From the generating functional averaged over force (C.27) we get the Feynman rules ($\langle \rangle_f$ denotes averaging over force). All the terms in the exponent can be represented as $i\mathcal{I}$, \mathcal{I} has the role of action and we will call it Martin-Siggia-Rose action [5, 36, 70, 71, 110]. The correlations functions of fields a are proven to be

given [36, 71, 110] by the following functional integrals

$$\begin{aligned} & \langle a(\mathbf{k}_1, t_1) \dots a(\mathbf{k}_n, t_n) a^*(\mathbf{k}_{n+1}, t_{n+1}) \dots a^*(\mathbf{k}_m, t_m) \rangle = \\ & = Z^{-1}[0, 0] \frac{\delta^m Z[l, l^*]}{\delta l(\mathbf{k}_1, t_1) \dots \delta l(\mathbf{k}_n, t_n) \delta l^*(\mathbf{k}_{n+1}, t_{n+1}) \dots \delta l^*(\mathbf{k}_m, t_m)} \Big|_{l=0, l^*=0}. \end{aligned} \quad (\text{C.28})$$

We are considering a case of the weak nonlinearity. The main objects of the analysis are the pair correlation function $F(\mathbf{k}, t)$ and the Green's function $G(\mathbf{k}, t)$. They are determined as the following averages

$$F(\mathbf{k}, t) (2\pi)^d \delta(\mathbf{k} - \mathbf{k}') \equiv \langle a^*(\mathbf{k}, 0) a(\mathbf{k}', 0) \rangle \quad (\text{C.29})$$

$$G(\mathbf{k}, t) (2\pi)^d \delta(\mathbf{k} - \mathbf{k}') \equiv \left\langle \frac{\delta a(\mathbf{k}, t)}{\delta f(\mathbf{k}', 0)} \right\rangle, \quad (\text{C.30})$$

where δa designates the response of a solution of (C.20) to the variation δf of the pumping force. In the lowest order we already said we will take as known the form of F_q , while the bare propagator between $a(\mathbf{k}_1, \omega_1)$ and $p(\mathbf{k}_2, \omega_2)$ from the quadratic part of Martin-Siggia-Rose action. Let us look at

$$\begin{aligned} & i \int \frac{d\mathbf{k}_1}{(2\pi)^d} dt \frac{d\omega_1 d\omega_2}{(2\pi)^2} a_1(-i\omega_1 + i\Omega_1 - \gamma_{01}) p_2^* e^{-i(\omega_1 - \omega_2)t} \\ & = i \int \frac{d\mathbf{k}_1}{(2\pi)^d} d\mathbf{k}_2 dt \frac{d\omega_1 d\omega_2}{(2\pi)^2} e^{i(\omega_2 - \omega_1)t} a_1(-i\omega_1 + i\Omega_1 - \gamma_{01}) p_2^* \delta(\mathbf{k}_1 - \mathbf{k}_2) \\ & = \int \frac{dq_1 dq_2}{(2\pi)^{2d+2}} a_1(\omega_1 - \Omega_1 + i\gamma_{01}) p_2^* (2\pi)^{d+1} \delta(q_1 - q_2), \end{aligned}$$

here a_i and p_i are functions of q_i . This calculus gives us the bare propagator between a and p^*

$$G(\mathbf{k}, \omega) = \frac{1}{\omega - \Omega_{\mathbf{k}} + i\gamma_{0\mathbf{k}}} \quad (\text{C.31})$$

Let us recall the exact Dyson's equation for the dressed propagators ²

$$G(q) = [\omega - \Omega(\mathbf{k}) + i\gamma_0(\mathbf{k}) - \Sigma(q)]^{-1}, \quad \text{where} \quad (\text{C.32})$$

² Frequently the equation on F is called the Dyson-Wyld equation.

$$F(q) = [\Phi(q) + \Phi_0(q)] |G(q)|^2, \quad (\text{C.33})$$

$$\langle f^*(q)f(q') \rangle \equiv (2\pi)^{d+1} \Phi_0(q) \delta(q - q'), \quad (\text{C.34})$$

$$G_0(q) = [\omega - \Omega(\mathbf{k}) + i\gamma_0(\mathbf{k})]^{-1}. \quad (\text{C.35})$$

Above we introduced self-energy function Σ and the mass operator Φ and the forcing correlation function Φ_0 . The imaginary part of Σ determines the damping of waves, the real part shifts the frequency from Ω_k , while Φ is the renormalized pumping. Due to small nonlinearity

$$\Sigma(\mathbf{k}, \omega) \propto \epsilon^2 \ll \Omega(\mathbf{k}), \quad (\text{C.36})$$

thus (C.31) has a sharp peak in the vicinity of $\Omega(\mathbf{k})$. As a first step in analysis one may neglect the ω dependence of $\Sigma(\mathbf{k}, \omega)$ and use

$$\Sigma(\mathbf{k}, \omega) \simeq \Sigma(\mathbf{k}, \Omega(\mathbf{k})). \quad (\text{C.37})$$

With this approximation for the self-energy we get that (C.32) looks like

$$G(q) \simeq \tilde{G}(q) = [\omega - \Omega_R(\mathbf{k}) + i\gamma(\mathbf{k})]^{-1}, \quad (\text{C.38})$$

$$\Omega_R(\mathbf{k}) \equiv \Omega(\mathbf{k}) + \text{Re}\Sigma(\mathbf{k}, \Omega(\mathbf{k})), \quad (\text{C.39})$$

$$\gamma(\mathbf{k}) \equiv \gamma_0(\mathbf{k}) - \text{Im}\Sigma(\mathbf{k}, \Omega(\mathbf{k})), \quad (\text{C.40})$$

$$\Phi(q) \simeq \tilde{\Phi}(q) = \Phi(\mathbf{k}, \Omega(\mathbf{k})), \quad (\text{C.41})$$

$$F(q) \simeq \tilde{F}(q) = |\tilde{G}(q)|^2 [\Phi_0(q) + \tilde{\Phi}(q)]. \quad (\text{C.42})$$

Thus, in the lowest order we have

$$F(\mathbf{k}, \omega) \simeq n(\mathbf{k}) (2\pi) \delta(\omega - \Omega(\mathbf{k})) \quad (\text{C.43})$$

Recall that we take wave spectrum $n(\mathbf{k})$ as given. We will also assume that $n(\mathbf{k})$ is a steady state, since the sum of Lyapunov exponents can be written as (1.1) only for a steady state. This steady state imposes $\Phi(q)/\gamma(\mathbf{k}) = \text{const}$, however this alone does not help, since we assume

nothing about the forcing that created the wave spectra. The vertices and propagators that appear in this field theory are listed bellow.

C.2 Rules and vertices

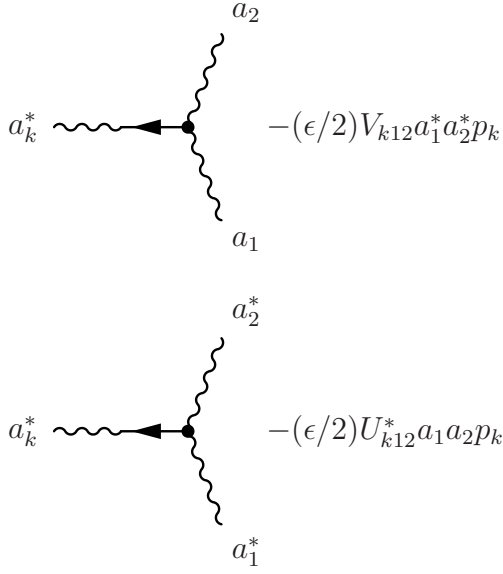
$$\begin{aligned}
 a \text{ --- } \longrightarrow p^* & \quad G_1(2\pi)^{d+1}\delta(q_1 - q_2) \equiv \langle a_1 p_2^* \rangle \\
 a \text{ --- } a^* & \quad F_1(2\pi)^{d+1}\delta(q_1 - q_2) \equiv \langle a_1^* a_2 \rangle \\
 a \text{ --- } a^* & \quad \text{emphasizes that the F is taken as dressed}
 \end{aligned}$$

$$\begin{array}{c}
 a_2 \\
 | \\
 a_k \text{ --- } \bullet \\
 | \\
 a_1^*
 \end{array}
 \quad -\epsilon V_{12k} a_1 a_2^* p_k^*$$

$$\begin{array}{c}
 a_2^* \\
 | \\
 a_k \text{ --- } \bullet \\
 | \\
 a_1^*
 \end{array}
 \quad -(\epsilon/2) V_{k12}^* a_1 a_2 p_k^*$$

$$\begin{array}{c}
 a_2 \\
 | \\
 a_k \text{ --- } \bullet \\
 | \\
 a_1
 \end{array}
 \quad -(\epsilon/2) U_{k12} a_1^* a_2^* p_k^*$$

$$\begin{array}{c}
 a_2^* \\
 | \\
 a_k^* \text{ --- } \bullet \\
 | \\
 a_1
 \end{array}
 \quad -\epsilon V_{12k}^* a_1^* a_2 p_k$$



Note that the direction of G and G^* is opposite, while $F = F^*$ can have both directions. We will use bold lines to denote the dressed propagator and pair correlation function. The momentum is conserved at each vertex.

Let us look at a wave field a

$$a(\mathbf{k}, t) = \int \frac{d\omega}{2\pi} a(\mathbf{k}, \omega) e^{-i\omega t} \quad (\text{C.44})$$

We introduce a cut-off ω_b such that $\omega_b \ll \Omega(\mathbf{k}_p)$, where \mathbf{k}_p is the characteristic wavenumber of the pumping scale. Now $a(\mathbf{k}, t)$ can be decomposed into a slow a' and fast \tilde{a} part as follows

$$a(\mathbf{k}, t) = a' + \tilde{a}, \quad a' \equiv \int_{|\omega| < \omega_b} \frac{d\omega}{2\pi} a(\mathbf{k}, \omega) e^{-i\omega t}, \quad \tilde{a} \equiv \int_{|\omega| \geq \omega_b} \frac{d\omega}{2\pi} a(\mathbf{k}, \omega) e^{-i\omega t} \quad (\text{C.45})$$

Note that at those frequencies $G'_q \simeq -1/\Omega_k$.

C.3 Correlation function $\langle a'^* a' \rangle$

Let us look at following quantity

$$\int_{-\infty}^{\infty} dt \langle a^*(\mathbf{k}_1, 0) a(\mathbf{k}_2, t) \rangle = F(\mathbf{k}_1, \omega = 0) \delta(\mathbf{k}_1 - \mathbf{k}_2) (2\pi)^d \quad (\text{C.46})$$

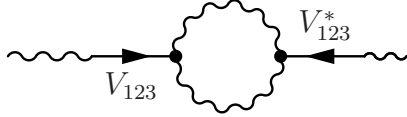
We see that the main contribution to these quantity will be given from small frequencies, i.e. a' wave amplitudes. Since there is no pumping on those scales in the lowest order $\langle a'^* a' \rangle$ is zero.

The first non-vanishing order is ϵ^2 . The graph that contributes to this correlation function is

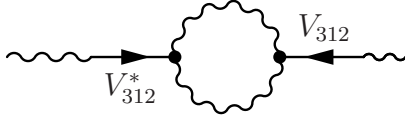
$$\langle a'^* a' \rangle = \text{---} \xrightarrow{V_{123}} \text{---} \text{---} \xleftarrow{V_{123}^*} \text{---} \quad (C.47)$$

here we used a bold way line to emphasize that the correlation functions F should be taken as dressed. With the vertices we have on disposal we can make the following graphs

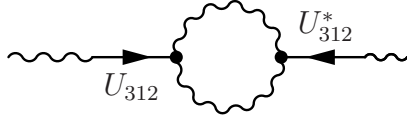
$$F(\mathbf{k}_3, \omega_3 = 0) = \Phi_1(\mathbf{k}_3, \omega_3 = 0) + \Phi_2(\mathbf{k}_3, \omega_3 = 0) + \Phi_3(\mathbf{k}_3, \omega_3 = 0) \quad (C.48)$$



$$\begin{aligned} \Phi_1(\mathbf{k}_3, \omega_3 = 0) &= \epsilon^2 (2\pi)^{d-1} |G'_3|^2 \int dq_{12} |V_{123}|^2 \delta q_{1-2-3} F(q_1) F(q_2) = \\ &= \epsilon^2 (2\pi)^{d+1} \frac{1}{\Omega_3^2} \int d\mathbf{k}_{12} |V_{123}|^2 \delta \mathbf{k}_{1-2-3} n_1 n_2 \delta(\Omega_1 - \Omega_2) \end{aligned} \quad (C.49)$$



$$\begin{aligned} \Phi_2(\mathbf{k}_3, \omega_3 = 0) &= 2 \frac{\epsilon^2}{4} (2\pi)^{d-1} |G'_3|^2 \int dq_{12} |V_{312}|^2 \delta q_{3-1-2} F(q_1) F(q_2) = \\ &= \frac{\epsilon^2}{2} (2\pi)^{d+1} \frac{1}{\Omega_3^2} \int d\mathbf{k}_{12} |V_{312}|^2 \delta \mathbf{k}_{3-1-2} n_1 n_2 \delta(\Omega_1 + \Omega_2) \end{aligned} \quad (C.50)$$



$$\Phi_3(\mathbf{k}_3, \omega_3 = 0) = 2\frac{\epsilon^2}{4}(2\pi)^{d-1}|G'_3|^2 \int dq_{12}|U_{123}|^2 \delta_{q_1+2+3} F(q_1)F(q_2) = \quad (C.51)$$

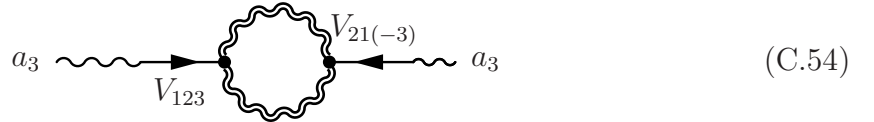
$$= \frac{\epsilon^2}{2}(2\pi)^{d+1} \frac{1}{\Omega_3^2} \int d\mathbf{k}_{12}|U_{123}|^2 n_1 n_2 \delta(\Omega_1 + \Omega_2) \quad (C.52)$$

Adding all terms (C.49,C.50 and C.52) we get

$$F(\mathbf{k}_3, \omega_3 = 0) = \frac{\epsilon^2}{2}(2\pi)^{d+1} \frac{1}{\Omega_3^2} \int d\mathbf{k}_{12} n_1 n_2 [2|V_{123}|^2 \delta_{\mathbf{k}_{1-2-3}} \delta(\Omega_1 - \Omega_2) + |V_{312}|^2 \delta_{\mathbf{k}_{3-1-2}} \delta(\Omega_1 + \Omega_2) + |U_{123}|^2 \delta_{\mathbf{k}_{3+1+2}} \delta(\Omega_1 + \Omega_2)] \quad (C.53)$$

C.4 Correlation function $\langle a' a' \rangle$

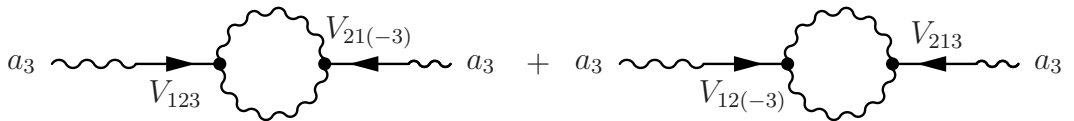
We notice again that there is no zeroth order contribution to $\langle a' a' \rangle$ since there is no pumping at those scale. The main contribution comes graph bellow



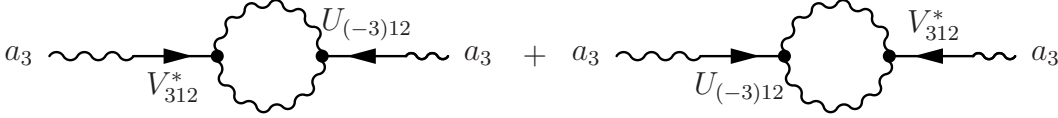
$$(C.54)$$

With the vertices we have on disposal we can make the following graphs

$$H(\mathbf{k}_3, \omega_3 = 0) = \Xi_1(\mathbf{k}_3, \omega_3 = 0) + \Xi_2(\mathbf{k}_3, \omega_3 = 0) \quad (C.55)$$



$$\begin{aligned}
 \Xi_1(\mathbf{k}_3, \omega_3 = 0) &= \frac{\epsilon^2}{2} (2\pi)^{d-1} G'_3 G'_{-3} \int dq_{12} F_1 F_2 [V_{123} V_{21(-3)} \delta q_{1-2-3} + V_{12(-3)} V_{213} \delta q_{1-2+3}] \\
 &= \frac{\epsilon^2}{2} (2\pi)^{d+1} \frac{1}{\Omega_3 \Omega_{-3}} \int d\mathbf{k}_{12} n_1 n_2 \delta(\Omega_1 - \Omega_2) [V_{123} V_{21(-3)} \delta \mathbf{k}_{1-2-3} + V_{12(-3)} V_{213} \delta \mathbf{k}_{1-2+3}] \quad (\text{C.56})
 \end{aligned}$$

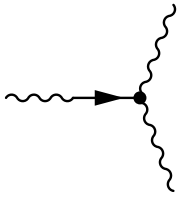


$$\begin{aligned}
 \Xi_2(\mathbf{k}_3, \omega_3 = 0) &= \frac{\epsilon^2}{4} (2\pi)^{d-1} G'_3 G'_{-3} \int dq_{12} F_1 F_2 [V_{312}^* U_{12(-3)} \delta q_{3-1-2} + V_{(-3)12}^* U_{123} \delta q_{1+2+3}] \\
 &= \frac{\epsilon^2}{2} (2\pi)^{d+1} \frac{1}{\Omega_3 \Omega_{-3}} \int d\mathbf{k}_{12} n_1 n_2 \delta(\Omega_1 + \Omega_2) [V_{312}^* U_{12(-3)} \delta \mathbf{k}_{3-1-2} + V_{(-3)12}^* U_{123} \delta \mathbf{k}_{1+2+3}] \quad (\text{C.57})
 \end{aligned}$$

Hence from (C.56,) we get the $\langle a'a' \rangle$ correlator

$$\begin{aligned}
 H(\mathbf{k}_3, \omega_3 = 0) &= \frac{\epsilon^2}{4} (2\pi)^{d+1} \frac{1}{\Omega_3 \Omega_{-3}} \int d\mathbf{k}_{12} n_1 n_2 \times \\
 &\quad \times [2(V_{123} V_{21(-3)} \delta \mathbf{k}_{1-2-3} + V_{12(-3)} V_{213} \delta \mathbf{k}_{1-2+3}) \delta(\Omega_1 - \Omega_2) \\
 &\quad + (V_{312}^* U_{12(-3)} \delta \mathbf{k}_{3-1-2} + V_{(-3)12}^* U_{123} \delta \mathbf{k}_{1+2+3}) \delta(\Omega_1 + \Omega_2)] \quad (\text{C.58})
 \end{aligned}$$

C.5 Correlation function $\langle a_1 a_2 a_3 \rangle$



$$(\text{C.59})$$

$$\begin{aligned}
 J_{123} &= -\epsilon (2\pi)^d U_{123} (G_1 F_2 F_3 + G_2 F_1 F_3 + G_3 F_1 F_2) \\
 &= -\epsilon (2\pi)^{d+2} U_{123} [G_1 n_2 n_3 \delta(\omega_2 - \Omega_2) \delta(\omega_3 - \Omega_3) + G_2 n_1 n_3 \delta(\omega_1 - \Omega_1) \delta(\omega_3 - \Omega_3) + \\
 &\quad + G_3 n_1 n_2 \delta(\omega_1 - \Omega_1) \delta(\omega_2 - \Omega_2)] \quad (\text{C.60})
 \end{aligned}$$

here G_i is the bare Green's function.

C.6 Correlation function $\langle a_1^* a_2 a_3 \rangle$



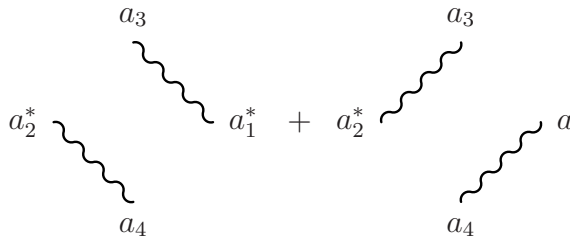
$$(C.61)$$

$$\begin{aligned}
 K_{123} &= -\epsilon(2\pi)^d V_{123} (G_1^* F_2 F_3 + G_2 F_1 F_3 + G_3 F_1 F_2) \\
 &= -\epsilon(2\pi)^{d+2} V_{123} [G_1^* n_2 n_3 \delta(\omega_2 - \Omega_2) \delta(\omega_3 - \Omega_3) + G_2 n_1 n_3 \delta(\omega_1 - \Omega_1) \delta(\omega_3 - \Omega_3) + \\
 &\quad + G_3 n_1 n_2 \delta(\omega_1 - \Omega_1) \delta(\omega_2 - \Omega_2)]
 \end{aligned}
 \tag{C.62}$$

here also G_i is the bare Green's function.

C.7 Correlation function $\langle \tilde{a}_1^* \tilde{a}_2^* \tilde{a}_3 \tilde{a}_4 \rangle$

All correlation function of four a that appear in (1.3) need to be taken in the zeroth order, since there is already an ϵ^2 factor in front. Hence all a should be taken as \tilde{a} . These guys correspond to fast frequencies and also can arise directly from pumping. The diagrams that contribute to them are

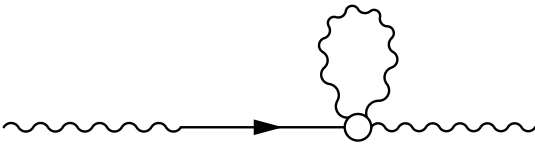


$$\begin{aligned}
 \langle \tilde{a}_1^* \tilde{a}_2^* \tilde{a}_3 \tilde{a}_4 \rangle &= (2\pi)^{2d+2} (\delta q_{1-3} \delta q_{2-4} + \delta q_{1-4} \delta q_{2-3}) F_1 F_2 \\
 &= (2\pi)^{2d+4} [\delta q_{1-3} \delta q_{2-4} + \delta q_{1-4} \delta q_{2-3}] \delta(\omega_1 - \Omega_1) \delta(\omega_2 - \Omega_2) n_1 n_2
 \end{aligned}
 \tag{C.63}$$

Note that the correlation function $\langle \tilde{a} \tilde{a} \rangle$ only appears in the ϵ^2 orders, since there are no bare vertex of p interacting with p (there is a vertex however of p interacting with p^*).

C.8 Four wave interaction

In the rescaled wave equation the four-wave interaction terms comes with ϵ^2 smallness, thus to the order of ϵ^4 in λ such a term could enter only correlation functions $\langle a'_1 a'_1 \rangle$ and $\langle a'^* a' \rangle$. The only possible diagram that could contribute is


(C.64)

However we notice that this diagram actually in ϵ^2 corresponds to pair correlation functions of $\langle \tilde{a}_1 \tilde{a}_1 \rangle$ and $\langle \tilde{a}^* \tilde{a} \rangle$. Contributions to $\langle a'_1 a'_1 \rangle$ and $\langle a'^* a' \rangle$ would be of orders higher than ϵ^2 .

Some questions arise: Could it have been anticipated that λ is to depend on the sign of interaction? Can it be then guessed that a term with four-wave interaction in ϵ^2 order would not enter?

C.9 Higher than ϵ^4

The next order terms to a field theory with vertices of three-, four- and five-wave interactions (five-wave interaction vertex is of order ϵ^3) show that the ϵ^5 order does not exist. We see this by trying to draw diagrams of ϵ^5 order for correlation functions $\langle a_i'^* a_j' \rangle$, $\langle a_i' a_j' \rangle$, $\langle a_i a_j a_k \rangle$, $\langle a_i^* a_j a_k \rangle$ and four and five a and a^* fields correlation functions.

C.10 Calculating the sum of Lyapunov exponents

Now we recall the derived formula for the sum of Lyapunov exponents (C.19), we write it in terms of rescaled fields a and plugg the correlation functions expressed in terms of unknown

wave spectra $n(\mathbf{k})$ (C.53–C.63)

$$\begin{aligned}
\lambda = & \epsilon^4 (2\pi) \int d\mathbf{k}_{123} k_3^4 A_3 A_{-3} n_1 n_2 \left\{ \text{Re} \left[\frac{1}{4\Omega_3 \Omega_{-3}} [2(V_{123} V_{21(-3)} \delta \mathbf{k}_{1-2-3} + \right. \right. \\
& + V_{12(-3)} V_{213} \delta \mathbf{k}_{1-2+3}) \delta(\Omega_1 - \Omega_2) + (V_{312}^* U_{12(-3)} \delta \mathbf{k}_{3-1-2} + V_{(-3)12}^* U_{123} \delta \mathbf{k}_{1+2+3}) \delta(\Omega_1 + \Omega_2)] \left. \right] - \\
& - \frac{1}{2\Omega_3^2} [2|V_{123}|^2 \delta \mathbf{k}_{1-2-3} \delta(\Omega_1 - \Omega_2) + |V_{312}|^2 \delta \mathbf{k}_{3-1-2} \delta(\Omega_1 + \Omega_2) + |U_{123}|^2 \delta \mathbf{k}_{3+1+2} \delta(\Omega_1 + \Omega_2)] \left. \right\} \\
& + \epsilon^4 \int \frac{dq_{123}}{(2\pi)^{d+2}} \delta q_{1+2+3} \left\{ |k_1| k_3^2 (\mathbf{k}_1 \cdot \mathbf{k}_2 + k_2^2) (2\pi) \delta(\omega_3) A_1 B_2 A_3 \times \right. \\
& \times [U_{123}(G_1 F_2 F_3 + G_2 F_1 F_3 + G_3 F_1 F_2) + U_{-1-2-3}^*(G_{-1}^* F_{-2} F_{-3} + G_{-2}^* F_{-1} F_{-3} + G_{-3}^* F_{-1} F_{-2}) \\
& - V_{-123}(G_{-1}^* F_2 F_3 + G_2 F_{-1} F_3 + G_3 F_{-1} F_2) - V_{1-2-3}^*(G_1 F_{-2} F_{-3} + G_{-2}^* F_1 F_{-3} + G_{-3}^* F_1 F_{-2}) \\
& + V_{-213}(G_1 F_{-2} F_3 + G_{-2}^* F_1 F_3 + G_3 F_1 F_{-2}) + V_{2-1-3}^*(G_{-1}^* F_2 F_{-3} + G_2 F_{-1} F_{-3} + G_{-3}^* F_{-1} F_2) \\
& - V_{-312}(G_1 F_2 F_{-3} + G_2 F_1 F_{-3} + G_{-3}^* F_1 F_2) - V_{3-1-2}^*(G_{-1}^* F_{-2} F_3 + G_{-2}^* F_{-1} F_3 + G_3 F_{-1} F_{-2})] \\
& + k_1^2 k_2^2 (\mathbf{k}_2 \cdot \mathbf{k}_3) \left(\frac{i\pi}{\omega_3} (\delta(\omega_1) - \delta(\omega_2)) + \frac{1}{\omega_1 \omega_2} \right) A_1 A_2 A_3 \times \\
& \times [U_{123}(G_1 F_2 F_3 + G_2 F_1 F_3 + G_3 F_1 F_2) - U_{-1-2-3}^*(G_{-1}^* F_{-2} F_{-3} + G_{-2}^* F_{-1} F_{-3} + G_{-3}^* F_{-1} F_{-2}) \\
& - V_{-123}(G_{-1}^* F_2 F_3 + G_2 F_{-1} F_3 + G_3 F_{-1} F_2) + V_{1-2-3}^*(G_1 F_{-2} F_{-3} + G_{-2}^* F_1 F_{-3} + G_{-3}^* F_1 F_{-2}) \\
& - V_{-213}(G_1 F_{-2} F_3 + G_{-2}^* F_1 F_3 + G_3 F_1 F_{-2}) + V_{2-1-3}^*(G_{-1}^* F_2 F_{-3} + G_2 F_{-1} F_{-3} + G_{-3}^* F_{-1} F_2) \\
& - V_{-312}(G_1 F_2 F_{-3} + G_2 F_1 F_{-3} + G_{-3}^* F_1 F_2) + V_{3-1-2}^*(G_{-1}^* F_{-2} F_3 + G_{-2}^* F_{-1} F_3 + G_3 F_{-1} F_{-2})] \left. \right\} \\
& + \lambda_{aaaa} + \mathcal{O}(\epsilon^6). \tag{C.65}
\end{aligned}$$

here we introduced λ_{aaaa} as follows

$$\begin{aligned}
\lambda_{aaaa} \equiv & \lim_{t \rightarrow \infty} \epsilon^4 \int \frac{dq_{1234}}{(2\pi)^{4d+4}} (2\pi)^{2d+2} \times \tag{C.66} \\
& \times \left\{ \frac{|k_1|}{2} (\mathbf{k}_1 \cdot \mathbf{k}_2 + k_2^2) |k_3| (\mathbf{k}_3 \cdot \mathbf{k}_4 + k_4^2) (2\pi) \delta(\omega_3 + \omega_4) \times \right. \\
& \times A_1 B_2 A_3 B_4 [-(F_1 F_2 + F_{-1} F_{-2}) (\delta q_{1+3} \delta q_{2+4} + \delta q_{1+4} \delta q_{2+3}) \\
& + (F_{-1} F_{-3} + F_1 F_3) (\delta q_{1+2} \delta q_{3+4} + \delta q_{1+4} \delta q_{2+3}) - (F_{-1} F_{-4} + F_1 F_4) (\delta q_{1+2} \delta q_{3+4} + \delta q_{1+3} \delta q_{2+4})] \\
& + |k_1| (\mathbf{k}_1 \cdot \mathbf{k}_2 + k_2^2) k_3^2 (\mathbf{k}_3 \cdot \mathbf{k}_4) \left[-\frac{e^{-i(\omega_3 + \omega_4)t} - 1}{(\omega_3 + \omega_4)\omega_4} + \frac{e^{-i\omega_3 t} - 1}{\omega_3 \omega_4} \right] \times
\end{aligned}$$

$$\begin{aligned}
& \times A_1 B_2 A_3 A_4 [(F_1 F_2 - F_{-1} F_{-2})(\delta q_{1+3} \delta q_{2+4} + \delta q_{1+4} \delta q_{2+3}) \\
& + (F_{-1} F_{-3} - F_1 F_3)(\delta q_{1+2} \delta q_{3+4} + \delta q_{1+4} \delta q_{2+3}) + (F_{-1} F_{-4} - F_1 F_4)(\delta q_{1+2} \delta q_{3+4} + \delta q_{1+3} \delta q_{2+4})] \\
& + k_1^2 |k_2| (\mathbf{k}_2 \cdot \mathbf{k}_3 + k_3^2) (\mathbf{k}_2 \cdot \mathbf{k}_4 + \mathbf{k}_3 \cdot \mathbf{k}_4) \left[-\frac{e^{-i(\omega_2 + \omega_3 + \omega_4)t} - 1}{(\omega_2 + \omega_3 + \omega_4)\omega_4} + \frac{e^{-i(\omega_2 + \omega_3)t} - 1}{(\omega_2 + \omega_3)\omega_4} \right] \times \\
& \times A_1 A_2 B_3 A_4 [(F_1 F_3 - F_{-1} F_{-3})(\delta q_{1+2} \delta q_{3+4} + \delta q_{1+4} \delta q_{2+3}) \\
& + (F_{-1} F_{-2} - F_1 F_2)(\delta q_{1+3} \delta q_{2+4} + \delta q_{1+4} \delta q_{2+3}) + (F_{-1} F_{-4} - F_1 F_4)(\delta q_{1+3} \delta q_{2+4} + \delta q_{1+2} \delta q_{3+4})] \\
& + k_1^2 k_2^2 (\mathbf{k}_2 \cdot \mathbf{k}_4) |k_3| \left[-\frac{e^{-i(\omega_2 + \omega_3 + \omega_4)t} - 1}{(\omega_2 + \omega_3 + \omega_4)(\omega_3 + \omega_4)} + \frac{e^{-i\omega_2 t} - 1}{\omega_2(\omega_3 + \omega_4)} \right] \times \\
& \times A_1 A_2 A_3 B_4 [(F_1 F_4 - F_{-1} F_{-4})(\delta q_{1+3} \delta q_{2+4} + \delta q_{1+2} \delta q_{3+4}) \\
& + (F_{-1} F_{-3} - F_1 F_3)(\delta q_{1+4} \delta q_{2+3} + \delta q_{1+2} \delta q_{3+4}) + (F_{-1} F_{-2} - F_1 F_2)(\delta q_{1+4} \delta q_{2+3} + \delta q_{1+3} \delta q_{2+4})] \\
& + k_1^2 k_2^2 (\mathbf{k}_2 \cdot \mathbf{k}_3) (\mathbf{k}_3 \cdot \mathbf{k}_4) \left[\frac{e^{-i(\omega_2 + \omega_3 + \omega_4)t} - 1}{i(\omega_2 + \omega_3 + \omega_4)(\omega_3 + \omega_4)\omega_4} - \frac{e^{-i\omega_2 t} - 1}{i\omega_2(\omega_3 + \omega_4)\omega_4} - \right. \\
& \left. - \frac{e^{-i(\omega_2 + \omega_3)t} - 1}{i(\omega_2 + \omega_3)\omega_3\omega_4} + \frac{e^{-i\omega_2 t} - 1}{i\omega_2\omega_3\omega_4} \right] A_1 A_2 A_3 A_4 [(F_1 F_2 + F_{-1} F_{-2})(\delta q_{1+3} \delta q_{2+4} + \delta q_{1+4} \delta q_{2+3}) \\
& + (F_{-1} F_{-3} + F_1 F_3)(\delta q_{1+2} \delta q_{3+4} + \delta q_{1+4} \delta q_{2+3}) + (F_{-1} F_{-4} + F_1 F_4)(\delta q_{1+2} \delta q_{3+4} + \delta q_{1+3} \delta q_{2+4})] \\
& + \frac{1}{2} k_1^2 k_2^2 (\mathbf{k}_2 \cdot \mathbf{k}_3) (\mathbf{k}_2 \cdot \mathbf{k}_4) \left[\frac{e^{-i(\omega_2 + \omega_3 + \omega_4)t} - 1}{i(\omega_2 + \omega_3 + \omega_4)\omega_3\omega_4} - \frac{e^{-i(\omega_2 + \omega_4)t} - 1}{i(\omega_2 + \omega_4)\omega_3\omega_4} - \right. \\
& \left. - \frac{e^{-i(\omega_2 + \omega_3)t} - 1}{i(\omega_2 + \omega_3)\omega_3\omega_4} + \frac{e^{-i\omega_2 t} - 1}{i\omega_2\omega_3\omega_4} \right] A_1 A_2 A_3 A_4 [(F_1 F_2 + F_{-1} F_{-2})(\delta q_{1+3} \delta q_{2+4} + \delta q_{1+4} \delta q_{2+3}) \\
& + (F_{-1} F_{-3} + F_1 F_3)(\delta q_{1+2} \delta q_{3+4} + \delta q_{1+4} \delta q_{2+3}) + (F_{-1} F_{-4} + F_1 F_4)(\delta q_{1+2} \delta q_{3+4} + \delta q_{1+3} \delta q_{2+4})] \Big\}.
\end{aligned}$$

To manage the calculation of the length expression, given above, we brake it into a sum of three terms

$$\lambda = \lambda_{aa} + \lambda_{aaa} + \lambda_{aaaa} + \mathcal{O}(\epsilon^6), \quad (\text{C.67})$$

where λ_{aa} corresponds to the part where we use the pair correlation functions F and H in only ϵ^2 order, λ_{aaa} the part where we meet K and J correlation functions and the rest gives λ_{aaaa} . The next order it's ϵ^6 as explained in section C.9.

Also from now on we focus on gravity-capillary waves, hence it is worth to revise some characteristics of them that we will constantly use along the way

- We assume $F(\mathbf{k}, \omega = 0) = 0$ and from the definition of $n(\mathbf{k})$ from bare $F(\mathbf{k}, \omega)$ as $F(\mathbf{k}, \omega) = (2\pi)n(\mathbf{k})\delta(\omega - \Omega(\mathbf{k}))$ we get $F(\mathbf{k}, \omega = 0) = 0 \Rightarrow n(\mathbf{k})\delta(\Omega(\mathbf{k})) = 0 \Rightarrow n(\mathbf{k}) = 0$ for $\Omega(\mathbf{k}) = 0$;
- $\Omega(\mathbf{k}_i) = \Omega(-\mathbf{k}_i)$;
- Interaction coefficients V_{ijk}, U_{ijk} are real;
- $A(\mathbf{k}_i) = A(-\mathbf{k}_i)$ and $B(\mathbf{k}_i) = B(-\mathbf{k}_i)$ for gravity-capillary waves, but due to the fact that velocity has to be real we have $A(\mathbf{k}_i) = -A^*(-\mathbf{k}_i)$ and $B(\mathbf{k}_i) = B^*(-\mathbf{k}_i)$.

We will assume things related to gravity-capillary waves, as they become necessary.

Terms λ_{aa}

$$\begin{aligned} \lambda_{aa} \equiv & \epsilon^4 (2\pi) \int d\mathbf{k}_{123} k_3^4 A_3 A_{-3} n_1 n_2 \left\{ \text{Re} \left[\frac{1}{4\Omega_3 \Omega_{-3}} [2(V_{123} V_{21(-3)} \delta\mathbf{k}_{1-2-3} + \right. \right. \\ & + V_{12(-3)} V_{213} \delta\mathbf{k}_{1-2+3}) \delta(\Omega_1 - \Omega_2) + (V_{312}^* U_{12(-3)} \delta\mathbf{k}_{3-1-2} + V_{(-3)12}^* U_{123} \delta\mathbf{k}_{1+2+3}) \delta(\Omega_1 + \Omega_2)] \left. \right] - \\ & \left. - \frac{1}{2\Omega_3^2} [2|V_{123}|^2 \delta\mathbf{k}_{1-2-3} \delta(\Omega_1 - \Omega_2) + |V_{312}|^2 \delta\mathbf{k}_{3-1-2} \delta(\Omega_1 + \Omega_2) + |U_{123}|^2 \delta\mathbf{k}_{3+1+2} \delta(\Omega_1 + \Omega_2)] \right\} \end{aligned}$$

Since $\Omega_i \geq 0$ we have that $n_i n_j \delta(\Omega_i + \Omega_j)$ is non-zero only for $\Omega_i = \Omega_j = 0$ for which $n_i = n_j = 0$, hence we have

$$\begin{aligned} \lambda_{aa} &= \epsilon^4 (2\pi) \int d\mathbf{k}_{123} k_3^4 |A_3|^2 n_1 n_2 \left\{ \text{Re} \left[\frac{1}{2\Omega_3 \Omega_{-3}} (V_{123} V_{21(-3)} \delta\mathbf{k}_{1-2-3} + \right. \right. \\ & \left. \left. + V_{12(-3)} V_{213} \delta\mathbf{k}_{1-2+3}) \delta(\Omega_1 - \Omega_2) \right] - \frac{1}{\Omega_3^2} |V_{123}|^2 \delta\mathbf{k}_{1-2-3} \delta(\Omega_1 - \Omega_2) \right\} \\ &= \epsilon^4 (2\pi) \int d\mathbf{k}_{123} k_3^4 |A_3|^2 n_1 n_2 \left[\frac{|V_{123}|^2}{\Omega_3^2} - \frac{\text{Re}(V_{123} V_{21(-3)})}{\Omega_3 \Omega_{-3}} \right] \delta(\Omega_1 - \Omega_2) \delta\mathbf{k}_{1-2-3} \quad (\text{C.68}) \end{aligned}$$

For gravity-capillary waves λ_{aa} is

$$\begin{aligned} \lambda_{aa} &= \epsilon^4 (2\pi) \int d\mathbf{k}_{123} k_3^4 A_3^2 n_1 n_2 \frac{1}{\Omega_3^2} \delta\mathbf{k}_{1-2-3} \delta(\Omega_1 - \Omega_2) V_{123} (V_{21(-3)} - V_{123}) \\ &= 0 \end{aligned}$$

One can check [38] that $(V_{21(-3)} - V_{123})\delta\mathbf{k}_{1-2-3}\delta(\Omega_1 - \Omega_2) = 0$ for gravity-capillary waves.

Terms λ_{aaa}

$$\begin{aligned}
 \lambda_{aaa} \simeq & -\epsilon^4 \int \frac{dq_{123}}{(2\pi)^{d+2}} \delta q_{1+2+3} |k_1| k_3^2 (\mathbf{k}_2 \cdot \mathbf{k}_3) (2\pi) \delta(\omega_3) A_1 B_2 A_3 \times \\
 & \times [-V_{-123} G_3 F_{-1} F_2 - V_{1-2-3}^* G_{-3}^* F_1 F_{-2} + V_{-213} G_3 F_1 F_{-2} + V_{2-1-3}^* G_{-3}^* F_{-1} F_2] \\
 & + \epsilon^4 \int \frac{dq_{123}}{(2\pi)^{d+2}} \delta q_{1+2+3} k_1^2 k_2^2 (\mathbf{k}_2 \cdot \mathbf{k}_3) A_1 A_2 A_3 \frac{i\pi}{\omega_3} \delta(\omega_1) \times \\
 & \times [-V_{-213} G_1 F_{-2} F_3 + V_{2-1-3}^* G_{-1}^* F_2 F_{-3} - V_{-312} G_1 F_2 F_{-3} + V_{3-1-2}^* G_{-1}^* F_{-2} F_3] \\
 & - \epsilon^4 \int \frac{dq_{123}}{(2\pi)^{d+2}} \delta q_{1+2+3} k_1^2 k_2^2 (\mathbf{k}_2 \cdot \mathbf{k}_3) A_1 A_2 A_3 \frac{i\pi}{\omega_3} \delta(\omega_2) \times \\
 & \times [-V_{-123} G_2 F_{-1} F_3 + V_{1-2-3}^* G_{-2}^* F_1 F_{-3} - V_{-312} G_2 F_1 F_{-3} + V_{3-1-2}^* G_{-2}^* F_{-1} F_3] \\
 & - \epsilon^4 \int \frac{dq_{123}}{(2\pi)^{d+2}} \delta q_{1+2+3} \frac{1}{2} k_1^2 k_2^2 k_3^2 A_1 A_2 A_3 \frac{1}{\omega_1 \omega_2} \times \\
 & \times [U_{123} (G_1 F_2 F_3 + G_2 F_1 F_3 + G_3 F_1 F_2) - U_{-1-2-3}^* (G_{-1}^* F_{-2} F_{-3} + G_{-2}^* F_{-1} F_{-3} + G_{-3}^* F_{-1} F_{-2}) \\
 & - V_{-123} (G_{-1}^* F_2 F_3 + G_2 F_{-1} F_3 + G_3 F_{-1} F_2) + V_{1-2-3}^* (G_1 n_{-2} F_{-3} + G_{-2}^* F_1 F_{-3} + G_{-3}^* F_1 F_{-2}) \\
 & - V_{-213} (G_1 F_{-2} F_3 + G_{-2}^* F_1 F_3 + G_3 F_1 F_{-2}) + V_{2-1-3}^* (G_{-1}^* F_2 F_{-3} + G_2 F_{-1} F_{-3} + G_{-3}^* F_{-1} F_2) \\
 & - V_{-312} (G_1 F_2 F_{-3} + G_2 F_1 F_{-3} + G_{-3}^* F_1 F_2) + V_{3-1-2}^* (G_{-1}^* F_{-2} F_3 + G_{-2}^* F_{-1} F_3 + G_3 F_{-1} F_{-2})]
 \end{aligned} \tag{C.69}$$

To calculate λ_{aaa} we introduce three terms

$$\lambda_{aaa} \equiv \lambda_{aaa1} + \lambda_{aaa2} + \lambda_{aaa3} \tag{C.70}$$

Term λ_{aaa1}

$$\begin{aligned}
 \lambda_{aaa1} \equiv & -\epsilon^4 \int \frac{dq_{123}}{(2\pi)^{d+2}} \delta q_{1+2+3} |k_1| k_3^2 (\mathbf{k}_2 \cdot \mathbf{k}_3) (2\pi) \delta(\omega_3) A_1 B_2 A_3 \times \\
 & \times [-V_{-123} G_3 F_{-1} F_2 - V_{1-2-3}^* G_{-3}^* F_1 F_{-2} + V_{-213} G_3 F_1 F_{-2} + V_{2-1-3}^* G_{-3}^* F_{-1} F_2] \\
 & + \epsilon^4 \int \frac{dq_{123}}{(2\pi)^{d+2}} \delta q_{1+2+3} k_1^2 k_2^2 (\mathbf{k}_2 \cdot \mathbf{k}_3) A_1 A_2 A_3 \frac{i\pi}{\omega_3} \delta(\omega_1) \times \\
 & \times [-V_{-213} G_1 F_{-2} F_3 + V_{2-1-3}^* G_{-1}^* F_2 F_{-3} - V_{-312} G_1 F_2 F_{-3} + V_{3-1-2}^* G_{-1}^* F_{-2} F_3]
 \end{aligned} \tag{C.71}$$

$$\begin{aligned}
& -\epsilon^4 \int \frac{dq_{123}}{(2\pi)^{d+2}} \delta_{q_{1+2+3}} k_1^2 k_2^2 (\mathbf{k}_2 \cdot \mathbf{k}_3) A_1 A_2 A_3 \frac{i\pi}{\omega_3} \delta(\omega_2) \times \\
& \times [-V_{-123} G_2 F_{-1} F_3 + V_{1-2-3}^* G_{-2}^* F_1 F_{-3} - V_{-312} G_2 F_1 F_{-3} + V_{3-1-2}^* G_{-2}^* F_{-1} F_3] \\
& = -\epsilon^4 \int \frac{dq_{123}}{(2\pi)^{d+2}} \delta_{q_{1+2+3}} |k_1| k_3^2 (\mathbf{k}_2 \cdot \mathbf{k}_3) (2\pi) \delta(\omega_3) A_1 B_2 A_3 \times \\
& \times [-V_{-123} G_3 F_{-1} F_2 - V_{1-2-3}^* G_{-3}^* F_1 F_{-2} + V_{-213} G_3 F_1 F_{-2} + V_{2-1-3}^* G_{-3}^* F_{-1} F_2] \\
& + \epsilon^4 \int \frac{dq_{123}}{(2\pi)^{d+2}} \delta_{q_{1+2+3}} k_1^2 k_2^2 (\mathbf{k}_1 \cdot \mathbf{k}_3) A_1 A_2 A_3 \frac{i\pi}{\omega_3} \delta(\omega_2) \times \\
& \times [-V_{-123} G_2 F_{-1} F_3 + V_{1-2-3}^* G_{-2}^* F_1 F_{-3} - V_{-312} G_2 F_1 F_{-3} + V_{3-1-2}^* G_{-2}^* F_{-1} F_3] \\
& - \epsilon^4 \int \frac{dq_{123}}{(2\pi)^{d+2}} \delta_{q_{1+2+3}} k_1^2 k_2^2 (\mathbf{k}_2 \cdot \mathbf{k}_3) A_1 A_2 A_3 \frac{i\pi}{\omega_3} \delta(\omega_2) \times \\
& \times [-V_{-123} G_2 F_{-1} F_3 + V_{1-2-3}^* G_{-2}^* F_1 F_{-3} - V_{-312} G_2 F_1 F_{-3} + V_{3-1-2}^* G_{-2}^* F_{-1} F_3]
\end{aligned}$$

here we exchanged q_1 and q_2 in integrals that were with $\delta(\omega_1)$. This gave us

$$\begin{aligned}
\lambda_{aaa1} & = -\epsilon^4 \int \frac{dq_{123}}{(2\pi)^{d+2}} \delta_{q_{1+2+3}} |k_1| k_3^2 (\mathbf{k}_2 \cdot \mathbf{k}_3) (2\pi) \delta(\omega_3) A_1 B_2 A_3 \times \\
& \times [-V_{-123} G_3 F_{-1} F_2 - V_{1-2-3}^* G_{-3}^* F_1 F_{-2} + V_{-213} G_3 F_1 F_{-2} + V_{2-1-3}^* G_{-3}^* F_{-1} F_2] \\
& + \epsilon^4 \int \frac{dq_{123}}{(2\pi)^{d+2}} \delta_{q_{1+2+3}} k_1^2 k_2^2 ((\mathbf{k}_1 - \mathbf{k}_2) \cdot \mathbf{k}_3) A_1 A_2 A_3 \frac{i\pi}{\omega_3} \delta(\omega_2) \times \\
& \times [V_{3-1-2}^* G_{-2}^* F_{-1} F_3 - V_{-123} G_2 F_{-1} F_3] \\
& - \epsilon^4 \int \frac{dq_{123}}{(2\pi)^{d+2}} \delta_{q_{1+2+3}} k_1^2 k_2^2 ((\mathbf{k}_1 - \mathbf{k}_2) \cdot \mathbf{k}_3) A_1^* A_2^* A_3^* \frac{i\pi}{\omega_3} \delta(\omega_2) \times \\
& \times [V_{3-1-2} G_{-2} F_{-1} F_3 - V_{-123}^* G_2^* F_{-1} F_3]
\end{aligned}$$

Hence we get

$$\begin{aligned}
\lambda_{aaa1} & = -\epsilon^4 \int \frac{dq_{123}}{(2\pi)^{d+2}} \delta_{q_{1+2+3}} |k_1| k_3^2 (\mathbf{k}_2 \cdot \mathbf{k}_3) (2\pi) \delta(\omega_3) A_1 B_2 A_3 \times \\
& \times [-V_{-123} G_3 F_{-1} F_2 - V_{1-2-3}^* G_{-3}^* F_1 F_{-2} + V_{-213} G_3 F_1 F_{-2} + V_{2-1-3}^* G_{-3}^* F_{-1} F_2] \\
& + 2\text{Re} \left[\epsilon^4 \int \frac{dq_{123}}{(2\pi)^{d+2}} \delta_{q_{1+2+3}} k_1^2 k_2^2 ((\mathbf{k}_1 - \mathbf{k}_2) \cdot \mathbf{k}_3) A_1 A_2 A_3 \frac{i\pi}{\omega_3} \delta(\omega_2) \times \right. \\
& \left. \times [V_{3-1-2}^* G_{-2}^* - V_{-123} G_2] F_{-1} F_3 \right]
\end{aligned}$$

$$\begin{aligned}
 \lambda_{aaa1} &= 2\text{Re} \left[\epsilon^4 \pi \int \frac{dq_{123}}{(2\pi)^{d+2}} \delta q_{1+2+3} |k_1| k_3^2 (\mathbf{k}_2 \cdot \mathbf{k}_3) (2\pi) \delta(\omega_3) A_1 B_2 A_3 \times \right. \\
 &\quad \left. \times [V_{1-2-3}^* G_{-3}^* - V_{-213} G_3] F_1 F_{-2} \right] \\
 &+ 2\text{Re} \left[\epsilon^4 \int \frac{dq_{123}}{(2\pi)^{d+2}} \delta q_{1+2+3} k_1^2 k_2^2 ((\mathbf{k}_1 - \mathbf{k}_2) \cdot \mathbf{k}_3) A_1 A_2 A_3 \frac{i\pi}{\omega_3} \delta(\omega_2) \times \right. \\
 &\quad \left. \times [V_{3-1-2}^* G_{-2}^* - V_{-123} G_2] F_{-1} F_3 \right] \tag{C.72}
 \end{aligned}$$

The difference $(V_{3-1-2}^* G_{-2}^* - V_{-123} G_2) \delta q_{1+2+3} \delta(\omega_2)$ gives zero for gravity-capillary waves and both terms can be reduced to this difference.

Term λ_{aaa2}

$$\begin{aligned}
 \lambda_{aaa2} &\equiv -\epsilon^4 \int \frac{dq_{123}}{(2\pi)^{d+2}} \delta q_{1+2+3} \frac{1}{2} k_1^2 k_2^2 k_3^2 A_1 A_2 A_3 \frac{1}{\omega_1 \omega_2} \times \\
 &\quad \times [U_{123} (G_1 F_2 F_3 + G_2 F_1 F_3 + G_3 F_1 F_2) - U_{-1-2-3}^* (G_{-1}^* F_{-2} F_{-3} + G_{-2}^* F_{-1} F_{-3} + G_{-3}^* F_{-1} F_{-2}) \\
 &\quad - \epsilon^4 \int \frac{dq_{123}}{(2\pi)^{d+2}} \delta q_{1+2+3} \frac{1}{2} k_1^2 k_2^2 k_3^2 \frac{1}{\omega_1 \omega_2} \times \\
 &\quad \times [A_1 A_2 A_3 U_{123} (G_1 F_2 F_3 + G_2 F_1 F_3 + G_3 F_1 F_2) + A_1^* A_2^* A_3^* U_{123}^* (G_1^* F_2 F_3 + G_2^* F_1 F_3 + G_3^* F_1 F_2)
 \end{aligned} \tag{C.73}$$

where we changed variables $q_i \rightarrow -q_i$ in the term with U_{-1-2-3}^* . $A_{-1} = -A_1^*$ comes from asking the velocity to be real, however for gravity capillary waves even more is true $A_1 = A_{-1} = -A_1^*$.

$$\begin{aligned}
 \lambda_{aaa2} &= -\text{Re} \left[\epsilon^4 \int \frac{dq_{123}}{(2\pi)^{d+2}} \delta q_{1+2+3} \frac{k_1^2 k_2^2 k_3^2 A_1 A_2 A_3 U_{123}}{\omega_1 \omega_2} (G_1 F_2 F_3 + G_2 F_1 F_3 + G_3 F_1 F_2) \right] \\
 &= \text{Re} \left[\epsilon^4 \int \frac{d\mathbf{k}_{123} \delta \mathbf{k}_{1+2+3} k_1^2 k_2^2 k_3^2 A_1 A_2 A_3 U_{123}}{(2\pi)^d (\Omega_1 + \Omega_2 + \Omega_3 - i\gamma_0)} \left(\frac{n_1 n_2}{\Omega_1 \Omega_2} - \frac{n_1 n_3}{\Omega_1 (\Omega_1 + \Omega_3)} - \frac{n_2 n_3}{\Omega_2 (\Omega_2 + \Omega_3)} \right) \right] \\
 &= \text{Re} \left[\epsilon^4 \int \frac{d\mathbf{k}_{123} \delta \mathbf{k}_{1+2+3} k_1^2 k_2^2 k_3^2 A_1 A_2 A_3 U_{123} n_1 n_2}{(2\pi)^d (\Omega_1 + \Omega_2 + \Omega_3 - i\gamma_0)} \left(\frac{1}{\Omega_1 \Omega_2} - \frac{1}{\Omega_1 (\Omega_1 + \Omega_2)} - \frac{1}{(\Omega_1 + \Omega_2) \Omega_2} \right) \right] \\
 \lambda_{aaa2} &= 0 \tag{C.74}
 \end{aligned}$$

here we assumed $\gamma_0(\mathbf{k}) \equiv \gamma_0$ does not depend on \mathbf{k} , which is fine, since no result should depend on γ_0 and it is small. It just shows how to take the contour integrals. Also to make the last step we changed in such way indices to have all terms with $n_1 n_2$.

Term λ_{aaa3}

$$\begin{aligned}
\lambda_{aaa3} &\equiv -\epsilon^4 \int \frac{dq_{123}}{(2\pi)^{d+2}} \delta q_{1+2+3} \frac{1}{2} k_1^2 k_2^2 k_3^2 A_1 A_2 A_3 \frac{1}{\omega_1 \omega_2} \times \\
&\times [V_{1-2-3}^*(G_1 n_{-2} F_{-3} + G_{-2}^* F_1 F_{-3} + G_{-3}^* F_1 F_{-2}) - V_{-123}(G_{-1}^* F_2 F_3 + G_2 F_{-1} F_3 + G_3 F_{-1} F_2) + \\
&+ V_{2-1-3}^*(G_{-1}^* F_2 F_{-3} + G_2 F_{-1} F_{-3} + G_{-3}^* F_{-1} F_2) - V_{-213}(G_1 F_{-2} F_3 + G_{-2}^* F_1 F_3 + G_3 F_1 F_{-2}) + \\
&+ V_{3-1-2}^*(G_{-1}^* F_{-2} F_3 + G_{-2}^* F_{-1} F_3 + G_3 F_{-1} F_{-2}) - V_{-312}(G_1 F_2 F_{-3} + G_2 F_1 F_{-3} + G_{-3}^* F_1 F_2)] \\
&= -\epsilon^4 \int \frac{dq_{123}}{(2\pi)^{d+2}} \delta q_{1+2+3} \frac{1}{2} k_1^2 k_2^2 k_3^2 A_1 A_2 A_3 \frac{1}{\omega_1} \left(\frac{1}{\omega_2} - \frac{1}{\omega_3} \right) \times \\
&\times [V_{1-2-3}^*(G_1 n_{-2} F_{-3} + G_{-2}^* F_1 F_{-3} + G_{-3}^* F_1 F_{-2}) - V_{-123}(G_{-1}^* F_2 F_3 + G_2 F_{-1} F_3 + G_3 F_{-1} F_2)] \\
\lambda_{aaa3} &= 0
\end{aligned} \tag{C.75}$$

here we changed variables of integration so that all terms depend on V_{1-2-3}^* and V_{-123} and used $\delta\omega_{1+2+3}$, then we arrived expression above, which to show that it is zero it is enough to change $q_2 \leftrightarrow q_3$ in $1/\omega_3$ term.

C.11 Term λ_{aaaa}

$$\begin{aligned}
\lambda_{aaaa} &= \epsilon^4 \int \frac{dq_{1234}}{(2\pi)^{4d+4}} (2\pi)^{2d+2} \times \\
&\times \left\{ \frac{|k_1|}{2} (\mathbf{k}_1 \cdot \mathbf{k}_2 + k_2^2) |k_3| (\mathbf{k}_3 \cdot \mathbf{k}_4 + k_4^2) (2\pi) \delta(\omega_3 + \omega_4) \times \right. \\
&\times A_1 B_2 A_3 B_4 [-(F_1 F_2 + F_{-1} F_{-2}) (\delta q_{1+3} \delta q_{2+4} + \delta q_{1+4} \delta q_{2+3}) \\
&+ (F_{-1} F_{-3} + F_1 F_3) (\delta q_{1+2} \delta q_{3+4} + \delta q_{1+4} \delta q_{2+3}) - (F_{-1} F_{-4} + F_1 F_4) (\delta q_{1+2} \delta q_{3+4} + \delta q_{1+3} \delta q_{2+4})] \\
&+ |k_1| (\mathbf{k}_1 \cdot \mathbf{k}_2 + k_2^2) k_3^2 (\mathbf{k}_3 \cdot \mathbf{k}_4) \left[\frac{i\pi \delta(\omega_3 + \omega_4)}{\omega_4} - \frac{i\pi \delta(\omega_3)}{\omega_4} - \frac{1}{\omega_3(\omega_3 + \omega_4)} \right] \times \\
&\times A_1 B_2 A_3 A_4 [(F_1 F_2 - F_{-1} F_{-2}) (\delta q_{1+3} \delta q_{2+4} + \delta q_{1+4} \delta q_{2+3}) + (F_{-1} F_{-3} - F_1 F_3) (\delta q_{1+2} \delta q_{3+4} + \\
&+ \delta q_{1+4} \delta q_{2+3}) + (F_{-1} F_{-4} - F_1 F_4) (\delta q_{1+2} \delta q_{3+4} + \delta q_{1+3} \delta q_{2+4})] + k_1^2 |k_2| (\mathbf{k}_2 \cdot \mathbf{k}_3 + k_3^2) \times \\
&\times (\mathbf{k}_2 \cdot \mathbf{k}_4 + \mathbf{k}_3 \cdot \mathbf{k}_4) \left[\frac{i\pi [\delta(\omega_2 + \omega_3 + \omega_4) - \delta(\omega_2 + \omega_3)]}{\omega_4} - \frac{1}{(\omega_2 + \omega_3)(\omega_2 + \omega_3 + \omega_4)} \right] \times
\end{aligned} \tag{C.77}$$

$$\begin{aligned}
 & \times A_1 A_2 B_3 A_4 [(F_1 F_3 - F_{-1} F_{-3})(\delta q_{1+2} \delta q_{3+4} + \delta q_{1+4} \delta q_{2+3}) \\
 & + (F_{-1} F_{-2} - F_1 F_2)(\delta q_{1+3} \delta q_{2+4} + \delta q_{1+4} \delta q_{2+3}) + (F_{-1} F_{-4} - F_1 F_4)(\delta q_{1+3} \delta q_{2+4} + \delta q_{1+2} \delta q_{3+4})] \\
 & + k_1^2 k_2^2 (\mathbf{k}_2 \cdot \mathbf{k}_4) |k_3| \left[\frac{i\pi \delta(\omega_2 + \omega_3 + \omega_4)}{\omega_3 + \omega_4} - \frac{1}{\omega_2(\omega_2 + \omega_3 + \omega_4)} - \frac{i\pi \delta(\omega_2)}{\omega_3 + \omega_4} \right] \times \\
 & \times A_1 A_2 A_3 B_4 [(F_1 F_4 - F_{-1} F_{-4})(\delta q_{1+3} \delta q_{2+4} + \delta q_{1+2} \delta q_{3+4}) + \\
 & + (F_{-1} F_{-3} - F_1 F_3)(\delta q_{1+4} \delta q_{2+3} + \delta q_{1+2} \delta q_{3+4}) + (F_{-1} F_{-2} - F_1 F_2)(\delta q_{1+4} \delta q_{2+3} + \delta q_{1+3} \delta q_{2+4})] \\
 & + k_1^2 k_2^2 (\mathbf{k}_2 \cdot \mathbf{k}_3) (\mathbf{k}_3 \cdot \mathbf{k}_4) \left[-\frac{\pi \delta(\omega_2 + \omega_3 + \omega_4)}{(\omega_3 + \omega_4) \omega_4} + \frac{1}{i\omega_2(\omega_2 + \omega_3 + \omega_4) \omega_4} + \right. \\
 & \left. + \frac{\pi \delta(\omega_2)}{(\omega_3 + \omega_4) \omega_4} + \frac{\pi \delta(\omega_2 + \omega_3)}{\omega_3 \omega_4} - \frac{\pi \delta(\omega_2)}{\omega_3 \omega_4} - \frac{1}{i\omega_2(\omega_2 + \omega_3) \omega_4} \right] \times \\
 & \times A_1 A_2 A_3 A_4 [(F_1 F_2 + F_{-1} F_{-2})(\delta q_{1+3} \delta q_{2+4} + \delta q_{1+4} \delta q_{2+3}) \\
 & + (F_{-1} F_{-3} + F_1 F_3)(\delta q_{1+2} \delta q_{3+4} + \delta q_{1+4} \delta q_{2+3}) + (F_{-1} F_{-4} + F_1 F_4)(\delta q_{1+2} \delta q_{3+4} + \delta q_{1+3} \delta q_{2+4})] \\
 & + \frac{1}{2} k_1^2 k_2^2 (\mathbf{k}_2 \cdot \mathbf{k}_3) (\mathbf{k}_2 \cdot \mathbf{k}_4) \left[-\frac{\pi \delta(\omega_2 + \omega_3 + \omega_4)}{\omega_3 \omega_4} + \frac{1}{i(\omega_2 + \omega_3 + \omega_4)(\omega_2 + \omega_4) \omega_4} + \frac{\pi \delta(\omega_2 + \omega_4)}{\omega_3 \omega_4} \right. \\
 & \left. + \frac{\pi \delta(\omega_2 + \omega_3)}{\omega_3 \omega_4} - \frac{1}{i\omega_2(\omega_2 + \omega_3) \omega_4} - \frac{\delta(\omega_2)}{\omega_3 \omega_4} \right] \times \\
 & \times A_1 A_2 A_3 A_4 [(F_1 F_2 + F_{-1} F_{-2})(\delta q_{1+3} \delta q_{2+4} + \delta q_{1+4} \delta q_{2+3}) \\
 & + (F_{-1} F_{-3} + F_1 F_3)(\delta q_{1+2} \delta q_{3+4} + \delta q_{1+4} \delta q_{2+3}) + (F_{-1} F_{-4} + F_1 F_4)(\delta q_{1+2} \delta q_{3+4} + \delta q_{1+3} \delta q_{2+4})] \Big\}
 \end{aligned}$$

Since we assume $F(\mathbf{k}, \omega = 0) = 0$ all $\delta(\omega_i + \omega_j + \omega_k)$ and $\delta(\omega_i)$ give zero and we obtain

$$\begin{aligned}
 \lambda_{aaaa} &= \epsilon^4 \int \frac{dq_{1234}}{(2\pi)^{4d+4}} (2\pi)^{2d+2} \times \tag{C.78} \\
 & \times \left\{ \frac{|k_1|}{2} (\mathbf{k}_1 \cdot \mathbf{k}_2 + k_2^2) |k_3| (\mathbf{k}_3 \cdot \mathbf{k}_4 + k_4^2) (2\pi) \delta(\omega_3 + \omega_4) \times \right. \\
 & \times A_1 B_2 A_3 B_4 [-(F_1 F_2 + F_{-1} F_{-2})(\delta q_{1+3} \delta q_{2+4} + \delta q_{1+4} \delta q_{2+3}) \\
 & + (F_{-1} F_{-3} + F_1 F_3)(\delta q_{1+2} \delta q_{3+4} + \delta q_{1+4} \delta q_{2+3}) - (F_{-1} F_{-4} + F_1 F_4)(\delta q_{1+2} \delta q_{3+4} + \delta q_{1+3} \delta q_{2+4})] \\
 & + |k_1| (\mathbf{k}_1 \cdot \mathbf{k}_2 + k_2^2) k_3^2 (\mathbf{k}_3 \cdot \mathbf{k}_4) \left[\frac{i\pi \delta(\omega_3 + \omega_4)}{\omega_4} - \frac{1}{\omega_3(\omega_3 + \omega_4)} \right] \times \\
 & \times A_1 B_2 A_3 A_4 [(F_1 F_2 - F_{-1} F_{-2})(\delta q_{1+3} \delta q_{2+4} + \delta q_{1+4} \delta q_{2+3}) + (F_{-1} F_{-3} - F_1 F_3)(\delta q_{1+2} \delta q_{3+4} + \\
 & + \delta q_{1+4} \delta q_{2+3}) + (F_{-1} F_{-4} - F_1 F_4)(\delta q_{1+2} \delta q_{3+4} + \delta q_{1+3} \delta q_{2+4})] + k_1^2 |k_2| (\mathbf{k}_2 \cdot \mathbf{k}_3 + k_3^2) \times
 \end{aligned}$$

$$\begin{aligned}
& \times (\mathbf{k}_2 \cdot \mathbf{k}_4 + \mathbf{k}_3 \cdot \mathbf{k}_4) \left[-\frac{i\pi\delta(\omega_2 + \omega_3)}{\omega_4} - \frac{1}{(\omega_2 + \omega_3)(\omega_2 + \omega_3 + \omega_4)} \right] \times \\
& \times A_1 A_2 B_3 A_4 [(F_1 F_3 - F_{-1} F_{-3})(\delta q_{1+2} \delta q_{3+4} + \delta q_{1+4} \delta q_{2+3}) \\
& + (F_{-1} F_{-2} - F_1 F_2)(\delta q_{1+3} \delta q_{2+4} + \delta q_{1+4} \delta q_{2+3}) + (F_{-1} F_{-4} - F_1 F_4)(\delta q_{1+3} \delta q_{2+4} + \delta q_{1+2} \delta q_{3+4})] \\
& + k_1^2 k_2^2 (\mathbf{k}_2 \cdot \mathbf{k}_4) |k_3| \left[-\frac{1}{\omega_2(\omega_2 + \omega_3 + \omega_4)} \right] \times \\
& \times A_1 A_2 A_3 B_4 [(F_1 F_4 - F_{-1} F_{-4})(\delta q_{1+3} \delta q_{2+4} + \delta q_{1+2} \delta q_{3+4}) + \\
& + (F_{-1} F_{-3} - F_1 F_3)(\delta q_{1+4} \delta q_{2+3} + \delta q_{1+2} \delta q_{3+4}) + (F_{-1} F_{-2} - F_1 F_2)(\delta q_{1+4} \delta q_{2+3} + \delta q_{1+3} \delta q_{2+4})] \\
& + k_1^2 k_2^2 (\mathbf{k}_2 \cdot \mathbf{k}_3) (\mathbf{k}_3 \cdot \mathbf{k}_4) \left[-\frac{1}{i\omega_2(\omega_2 + \omega_3)(\omega_2 + \omega_3 + \omega_4)} + \frac{\pi\delta(\omega_2 + \omega_3)}{\omega_3\omega_4} \right] \times \\
& \times A_1 A_2 A_3 A_4 [(F_1 F_2 + F_{-1} F_{-2})(\delta q_{1+3} \delta q_{2+4} + \delta q_{1+4} \delta q_{2+3}) \\
& + (F_{-1} F_{-3} + F_1 F_3)(\delta q_{1+2} \delta q_{3+4} + \delta q_{1+4} \delta q_{2+3}) + (F_{-1} F_{-4} + F_1 F_4)(\delta q_{1+2} \delta q_{3+4} + \delta q_{1+3} \delta q_{2+4})] \\
& + \frac{1}{2} k_1^2 k_2^2 (\mathbf{k}_2 \cdot \mathbf{k}_3) (\mathbf{k}_2 \cdot \mathbf{k}_4) \left[\frac{1}{i(\omega_2 + \omega_3 + \omega_4)(\omega_2 + \omega_4)\omega_4} + \frac{\pi\delta(\omega_2 + \omega_4)}{\omega_3\omega_4} \right. \\
& \left. + \frac{\pi\delta(\omega_2 + \omega_3)}{\omega_3\omega_4} - \frac{1}{i\omega_2(\omega_2 + \omega_3)\omega_4} \right] A_1 A_2 A_3 A_4 [(F_1 F_2 + F_{-1} F_{-2})(\delta q_{1+3} \delta q_{2+4} + \delta q_{1+4} \delta q_{2+3}) \\
& + (F_{-1} F_{-3} + F_1 F_3)(\delta q_{1+2} \delta q_{3+4} + \delta q_{1+4} \delta q_{2+3}) + (F_{-1} F_{-4} + F_1 F_4)(\delta q_{1+2} \delta q_{3+4} + \delta q_{1+3} \delta q_{2+4})] \Big\}
\end{aligned}$$

We calculate λ_{aaaa} as a sum of five terms

$$\lambda_{aaaa} \equiv \lambda_{aaaa1} + \lambda_{aaaa2} + \lambda_{aaaa3} + \lambda_{aaaa4} + \lambda_{aaaa5} \quad (\text{C.79})$$

Term λ_{aaaa1}

$$\begin{aligned}
\lambda_{aaaa1} & \equiv \epsilon^4 \int \frac{dq_{1234}}{(2\pi)^{4d+4}} (2\pi)^{2d+2} \times \quad (\text{C.80}) \\
& \frac{|k_1|}{2} (\mathbf{k}_1 \cdot \mathbf{k}_2 + k_2^2) |k_3| (\mathbf{k}_3 \cdot \mathbf{k}_4 + k_4^2) (2\pi) \delta(\omega_3 + \omega_4) \times \\
& \times A_1 B_2 A_3 B_4 [-(F_1 F_2 + F_{-1} F_{-2})(\delta q_{1+3} \delta q_{2+4} + \delta q_{1+4} \delta q_{2+3}) \\
& + (F_{-1} F_{-3} + F_1 F_3)(\delta q_{1+2} \delta q_{3+4} + \delta q_{1+4} \delta q_{2+3}) - (F_{-1} F_{-4} + F_1 F_4)(\delta q_{1+2} \delta q_{3+4} + \delta q_{1+3} \delta q_{2+4})] \\
& = -\pi \epsilon^4 \int \frac{dq_{1234}}{(2\pi)^{2d+2}} (F_1 F_2 + F_{-1} F_{-2})(\delta q_{1+3} \delta q_{2+4} + \delta q_{1+4} \delta q_{2+3}) \times
\end{aligned}$$

$$\begin{aligned}
 & \times \left[|k_1|(\mathbf{k}_1 \cdot \mathbf{k}_2 + k_2^2)|k_3|(\mathbf{k}_3 \cdot \mathbf{k}_4 + k_4^2)\delta(\omega_3 + \omega_4)A_1B_2A_3B_4 - \right. \\
 & - |k_1|(\mathbf{k}_1 \cdot \mathbf{k}_3 + k_3^2)|k_2|(\mathbf{k}_2 \cdot \mathbf{k}_4 + k_4^2)\delta(\omega_2 + \omega_4)A_1A_2B_3B_4 \\
 & \left. + |k_1|(\mathbf{k}_1 \cdot \mathbf{k}_4 + k_4^2)|k_3|(\mathbf{k}_2 \cdot \mathbf{k}_3 + k_2^2)\delta(\omega_2 + \omega_3)A_1B_2A_3B_4 \right] \\
 & = -\pi\epsilon^4 \int \frac{dq_{12}}{(2\pi)^{2d+2}} (F_1F_2 + F_{-1}F_{-2})|k_1|(\mathbf{k}_1 \cdot \mathbf{k}_2 - k_2^2)\delta(\omega_1 - \omega_2) \times \\
 & \times \left[|k_1|(\mathbf{k}_2 \cdot \mathbf{k}_1 - k_1^2)A_1B_2A_{-1}B_{-2} - |k_2|(\mathbf{k}_2 \cdot \mathbf{k}_1 - k_1^2)A_1A_2B_{-1}B_{-2} \right] \\
 & = 2\pi\epsilon^4 \int \frac{dq_{12}}{(2\pi)^{2d+2}} F_1F_2|k_1|(\mathbf{k}_1 \cdot \mathbf{k}_2 - k_2^2)\delta(\omega_1 - \omega_2) \times \\
 & \times \left[|k_1|(\mathbf{k}_1 \cdot \mathbf{k}_2 - k_2^2)|A_1B_2|^2 + |k_2|(\mathbf{k}_1 \cdot \mathbf{k}_2 - k_1^2)\text{Re}(A_1A_2B_1^*B_2^*) \right]
 \end{aligned}$$

$$\begin{aligned}
 \lambda_{aaaa1} &= 2\pi\epsilon^4 \int \frac{d\mathbf{k}_{12}}{(2\pi)^{2d}} n_1n_2\delta(\Omega_1 - \Omega_2) \times \\
 & \times \left[|k_1|^2(\mathbf{k}_1 \cdot \mathbf{k}_2 - k_2^2)^2|A_1B_2|^2 + |k_2||k_1|(\mathbf{k}_1 \cdot \mathbf{k}_2 - k_2^2)(\mathbf{k}_1 \cdot \mathbf{k}_2 - k_1^2)\text{Re}(A_1A_2B_1^*B_2^*) \right]
 \end{aligned} \tag{C.81}$$

For gravity-capillary waves

$$\begin{aligned}
 \lambda_{aaaa1} &= \frac{\pi}{2}\epsilon^4 \int \frac{d\mathbf{k}_{12}}{(2\pi)^{2d}} n_1n_2\delta(\Omega_1 - \Omega_2)|k_1||k_2| \times \\
 & \times \left[(\mathbf{k}_1 \cdot \mathbf{k}_2 - k_2^2)^2 - (\mathbf{k}_1 \cdot \mathbf{k}_2 - k_2^2)(\mathbf{k}_1 \cdot \mathbf{k}_2 - k_1^2) \right] \\
 & = \frac{\pi}{2}\epsilon^4 \int \frac{d\mathbf{k}_{12}}{(2\pi)^{2d}} n_1n_2\delta(\Omega_1 - \Omega_2)|k_1||k_2|(\mathbf{k}_1 \cdot \mathbf{k}_2 - k_2^2)(k_1^2 - k_2^2) \\
 & = 0
 \end{aligned} \tag{C.82}$$

Term λ_{aaaa2}

$$\begin{aligned}
 \lambda_{aaaa2} &\equiv \epsilon^4 \int \frac{dq_{1234}}{(2\pi)^{4d+4}} (2\pi)^{2d+2} \times \\
 & \times |k_1|(\mathbf{k}_1 \cdot \mathbf{k}_2 + k_2^2)k_3^2(\mathbf{k}_3 \cdot \mathbf{k}_4) \left[\frac{i\pi\delta(\omega_3 + \omega_4)}{\omega_4} - \frac{1}{\omega_3(\omega_3 + \omega_4)} \right] \times \\
 & \times A_1B_2A_3A_4[(F_1F_2 - F_{-1}F_{-2})(\delta q_{1+3}\delta q_{2+4} + \delta q_{1+4}\delta q_{2+3}) + (F_{-1}F_{-3} - F_1F_3)(\delta q_{1+2}\delta q_{3+4} +
 \end{aligned} \tag{C.83}$$

$$\begin{aligned}
& + \delta q_{1+4} \delta q_{2+3}) + (F_{-1} F_{-4} - F_1 F_4) (\delta q_{1+2} \delta q_{3+4} + \delta q_{1+3} \delta q_{2+4})] \\
& = \epsilon^4 \int \frac{dq_{1234}}{(2\pi)^{4d+4}} (2\pi)^{2d+2} (F_1 F_2 - F_{-1} F_{-2}) (\delta q_{1+3} \delta q_{2+4} + \delta q_{1+4} \delta q_{2+3}) \times \\
& \times \left[|k_1| (\mathbf{k}_1 \cdot \mathbf{k}_2 + k_2^2) k_3^2 (\mathbf{k}_3 \cdot \mathbf{k}_4) \left[\frac{i\pi \delta(\omega_3 + \omega_4)}{\omega_4} - \frac{1}{\omega_3(\omega_3 + \omega_4)} \right] A_1 B_2 A_3 A_4 \right. \\
& - |k_1| (\mathbf{k}_1 \cdot \mathbf{k}_3 + k_3^2) k_2^2 (\mathbf{k}_2 \cdot \mathbf{k}_4) \left[\frac{i\pi \delta(\omega_2 + \omega_4)}{\omega_4} - \frac{1}{\omega_2(\omega_2 + \omega_4)} \right] A_1 A_2 B_3 A_4 \\
& \left. - |k_1| (\mathbf{k}_1 \cdot \mathbf{k}_4 + k_4^2) k_3^2 (\mathbf{k}_2 \cdot \mathbf{k}_3) \left[\frac{i\pi \delta(\omega_2 + \omega_3)}{\omega_2} - \frac{1}{\omega_3(\omega_2 + \omega_3)} \right] A_1 A_3 A_2 B_4 \right] \\
& = \epsilon^4 \int \frac{dq_{12}}{(2\pi)^{4d+4}} (2\pi)^{2d+2} (F_1 F_2 - F_{-1} F_{-2}) \times \\
& \times \left[- |k_1| (\mathbf{k}_1 \cdot \mathbf{k}_2 + k_2^2) k_1^2 (\mathbf{k}_1 \cdot \mathbf{k}_2) \frac{1}{\omega_1(\omega_1 + \omega_2)} A_1 B_2 A_{-1} A_{-2} \right. \\
& + |k_1| (-\mathbf{k}_1 \cdot \mathbf{k}_2 + k_2^2) k_1^2 (\mathbf{k}_1 \cdot \mathbf{k}_2) \left[\frac{i\pi \delta(\omega_1 - \omega_2)}{\omega_1} - \frac{1}{\omega_1(\omega_1 - \omega_2)} \right] A_1 A_{-1} A_2 B_{-2} \\
& - |k_1| (\mathbf{k}_1 \cdot \mathbf{k}_2 + k_2^2) k_2^2 (\mathbf{k}_1 \cdot \mathbf{k}_2) \frac{1}{\omega_2(\omega_1 + \omega_2)} A_1 A_{-1} A_{-2} B_2 \\
& \left. - |k_1| (-\mathbf{k}_1 \cdot \mathbf{k}_2 + k_2^2) k_2^2 (\mathbf{k}_1 \cdot \mathbf{k}_2) \left[\frac{i\pi \delta(\omega_1 - \omega_2)}{\omega_1} - \frac{1}{\omega_2(\omega_1 - \omega_2)} \right] A_1 A_{-1} A_2 B_{-2} \right] = \\
& = \epsilon^4 \int \frac{dq_{12}}{(2\pi)^{4d+4}} (2\pi)^{2d+2} F_1 F_2 \left\{ |k_1| (\mathbf{k}_1 \cdot \mathbf{k}_2) \times \right. \\
& \times \left[- (\mathbf{k}_1 \cdot \mathbf{k}_2 + k_2^2) k_1^2 \frac{1}{\omega_1(\omega_1 + \omega_2)} A_1 A_{-1} A_{-2} B_2 + (-\mathbf{k}_1 \cdot \mathbf{k}_2 + k_2^2) k_1^2 \frac{1}{\omega_1(\omega_1 - \omega_2)} A_1 A_{-1} A_2 B_{-2} \right. \\
& + (-\mathbf{k}_1 \cdot \mathbf{k}_2 + k_2^2) k_2^2 \frac{1}{\omega_2(\omega_1 - \omega_2)} A_1 A_{-1} A_2 B_{-2} - (\mathbf{k}_1 \cdot \mathbf{k}_2 + k_2^2) k_2^2 \frac{1}{\omega_2(\omega_1 + \omega_2)} A_1 A_{-1} A_{-2} B_2 \\
& + (\mathbf{k}_1 \cdot \mathbf{k}_2 + k_2^2) k_1^2 \frac{1}{\omega_1(\omega_1 + \omega_2)} A_1 A_{-1} A_2 B_{-2} - (-\mathbf{k}_1 \cdot \mathbf{k}_2 + k_2^2) k_1^2 \frac{1}{\omega_1(\omega_1 - \omega_2)} A_1 A_{-1} A_{-2} B_2 \\
& \left. - (-\mathbf{k}_1 \cdot \mathbf{k}_2 + k_2^2) k_2^2 \frac{1}{\omega_2(\omega_1 - \omega_2)} A_1 A_{-1} A_{-2} B_2 + (\mathbf{k}_1 \cdot \mathbf{k}_2 + k_2^2) k_2^2 \frac{1}{\omega_2(\omega_1 + \omega_2)} A_1 A_{-1} A_2 B_{-2} \right] \\
& \left. + |k_1| (-\mathbf{k}_1 \cdot \mathbf{k}_2 + k_2^2) (k_1^2 - k_2^2) (\mathbf{k}_1 \cdot \mathbf{k}_2) \frac{i\pi \delta(\omega_1 - \omega_2)}{\omega_1} (A_1 A_{-1} A_{-2} B_2 + A_1 A_{-1} A_2 B_{-2}) \right\}
\end{aligned}$$

If we take $A_i = A_{-i}$ and $B_i = B_{-i}$, which is true for gravity-capillary waves we get

$$\begin{aligned}
\lambda_{aaaa2} & = \frac{\pi}{2} \epsilon^4 \int \frac{d\mathbf{k}_{12}}{(2\pi)^{2d}} n_1 n_2 (k_2^2 - \mathbf{k}_1 \cdot \mathbf{k}_2) (k_1^2 - k_2^2) (\mathbf{k}_1 \cdot \mathbf{k}_2) \delta(\Omega_1 - \Omega_2) \\
& = 0
\end{aligned} \tag{C.84}$$

Term λ_{aaaa3}

$$\begin{aligned}
 \lambda_{aaaa3} &\equiv \epsilon^4 \int \frac{dq_{1234}}{(2\pi)^{4d+4}} (2\pi)^{2d+2} k_1^2 |k_2| (\mathbf{k}_2 \cdot \mathbf{k}_3 + k_3^2) \times \\
 &\times (\mathbf{k}_2 \cdot \mathbf{k}_4 + \mathbf{k}_3 \cdot \mathbf{k}_4) \left[\frac{-i\pi\delta(\omega_2 + \omega_3)}{\omega_4} - \frac{1}{(\omega_2 + \omega_3)(\omega_2 + \omega_3 + \omega_4)} \right] \times \\
 &\times A_1 A_2 B_3 A_4 [(F_1 F_3 - F_{-1} F_{-3})(\delta q_{1+2} \delta q_{3+4} + \delta q_{1+4} \delta q_{2+3}) \\
 &+ (F_{-1} F_{-2} - F_1 F_2)(\delta q_{1+3} \delta q_{2+4} + \delta q_{1+4} \delta q_{2+3}) + (F_{-1} F_{-4} - F_1 F_4)(\delta q_{1+3} \delta q_{2+4} + \delta q_{1+2} \delta q_{3+4})] \\
 &= \epsilon^4 \int \frac{dq_{1234}}{(2\pi)^{4d+4}} (2\pi)^{2d+2} (F_1 F_2 - F_{-1} F_{-2})(\delta q_{1+3} \delta q_{2+4} + \delta q_{1+4} \delta q_{2+3}) \times \\
 &\times \left\{ k_1^2 |k_2| (\mathbf{k}_2 \cdot \mathbf{k}_3 + k_3^2) (\mathbf{k}_2 + \mathbf{k}_3) \cdot \mathbf{k}_4 \left[\frac{i\pi\delta(\omega_2 + \omega_3)}{\omega_4} + \frac{1}{(\omega_2 + \omega_3)(\omega_2 + \omega_3 + \omega_4)} \right] A_1 A_2 B_3 A_4 \right. \\
 &- k_1^2 |k_3| (\mathbf{k}_2 \cdot \mathbf{k}_3 + k_3^2) (\mathbf{k}_2 + \mathbf{k}_3) \cdot \mathbf{k}_4 \left[\frac{i\pi\delta(\omega_2 + \omega_3)}{\omega_4} + \frac{1}{(\omega_2 + \omega_3)(\omega_2 + \omega_3 + \omega_4)} \right] A_1 B_2 A_3 A_4 \\
 &+ k_1^2 |k_4| (\mathbf{k}_3 \cdot \mathbf{k}_4 + k_4^2) (\mathbf{k}_3 + \mathbf{k}_4) \cdot \mathbf{k}_2 \left[\frac{i\pi\delta(\omega_3 + \omega_4)}{\omega_2} + \frac{1}{(\omega_3 + \omega_4)(\omega_2 + \omega_3 + \omega_4)} \right] A_1 A_2 B_3 A_4 \left. \right\} \\
 &= \epsilon^4 \int \frac{dq_{12}}{(2\pi)^{2d+2}} (F_1 F_2 - F_{-1} F_{-2}) \times \\
 &\times \left\{ k_1^2 |k_2| (k_1^2 - \mathbf{k}_1 \cdot \mathbf{k}_2) (k_2^2 - \mathbf{k}_1 \cdot \mathbf{k}_2) \left[\frac{i\pi\delta(\omega_1 - \omega_2)}{\omega_1} + \frac{1}{\omega_1(\omega_1 - \omega_2)} \right] A_1 A_2 A_{-2} B_{-1} \right. \\
 &- k_1^2 |k_1| (k_2^2 - \mathbf{k}_1 \cdot \mathbf{k}_2)^2 \left[\frac{i\pi\delta(\omega_1 - \omega_2)}{\omega_1} + \frac{1}{\omega_1(\omega_1 - \omega_2)} \right] A_1 A_{-1} A_{-2} B_2 \\
 &+ k_1^2 |k_2| (\mathbf{k}_1 \cdot \mathbf{k}_2 + k_1^2) (\mathbf{k}_1 + \mathbf{k}_2) \cdot \mathbf{k}_2 \frac{1}{\omega_1(\omega_1 + \omega_2)} A_1 A_2 A_{-2} B_{-1} \\
 &- k_1^2 |k_1| (\mathbf{k}_1 \cdot \mathbf{k}_2 + k_2^2) (\mathbf{k}_1 + \mathbf{k}_2) \cdot \mathbf{k}_2 \frac{1}{\omega_1(\omega_1 + \omega_2)} A_1 A_{-1} A_2 B_{-2} \left. \right\}
 \end{aligned} \tag{C.85}$$

$$\begin{aligned}
 \lambda_{aaaa3} &= \epsilon^4 \int \frac{dq_{12}}{(2\pi)^{2d+2}} (F_1 F_2 - F_{-1} F_{-2}) \left\{ k_1^2 (k_2^2 - \mathbf{k}_1 \cdot \mathbf{k}_2) \frac{i\pi\delta(\omega_1 - \omega_2)}{\omega_1} \times \right. \\
 &\times [|k_2| (k_1^2 - \mathbf{k}_1 \cdot \mathbf{k}_2) A_1 A_2 A_{-2} B_{-1} - |k_1| (k_2^2 - \mathbf{k}_1 \cdot \mathbf{k}_2) A_1 A_{-1} A_{-2} B_2] \\
 &+ k_1^2 |k_2| A_1 A_2 A_{-2} B_{-1} \left[[(\mathbf{k}_1 \cdot \mathbf{k}_2)^2 + k_1^2 k_2^2] \left(\frac{1}{\omega_1(\omega_1 + \omega_2)} - \frac{1}{\omega_1(\omega_1 - \omega_2)} \right) \right] + \left. \right\}
 \end{aligned} \tag{C.86}$$

$$\begin{aligned}
& + [k_1^2(\mathbf{k}_1 \cdot \mathbf{k}_2) + (\mathbf{k}_1 \cdot \mathbf{k}_2)k_2^2] \left(\frac{1}{\omega_1(\omega_1 + \omega_2)} + \frac{1}{\omega_1(\omega_1 - \omega_2)} \right) \Big] + \\
& - k_1^2 |k_1| A_1 A_{-1} A_{-2} B_2 \left[[(\mathbf{k}_1 \cdot \mathbf{k}_2)^2 + k_2^4] \left(\frac{1}{\omega_1(\omega_1 + \omega_2)} + \frac{1}{\omega_1(\omega_1 - \omega_2)} \right) \right. \\
& \left. + 2(\mathbf{k}_1 \cdot \mathbf{k}_2)k_2^2 \left(\frac{1}{\omega_1(\omega_1 + \omega_2)} - \frac{1}{\omega_1(\omega_1 - \omega_2)} \right) \right] \Big\}
\end{aligned}$$

Now we use symmetry properties of the following functions

$$f(A, B) \equiv \frac{1}{A} \left[\frac{1}{A+B} + \frac{1}{A-B} \right], \quad f(A, B) = f(-A, -B) \quad (\text{C.87})$$

$$g(A, B) \equiv \frac{1}{A} \left[\frac{1}{A+B} - \frac{1}{A-B} \right], \quad g(A, B) = g(-A, -B) \quad (\text{C.88})$$

and obtain

$$\begin{aligned}
\lambda_{aaaa3} &= -2\pi\epsilon^4 \int \frac{dq_{12}}{(2\pi)^{2d+2}} F_1 F_2 k_1^2 (k_2^2 - \mathbf{k}_1 \cdot \mathbf{k}_2) \frac{\delta(\omega_1 - \omega_2)}{\omega_1} \times \\
& \times \left(|k_2| (k_1^2 - \mathbf{k}_1 \cdot \mathbf{k}_2) \text{Re}(iA_1 B_1^*) |A_2|^2 + |k_1| (k_2^2 - \mathbf{k}_1 \cdot \mathbf{k}_2) |A_1|^2 \text{Re}(iA_2^* B_2) \right) \\
& = -2\pi\epsilon^4 \int \frac{d\mathbf{k}_{12}}{(2\pi)^{2d}} n_1 n_2 k_1^2 (k_2^2 - \mathbf{k}_1 \cdot \mathbf{k}_2) \frac{\delta(\Omega_1 - \Omega_2)}{\Omega_1} \times \\
& \times \left(|k_2| (k_1^2 - \mathbf{k}_1 \cdot \mathbf{k}_2) \text{Re}(iA_1 B_1^*) |A_2|^2 + |k_1| (k_2^2 - \mathbf{k}_1 \cdot \mathbf{k}_2) |A_1|^2 \text{Re}(iA_2^* B_2) \right)
\end{aligned} \quad (\text{C.89})$$

For gravity-capillary wave we have

$$\begin{aligned}
\lambda_{aaaa3} &= -\frac{\pi}{2}\epsilon^4 \int \frac{d\mathbf{k}_{12}}{(2\pi)^{2d}} n_1 n_2 k_1^2 (k_2^2 - \mathbf{k}_1 \cdot \mathbf{k}_2) \delta(\Omega_1 - \Omega_2) (k_1^2 - k_2^2) \\
& = 0
\end{aligned} \quad (\text{C.90})$$

Term λ_{aaaa4}

$$\begin{aligned}
\lambda_{aaaa4} &\equiv \epsilon^4 \int \frac{dq_{1234}}{(2\pi)^{4d+4}} (2\pi)^{2d+2} A_1 A_2 A_3 B_4 k_1^2 k_2^2 (\mathbf{k}_2 \cdot \mathbf{k}_4) |k_3| \left[-\frac{1}{\omega_2(\omega_2 + \omega_3 + \omega_4)} \right] \times \\
& \times [-(F_{-1} F_{-4} - F_1 F_4) (\delta q_{1+3} \delta q_{2+4} + \delta q_{1+2} \delta q_{3+4}) + \times
\end{aligned} \quad (\text{C.91})$$

$$\begin{aligned}
 & + (F_{-1}F_{-3} - F_1F_3)(\delta q_{1+4}\delta q_{2+3} + \delta q_{1+2}\delta q_{3+4}) + (F_{-1}F_{-2} - F_1F_2)(\delta q_{1+4}\delta q_{2+3} + \delta q_{1+3}\delta q_{2+4})] \\
 & = \epsilon^4 \int \frac{dq_{1234}}{(2\pi)^{4d+4}} (2\pi)^{2d+2} k_1^2 k_2^2 (F_{-1}F_{-2} - F_1F_2)(\delta q_{1+4}\delta q_{2+3} + \delta q_{1+3}\delta q_{2+4}) \\
 & \times \left\{ A_1 A_2 A_3 B_4(\mathbf{k}_2 \cdot \mathbf{k}_4) |k_3| \left[-\frac{1}{\omega_2(\omega_2 + \omega_3 + \omega_4)} \right] + \right. \\
 & + A_1 A_2 A_3 B_4(\mathbf{k}_3 \cdot \mathbf{k}_4) |k_2| \left[-\frac{1}{(\omega_2 + \omega_3 + \omega_4)\omega_3} \right] \\
 & \left. - A_1 B_2 A_3 A_4(\mathbf{k}_2 \cdot \mathbf{k}_4) |k_3| \left[-\frac{1}{(\omega_2 + \omega_3 + \omega_4)\omega_4} \right] \right\} \\
 & = -\epsilon^4 \int \frac{dq_{12}}{(2\pi)^{4d+4}} (2\pi)^{2d+2} k_1^2 k_2^2 (F_{-1}F_{-2} - F_1F_2) \left\{ 2A_1 A_2 A_{-2} B_{-1}(\mathbf{k}_1 \cdot \mathbf{k}_2) |k_2| \frac{1}{\omega_1 \omega_2} \right. \\
 & \left. + A_1 A_{-1} (A_{-2} B_2 + A_2 B_{-2})(\mathbf{k}_1 \cdot \mathbf{k}_2) |k_2| \frac{1}{\omega_1^2} + A_1 A_{-1} (A_2 B_{-2} + A_{-2} B_2) k_2^2 |k_1| \frac{1}{\omega_1 \omega_2} \right\} \\
 & = 2\epsilon^4 \int \frac{dq_{12}}{(2\pi)^{2d+2}} k_1^2 k_2^2 F_1 F_2 (A_1 A_2 A_{-2} B_{-1} - A_{-1} A_{-2} A_2 B_1)(\mathbf{k}_1 \cdot \mathbf{k}_2) |k_2| \frac{1}{\omega_1 \omega_2} \\
 \lambda_{aaaa4} & = 0 \tag{C.92}
 \end{aligned}$$

since $A(-\mathbf{k}) = A(\mathbf{k})$ and $B(-\mathbf{k}) = B(\mathbf{k})$.

Term λ_{aaaa5}

$$\begin{aligned}
 \lambda_{aaaa5} & \equiv \epsilon^4 \int \frac{dq_{1234}}{(2\pi)^{4d+4}} (2\pi)^{2d+2} A_1 A_2 A_3 A_4 \times \tag{C.93} \\
 & \times \left[k_1^2 k_2^2 (\mathbf{k}_2 \cdot \mathbf{k}_3) (\mathbf{k}_3 \cdot \mathbf{k}_4) \left(-\frac{1}{i\omega_2(\omega_2 + \omega_3)(\omega_2 + \omega_3 + \omega_4)} + \frac{\pi\delta(\omega_2 + \omega_3)}{\omega_3\omega_4} \right) \right. \\
 & + \frac{1}{2} k_1^2 k_2^2 (\mathbf{k}_2 \cdot \mathbf{k}_3) (\mathbf{k}_2 \cdot \mathbf{k}_4) \left(\frac{1}{i(\omega_2 + \omega_3 + \omega_4)(\omega_2 + \omega_4)\omega_4} + \frac{\pi\delta(\omega_2 + \omega_4)}{\omega_3\omega_4} \right) \\
 & \left. + \frac{\pi\delta(\omega_2 + \omega_3)}{\omega_3\omega_4} - \frac{1}{i\omega_2(\omega_2 + \omega_3)\omega_4} \right] \times \\
 & \times [(F_1 F_2 + F_{-1} F_{-2})(\delta q_{1+3}\delta q_{2+4} + \delta q_{1+4}\delta q_{2+3}) \\
 & + (F_{-1} F_{-3} + F_1 F_3)(\delta q_{1+2}\delta q_{3+4} + \delta q_{1+4}\delta q_{2+3}) + (F_{-1} F_{-4} + F_1 F_4)(\delta q_{1+2}\delta q_{3+4} + \delta q_{1+3}\delta q_{2+4})] \\
 & = \epsilon^4 \int \frac{dq_{1234}}{(2\pi)^{4d+4}} (2\pi)^{2d+2} A_1 A_2 A_3 A_4 (F_1 F_2 + F_{-1} F_{-2})(\delta q_{1+3}\delta q_{2+4} + \delta q_{1+4}\delta q_{2+3}) \times \\
 & \times \left\{ k_1^2 k_2^2 (\mathbf{k}_2 \cdot \mathbf{k}_3) (\mathbf{k}_3 \cdot \mathbf{k}_4) \left[-\frac{1}{i\omega_2(\omega_2 + \omega_3)(\omega_2 + \omega_3 + \omega_4)} + \frac{\pi\delta(\omega_2 + \omega_3)}{\omega_3\omega_4} \right] \right\}
 \end{aligned}$$

$$\begin{aligned}
& + k_1^2 k_3^2 (\mathbf{k}_2 \cdot \mathbf{k}_3) (\mathbf{k}_2 \cdot \mathbf{k}_4) \left[-\frac{1}{i(\omega_2 + \omega_3)(\omega_2 + \omega_3 + \omega_4)\omega_3} + \frac{\pi\delta(\omega_2 + \omega_3)}{\omega_2\omega_4} \right] + \\
& + k_1^2 k_4^2 (\mathbf{k}_3 \cdot \mathbf{k}_4) (\mathbf{k}_2 \cdot \mathbf{k}_3) \left[-\frac{1}{i(\omega_2 + \omega_3 + \omega_4)(\omega_3 + \omega_4)\omega_4} + \frac{\pi\delta(\omega_3 + \omega_4)}{\omega_2\omega_3} \right] \\
& + \frac{1}{2} k_1^2 k_2^2 (\mathbf{k}_2 \cdot \mathbf{k}_3) (\mathbf{k}_2 \cdot \mathbf{k}_4) \left[\frac{1}{i(\omega_2 + \omega_3 + \omega_4)(\omega_2 + \omega_4)\omega_4} + \frac{\pi\delta(\omega_2 + \omega_4)}{\omega_3\omega_4} \right. \\
& \left. + \frac{\pi\delta(\omega_2 + \omega_3)}{\omega_3\omega_4} - \frac{1}{i\omega_2(\omega_2 + \omega_3)\omega_4} \right] \\
& + \frac{1}{2} k_1^2 k_3^2 (\mathbf{k}_2 \cdot \mathbf{k}_3) (\mathbf{k}_3 \cdot \mathbf{k}_4) \left[\frac{1}{i(\omega_2 + \omega_3 + \omega_4)(\omega_3 + \omega_4)\omega_4} + \frac{\pi\delta(\omega_3 + \omega_4)}{\omega_2\omega_4} \right. \\
& \left. + \frac{\pi\delta(\omega_2 + \omega_3)}{\omega_2\omega_4} - \frac{1}{i(\omega_2 + \omega_3)\omega_3\omega_4} \right] \\
& + \frac{1}{2} k_1^2 k_4^2 (\mathbf{k}_3 \cdot \mathbf{k}_4) (\mathbf{k}_2 \cdot \mathbf{k}_4) \left[\frac{1}{i\omega_2(\omega_2 + \omega_3 + \omega_4)(\omega_2 + \omega_4)} + \frac{\pi\delta(\omega_2 + \omega_4)}{\omega_2\omega_3} \right. \\
& \left. + \frac{\pi\delta(\omega_3 + \omega_4)}{\omega_2\omega_3} - \frac{1}{i\omega_2(\omega_3 + \omega_4)\omega_4} \right] \Big\}
\end{aligned}$$

$$\begin{aligned}
\lambda_{aaaa5} &= \epsilon^4 \int \frac{dq_{12}}{(2\pi)^{4d+4}} (2\pi)^{2d+2} A_1 A_2 A_{-1} A_{-2} (F_1 F_2 + F_{-1} F_{-2}) \frac{\pi\delta(\omega_1 - \omega_2)}{\omega_1^2} \times & (C.94) \\
&\times \left\{ -k_1^2 k_2^2 (\mathbf{k}_1 \cdot \mathbf{k}_2)^2 + \frac{1}{2} k_1^2 k_2^4 (\mathbf{k}_1 \cdot \mathbf{k}_2) + \frac{1}{2} k_1^2 k_2^4 (\mathbf{k}_1 \cdot \mathbf{k}_2) + \right. \\
&\left. - k_1^4 k_2^2 (\mathbf{k}_1 \cdot \mathbf{k}_2) + \frac{1}{2} k_1^4 (\mathbf{k}_1 \cdot \mathbf{k}_2)^2 + \frac{1}{2} k_1^4 (\mathbf{k}_1 \cdot \mathbf{k}_2)^2 \right\} \\
&= 2\pi\epsilon^4 \int \frac{dq_{12}}{(2\pi)^{2d+2}} |A_1 A_2|^2 F_1 F_2 \frac{\delta(\omega_1 - \omega_2)}{\omega_1^2} \times \\
&\times \left\{ -k_1^2 k_2^2 (\mathbf{k}_1 \cdot \mathbf{k}_2)^2 + k_1^4 (\mathbf{k}_1 \cdot \mathbf{k}_2)^2 + k_1^2 k_2^4 (\mathbf{k}_1 \cdot \mathbf{k}_2) - k_1^4 k_2^2 (\mathbf{k}_1 \cdot \mathbf{k}_2) \right\} \\
&= 2\pi\epsilon^4 \int \frac{dq_{12}}{(2\pi)^{2d+2}} |A_1 A_2|^2 F_1 F_2 \frac{\delta(\omega_1 - \omega_2)}{\omega_1^2} \times \\
&\times \left\{ k_1^2 (k_1^2 - k_2^2) (\mathbf{k}_1 \cdot \mathbf{k}_2)^2 + (k_1^2 k_2^4 - k_1^4 k_2^2) (\mathbf{k}_1 \cdot \mathbf{k}_2) \right\} \\
&= \pi\epsilon^4 \int \frac{dq_{12}}{(2\pi)^{2d+2}} |A_1 A_2|^2 F_1 F_2 \frac{\delta(\omega_1 - \omega_2)}{\omega_1^2} \times \\
&\times \left\{ k_1^2 (k_1^2 - k_2^2) (\mathbf{k}_1 \cdot \mathbf{k}_2)^2 - k_2^2 (k_1^2 - k_2^2) (\mathbf{k}_1 \cdot \mathbf{k}_2)^2 + (k_1^2 k_2^4 - k_1^4 k_2^2 + k_2^2 k_1^4 - k_2^4 k_1^2) (\mathbf{k}_1 \cdot \mathbf{k}_2) \right\}
\end{aligned}$$

$$\begin{aligned}
 &= \pi \epsilon^4 \int \frac{dq_{12}}{(2\pi)^{2d+2}} |A_1 A_2|^2 F_1 F_2 \frac{\delta(\omega_1 - \omega_2)}{\omega_1^2} (k_1^2 - k_2^2)^2 (\mathbf{k}_1 \cdot \mathbf{k}_2)^2 \\
 &= \pi \epsilon^4 \int \frac{d\mathbf{k}_{12}}{(2\pi)^{2d}} |A_1 A_2|^2 n_1 n_2 \frac{\delta(\Omega_1 - \Omega_2)}{\Omega_1^2} (k_1^2 - k_2^2)^2 (\mathbf{k}_1 \cdot \mathbf{k}_2)^2
 \end{aligned}$$

For gravity-capillary waves we have

$$\lambda_{aaaa5} = \frac{\pi}{4} \epsilon^4 \int \frac{d\mathbf{k}_{12}}{(2\pi)^{2d}} \frac{1}{k_1 k_2} n_1 n_2 (k_1^2 - k_2^2)^2 (\mathbf{k}_1 \cdot \mathbf{k}_2)^2 \delta(\Omega_1 - \Omega_2) \quad (\text{C.95})$$

C.12 The sum of Lyapunov exponents for gravity-capillary waves

Gathering all the terms in (C.19) from equations (C.69,C.72,C.74,C.76,C.82,C.84,C.90,C.92 and C.95) we get

$$\lambda = 0 + \mathcal{O}(\epsilon^6). \quad (\text{C.96})$$

D The velocity field of floaters

Here we derive the velocity field of the floaters $\mathbf{v}(x, y, t)$ up to the third order in wave amplitude, which is sufficient to calculate λ to the fourth order in wave amplitude. We perform the calculation for arbitrary fluid depth h . Equation (1.9) from the main text can be rewritten as

$$\mathbf{v}(x, y, t) = \left(\frac{\partial \psi}{\partial x} - \frac{\partial \eta}{\partial x} \frac{\partial \phi}{\partial z} [z = \eta(x, y, t)], \frac{\partial \psi}{\partial y} - \frac{\partial \eta}{\partial y} \frac{\partial \phi}{\partial z} [z = \eta(x, y, t)] \right). \quad (\text{D.1})$$

We observe that in order to establish the expression for \mathbf{v} in terms of ψ and η up to the third order in wave amplitude, we need to find the expression for the potential ϕ up to the second order in wave amplitude. To do this we note that $\phi(x, y, z, t)$ satisfies the Laplace equation $\nabla^2 \phi + \partial_z^2 \phi = 0$ with the boundary conditions $\phi(x, y, \eta(x, y, t), t) = \psi(x, y, t)$ and $\partial_z \phi(z = -h) = 0$, see e.g. [66]. Here ∇ is the two-dimensional gradient operator. To the lowest order in wave amplitude the boundary condition $\phi(x, y, \eta(x, y, t), t) = \psi(x, y, t)$ can be substituted by $\phi(x, y, z = 0, t) = \psi(x, y, t)$. This gives the following expression for the lowest order approximation to ϕ :

$$\phi_0(x, y, z, t) = \int \frac{d\mathbf{k}}{(2\pi)^2} \frac{\cosh[k(z+h)]}{\cosh[kh]} \exp[i\mathbf{k} \cdot \mathbf{r}] \psi(\mathbf{k}, t), \quad (\text{D.2})$$

where $\psi(\mathbf{k}, t)$ is the Fourier transform of $\psi(x, y, t)$ and all the vectors above are two-dimensional, e.g. $\mathbf{r} = (x, y)$. To find the next order correction ϕ_1 we use the identity

$$\phi(x, y, z, t) = \int \frac{d\mathbf{k}}{(2\pi)^2} \frac{\cosh[k(z+h)]}{\cosh[kh]} e^{i\mathbf{k} \cdot \mathbf{r}} \int d\mathbf{r}' \phi(\mathbf{r}', z = 0, t) e^{-i\mathbf{k} \cdot \mathbf{r}'}, \quad (\text{D.3})$$

where $\phi(\mathbf{r}', z = 0, t)$ is the exact potential at the plane $z = 0$. Using

$$\phi(x, y, z, t) = \phi(x, y, \eta(x, y, t), t) + [z - \eta(x, y, t)] \frac{\partial \phi(x, y, z, t)}{\partial z} \Big|_{z=\eta(x, y, t)} + O[(z - \eta)^2],$$

we find

$$\phi(x, y, z = 0, t) = \psi(x, y, t) - \eta(x, y, t) \frac{\partial \phi_0(x, y, z, t)}{\partial z} [z = 0] + O(\eta^2). \quad (\text{D.4})$$

Substituting the above into Eq. (D.3) we obtain that the second order contribution to the potential is

$$\phi_1 = - \int \frac{d\mathbf{k}_{123}}{(2\pi)^4} \delta(\mathbf{k}_1 - \mathbf{k}_2 - \mathbf{k}_3) \frac{\cosh[|k_1|(z+h)]}{\cosh[|k_1|h]} \exp[i\mathbf{k}_1 \cdot \mathbf{r}] |k_2| \tanh(|k_2|h) \psi_2 \eta_3,$$

where we use the same shorthand notation as in Section 1.6.1. In the approximation of the infinitely deep fluid, $h \rightarrow \infty$, the above expression reproduces the result given in [113] (there is however a sign difference in the expressions - our sign can be verified by checking that the boundary condition $\phi(x, y, \eta(x, y), t) = \psi(x, y, t)$ is satisfied in the considered order). Using the above expression we find that the first, the second and the third order contributions to the velocity field of the floaters are given respectively by

$$\begin{aligned} \mathbf{v}_0 &= \nabla \psi = i \int \frac{d\mathbf{k}_1}{(2\pi)^2} \mathbf{k}_1 \exp[i\mathbf{k}_1 \cdot \mathbf{r}] \psi_1, \\ \mathbf{v}_1 &= - \left. \frac{\partial \phi_0}{\partial z} \right|_{z=0} \nabla \eta = -i \int \frac{d\mathbf{k}_{12}}{(2\pi)^4} \exp[i(\mathbf{k}_1 + \mathbf{k}_2) \cdot \mathbf{r}] |k_1| \tanh[|k_1|h] \mathbf{k}_2 \psi_1 \eta_2, \\ \mathbf{v}_2 &= -\nabla \eta \left(\eta \left. \frac{\partial^2 \phi_0}{\partial z^2} \right|_{z=0} + \left. \frac{\partial \phi_1}{\partial z} \right|_{z=0} \right) = -\frac{i}{2} \int \frac{d\mathbf{k}_{123}}{(2\pi)^6} e^{i(\mathbf{k}_1 + \mathbf{k}_2 + \mathbf{k}_3) \cdot \mathbf{r}} \psi_1 \eta_2 \eta_3 \\ &\times \left(|k_1|^2 \mathbf{k}_2 + |k_1|^2 \mathbf{k}_3 - 2\sqrt{k_1^2 + k_2^2} |k_1| \mathbf{k}_3 \right), \end{aligned} \quad (\text{D.5})$$

where we introduced the following shorthand notation $\bar{k} \equiv |k| \tanh(|k|h)$. The above expression is equivalent to Eq. (1.10) used in the main text.

E Calculation of the clustering rate of surface waves

In this Section we provide the calculation of λ to the fourth order in wave amplitude, based on the calculation of the different contributions λ_i , see (1.3)-(1.5). Some parts of this analysis deal with the same objects as those considered in [4, 104], however our analysis is different and it uses specific properties of surface waves. Below we provide a more detailed calculation, as compared to the short articles [4] and [104].

The general structure of the calculation is as follows. After one substitutes the expression (1.10) for the velocity into λ_i , one finds the expression for λ as a sum of the terms involving products of two, three and four fields. The latter terms are of the fourth order in wave amplitude already in the Gaussian approximation. Thus for them one can directly use Wick's theorem to express the answer in terms of the pair correlation functions given by Eqs. (1.13). As an example of such a computation, below we calculate λ_4 that contains the terms with four fields only. Also the calculation of λ_4 presents separate interest as will become clear in the end of the next subsection.

E.1 Calculation of λ_4

We consider the contribution λ_4 to λ . To calculate λ_4 to the fourth order in wave amplitude we may assume Gaussian non-interacting waves and use Wick's theorem to decouple the averages. Employing identities like $\langle v_\alpha(t_1) \partial_\alpha \partial_\beta w(t) \rangle = -\langle (\partial_\beta v_\alpha(t_1)) (\partial_\alpha w(t)) \rangle$, that follow by integration by parts, one finds

$$\begin{aligned} \lambda_4 = & - \int_0^\infty dt \int_0^t dt_1 \int_0^{t_1} dt_2 \left[\left\langle w(0) \frac{\partial w(t)}{\partial x_\alpha} \right\rangle \langle v_\alpha(t_1) w(t_2) \rangle + \left\langle w(0) \frac{\partial v_\alpha(t_1)}{\partial x_\beta} \right\rangle \left\langle w(t) \frac{\partial v_\beta(t_2)}{\partial x_\alpha} \right\rangle \right. \\ & \left. + \left\langle \frac{\partial w(0)}{\partial x_\alpha} \frac{\partial w(t)}{\partial x_\beta} \right\rangle \langle v_\alpha(t_1) v_\beta(t_2) \rangle + \left\langle w(t_2) \frac{\partial w(t)}{\partial x_\alpha} \right\rangle \langle v_\alpha(t_1) w(0) \rangle \right]. \end{aligned} \quad (\text{E.1})$$

Here we do not assume isotropy of the waves. Isotropy would make terms like $\langle v_\alpha(t_1) w(t_2) \rangle$ vanish. In the considered order, $\mathbf{v} = \nabla \psi$ is a potential field and spectral representation of the

pair-correlation function gives

$$\langle \psi(0)\psi(t) \rangle = \int \frac{d\mathbf{k}}{(2\pi)^2} E(\mathbf{k}) \cos(\Omega_{\mathbf{k}}t) \Rightarrow \langle v_\alpha(0)v_\beta(t) \rangle = \int \frac{d\mathbf{k}}{(2\pi)^2} k_\alpha k_\beta E(\mathbf{k}) \cos(\Omega_{\mathbf{k}}t),$$

where $E(\mathbf{k})$ is expressible in terms on $n(\mathbf{k})$ in Eqs. (1.13). Similar expressions hold for other correlation functions in (E.1). Note that the potentiality of surface waves, holding in the Gaussian approximation, makes the velocity spectrum vanish at $k = 0$ even if $E(k = 0) \neq 0$ [cf. [4, 104]]. We find

$$\begin{aligned} \lambda_4 = & \int \frac{d\mathbf{k}d\mathbf{q}E(\mathbf{k})E(\mathbf{q})}{(2\pi)^4} \int_0^\infty dt \int_0^t dt_1 \int_0^{t_1} dt_2 \left[k^4 q^2 (\mathbf{k} \cdot \mathbf{q}) \sin[\Omega_{\mathbf{k}}t] \sin[\Omega_{\mathbf{q}}(t_1 - t_2)] \right. \\ & - k^2 q^2 (\mathbf{k} \cdot \mathbf{q})^2 \cos[\Omega_{\mathbf{k}}t_1] \cos[\Omega_{\mathbf{q}}(t - t_2)] - k^4 (\mathbf{k} \cdot \mathbf{q})^2 \cos[\Omega_{\mathbf{k}}t] \cos[\Omega_{\mathbf{q}}(t_1 - t_2)] \\ & \left. + k^4 q^2 (\mathbf{k} \cdot \mathbf{q}) \sin[\Omega_{\mathbf{k}}(t - t_2)] \sin[\Omega_{\mathbf{q}}t_1] \right]. \end{aligned} \quad (\text{E.2})$$

To calculate the time-integrals we represent the products of trigonometric functions above as sums or differences of cosine functions and use

$$\begin{aligned} \int_0^\infty dt \int_0^t dt_1 \int_0^{t_1} dt_2 \cos(at + bt_1 + ct_2) &= -\frac{\pi\delta(a)}{b(b+c)} + \frac{\pi\delta(a+b)}{bc} - \frac{\pi\delta(a+b+c)}{c(b+c)}, \quad b \neq -c, \\ \int_0^\infty dt \int_0^t dt_1 \int_0^{t_1} dt_2 \cos(at - bt_1 + bt_2) &= -\frac{\pi\delta'(a)}{b} + \frac{\pi\delta(a)}{b^2} - \frac{\pi\delta(a-b)}{b^2}. \end{aligned} \quad (\text{E.3})$$

All terms which are supported only at the zero frequency in the frequency representation (δ -functions or their derivatives) are also supported only at the zero wavenumber, since the dispersion relation of surface waves vanishes at $k = 0$ only. As a result, due to the presence of positive powers of k in (E.2), these terms vanish (similarly to the vanishing of the velocity spectrum at $k = 0$ shown above). It is then easy to see that the first and the fourth terms in λ_4 (having the same dependence on the wavevectors) cancel each other, while the second and the third terms give

$$\lambda_4 = \int \frac{d\mathbf{k}d\mathbf{q}}{(2\pi)^4} E(\mathbf{k})E(\mathbf{q})k^2(\mathbf{k} \cdot \mathbf{q})^2(k^2 - q^2) \left(\frac{\pi\delta(\Omega_{\mathbf{k}} - \Omega_{\mathbf{q}})}{2\Omega_{\mathbf{q}}^2} \right). \quad (\text{E.4})$$

Since for the surface waves the equality of the frequencies of two waves implies the equality of their wavelengths, then the above terms cancel each other, $\lambda_4 = 0$. This reproduces in a simple way the result of [4] which says that in the Gaussian approximation λ vanishes for potential waves having the property that the equality of the frequencies implies the equality of the wavelengths.

E.2 Reduction to terms involving interactions and the zero frequency field

Having shown $\lambda_4 = 0$, let us consider λ_2 and λ_3 . The calculation of the terms in λ_2 and λ_3 that contain products of four fields can be done along the same lines as the calculation of λ_4 in the previous subsection. The calculations are brought in Appendix E.5 and they show that these terms vanish identically, just like λ_4 . One is left with (see Eq. (E.18) from Appendix E.5):

$$\begin{aligned} \lambda &= \frac{1}{2} \int \frac{k_1^2 k_2^2 d\mathbf{k}_{12} d\omega}{(2\pi)^5} \langle \psi_1(\omega) \psi_2(\omega = 0) \rangle \\ &- \int \frac{d\mathbf{k}_{123} d\omega_{12}}{(2\pi)^8} |k_1| k_3^2 (\mathbf{k}_1 \cdot \mathbf{k}_2 + k_2^2) \langle \psi_1(\omega_1) \eta_2(\omega_2) \psi_3(\omega = 0) \rangle \\ &- \int \frac{d\mathbf{k}_{123} d\omega_{123}}{(2\pi)^9} k_1^2 k_2^2 (\mathbf{k}_2 \cdot \mathbf{k}_3) \langle \psi_1(\omega_1) \psi_2(\omega_2) \psi_3(\omega_3) \rangle \frac{i\pi[\delta(\omega_2) - \delta(\omega_1)]}{\omega_3}, \end{aligned} \quad (\text{E.5})$$

where shorthand notation $d\omega_{i;jl} = d\omega_i d\omega_j d\omega_l \dots$ is employed and Fourier representation of the fields over the frequency is used. To calculate the above terms to the fourth order in wave amplitude, one needs to account for the nonlinear wave interactions. The calculation is facilitated by observing that the terms in Eq. (E.5) are special: they all contain the field amplitude at the zero frequency, $\psi(\mathbf{k}, \omega = 0)$. Note that the value of the random wave field at the zero frequency plays an important role also in the diffusion of the passive scalar. In that problem if the field vanishes at the zero frequency field, there is no turbulent diffusion at the order ϵ^2 , see [2, 52, 107].

We assume that the force that sustains the stationary wave turbulence vanishes at the zero frequency [note however that the first term on the RHS of Eq. (E.5) vanishes in the Gaussian approximation independently of this assumption, cf. [4] and [104]]. Then the nonzero value of $\psi(\mathbf{k}, \omega = 0)$ is solely due to the presence of nonlinear wave interactions. As a result, $\psi(\mathbf{k}, \omega = 0)$

is of at least second order in wave amplitude. Below we derive the corresponding expression for $\psi(\mathbf{k}, \omega = 0)$ in terms of the higher order terms. Substituting the resulting expressions into the correlation functions will already allow the use of Wick's theorem to complete the calculation.

E.3 The expression for ψ

To calculate λ we need to know $\psi(\mathbf{k}, \omega = 0)$ to the third order in wave amplitude. Consider the dynamical equation on the surface elevation η , see [9, 113],

$$\frac{\partial \eta}{\partial t} = \frac{\partial \phi}{\partial z}[z = \eta] - \nabla \eta \nabla \phi[z = \eta]. \quad (\text{E.6})$$

To order ϵ^2 , the equation reads

$$\frac{\partial \eta}{\partial t} = \frac{\partial \phi_0}{\partial z}[z = 0] + \eta \frac{\partial^2 \phi_0}{\partial z^2}[z = 0] + \frac{\partial \phi_1}{\partial z} - \nabla \eta \nabla \phi_0[z = 0] + O(\eta^3), \quad (\text{E.7})$$

where ϕ_0 and ϕ_1 are the terms of the expansion of the potential with respect to the surface elevation, see Appendix D and [113]. Using the expressions for ϕ_i , performing the Fourier transform over space and time coordinates, and setting the frequency $\omega = 0$, we find

$$\begin{aligned} 0 = & \overline{|k|} \psi(\mathbf{k}, \omega = 0) + \int \frac{d\mathbf{k}_1 d\omega}{(2\pi)^3} k_1^2 \psi(\mathbf{k}_1, \omega) \eta(\mathbf{k} - \mathbf{k}_1, -\omega) \\ & - \int \frac{d\mathbf{k}_1 d\omega}{(2\pi)^3} \overline{|k|} \overline{|k_1|} \psi(\mathbf{k}_1, \omega) \eta(\mathbf{k} - \mathbf{k}_1, -\omega) + \int \frac{d\mathbf{k}_1 d\omega}{(2\pi)^3} \mathbf{k}_1 \cdot (\mathbf{k} - \mathbf{k}_1) \psi(\mathbf{k}_1, \omega) \eta(\mathbf{k} - \mathbf{k}_1, -\omega), \end{aligned}$$

where we neglected terms of order ϵ^3 . It follows that in this order $\psi(\mathbf{k}, \omega = 0)$ is given by

$$\psi(\mathbf{k}, \omega = 0) = \int \frac{d\mathbf{k}_1 d\omega}{(2\pi)^3} \left(\overline{|k_1|} - \frac{\mathbf{k}_1 \cdot \mathbf{k}}{\overline{|k|}} \right) \psi(\mathbf{k}_1, \omega) \eta(\mathbf{k} - \mathbf{k}_1, -\omega). \quad (\text{E.8})$$

The physical meaning of the above representation is that the zero frequency field arises due to the nonlinear interactions only, and in the lowest order it can be represented as a result of a single wave scattering. The above formula suffices in order to calculate the last two terms in Eq. (E.5). Indeed, after we substitute into these terms the above expression for $\psi(\mathbf{k}, \omega = 0)$, we obtain correlation function of already four fields, which can be again calculated using Wick's

theorem. The corresponding calculation is straightforward but cumbersome and it is brought in Appendix F. As a result of the calculation one finds that these terms vanish identically so one is left with

$$\lambda = \frac{1}{2} \int \frac{k_1^2 k_2^2 d\mathbf{k}_{12} d\omega}{(2\pi)^5} \langle \psi_1(\omega) \psi_2(\omega = 0) \rangle. \quad (\text{E.9})$$

To calculate the above quadratic term we again use the fact that it involves $\psi(\mathbf{k}, \omega = 0)$ by slightly modifying the above computation.

E.4 Calculation of the quadratic term

To calculate the RHS of Eq. (E.9) we note that it is sufficient to know $\psi(\mathbf{k}_1, \omega)$ at an arbitrarily small but finite ω where the forcing is again negligible and one can use the dynamic equation (E.6) without the force. The Fourier transform of (E.7) taken now at a small but finite frequency, neglecting terms of order ϵ^3 , gives

$$\begin{aligned} i\omega\eta(\mathbf{k}, \omega) &= \overline{|k|} \psi(\mathbf{k}, \omega) + \int \frac{d\mathbf{k}_1 d\omega_1}{(2\pi)^3} k_1^2 \psi_1(\omega_1) \eta(\mathbf{k} - \mathbf{k}_1, \omega - \omega_1) - \int \frac{d\mathbf{k}_1 d\omega_1}{(2\pi)^3} \overline{|k|} \overline{|k_1|} \psi_1(\omega) \\ &\times \eta(\mathbf{k} - \mathbf{k}_1, \omega - \omega_1) + \int \frac{d\mathbf{k}_1 d\omega_1}{(2\pi)^3} \mathbf{k}_1 \cdot (\mathbf{k} - \mathbf{k}_1) \psi_1(\omega) \eta(\mathbf{k} - \mathbf{k}_1, \omega - \omega_1). \end{aligned} \quad (\text{E.10})$$

This gives

$$\psi(\mathbf{k}, \omega) = \frac{i\omega\eta(\mathbf{k}, \omega)}{\overline{|k|}} + \int \frac{d\mathbf{k}_1 d\omega_1}{(2\pi)^3} \left(\overline{|k_1|} - \frac{\mathbf{k}_1 \cdot \mathbf{k}}{\overline{|k|}} \right) \psi(\mathbf{k}_1, \omega_1) \eta(\mathbf{k} - \mathbf{k}_1, \omega - \omega_1) + O(\eta^3).$$

It follows that Eq. (E.9) can be written as

$$\begin{aligned} \lambda &= \frac{1}{2} \int \frac{k_1^2 k_2^2 d\mathbf{k}_{12}}{(2\pi)^4} \int \frac{d\omega}{2\pi} \left\langle \left[\frac{i\omega\eta(\mathbf{k}_1, \omega)}{\overline{|k_1|}} + \int \frac{d\mathbf{k}_3 d\omega_1}{(2\pi)^3} \left(\overline{|k_3|} - \frac{\mathbf{k}_3 \cdot \mathbf{k}_1}{\overline{|k_1|}} \right) \psi(\mathbf{k}_3, \omega_1) \right. \right. \\ &\times \eta(\mathbf{k}_1 - \mathbf{k}_3, \omega - \omega_1) + O(\eta^3) \left. \right] \psi(\mathbf{k}_2, \omega = 0) \left. \right\rangle = \frac{1}{2} \int \frac{k_1^2 k_2^2 d\mathbf{k}_{12}}{(2\pi)^4} \int \frac{d\omega_1}{2\pi} \left\langle \left[\int \frac{d\mathbf{k}_3 d\omega_3}{(2\pi)^3} \right. \right. \\ &\times \left. \left. \left(\overline{|k_3|} - \frac{\mathbf{k}_3 \cdot \mathbf{k}_1}{\overline{|k_1|}} \right) \psi(\mathbf{k}_3, \omega_3) \eta(\mathbf{k}_1 - \mathbf{k}_3, \omega_1 - \omega_3) + O(\eta^3) \right] \psi(\mathbf{k}_2, \omega = 0) \right. \left. \right\rangle, \end{aligned} \quad (\text{E.11})$$

where we used that $\omega \langle \eta(\mathbf{k}_1, \omega) \psi(\mathbf{k}_2, \omega = 0) \rangle \propto \omega \delta(\omega) = 0$. Next, using that $\psi(\mathbf{k}, \omega = 0)$ is by itself of order ϵ^2 , see the previous subsection, we conclude that in fact the $O(\eta^3)$ term in the above expression can be neglected. The physical reason for the possibility of such a neglect is that the quadratic term in fact contains correlations of two low-frequency fields where each one of them is of the order ϵ^2 . In the remaining expression, using Eq. (E.8), taking the integral over ω_3 and omitting the terms supported at the zero frequency, we find

$$\begin{aligned} \lambda = & \frac{1}{8} \int \frac{d\mathbf{k}_{13}}{(2\pi)^3} (\mathbf{k}_1 + \mathbf{k}_3)^4 \left(\overline{|k_3|} - \frac{\mathbf{k}_3 \cdot (\mathbf{k}_1 + \mathbf{k}_3)}{|\mathbf{k}_1 + \mathbf{k}_3|} \right) [n_3 n_{-1} \delta(\Omega_{-1} - \Omega_3) \\ & + n_{-3} n_1 \delta(\Omega_1 - \Omega_{-3})] \left(\overline{|k_3|} - \overline{|k_1|} + \frac{k_1^2 - k_3^2}{|\mathbf{k}_1 + \mathbf{k}_3|} \right) = 0. \end{aligned} \quad (\text{E.12})$$

The vanishing of the above expression can be easily verified by noting that the δ -functions imply $k_1 = k_3$. Thus we obtain that the sum of Lyapunov exponents for weakly interacting surface waves is identically zero at fourth order in wave amplitude.

E.5 Calculation of terms in λ involving products of four fields

Here we calculate those terms in λ_2 and λ_3 that contain products of four fields and allow for the direct use of Wick's theorem. We first consider λ_2 in (1.3).

E.6 Calculation of the fourth-order terms in λ_2

Using the explicit form of the surface velocity (1.10) we get

$$\begin{aligned} 2\lambda_2 = & \int \frac{k_1^2 k_2^2 d\mathbf{k}_{12} dt}{(2\pi)^4} \langle \psi_1(0) \psi_2(t) \rangle - 2 \int \frac{d\mathbf{k}_{123} dt}{(2\pi)^6} k_3^2 (\mathbf{k}_1 \cdot \mathbf{k}_2 + k_2^2) \langle \psi_1(0) \eta_2(0) \psi_3(t) \rangle \overline{|k_1|} \\ & - \int \frac{d\mathbf{k}_{1234} dt}{(2\pi)^8} \langle \psi_1(0) \eta_2(0) \eta_3(0) \psi_4(t) \rangle k_4^2 \left(|k_1|^2 (\mathbf{k}_1 \cdot \mathbf{k}_2 + k_2^2 + \mathbf{k}_2 \cdot \mathbf{k}_3) \right. \\ & \left. + \left(|k_1|^2 - 2\sqrt{k_1^2 + k_2^2} \overline{|k_1|} \right) (\mathbf{k}_1 \cdot \mathbf{k}_3 + \mathbf{k}_2 \cdot \mathbf{k}_3 + k_3^2) \right) \\ & + \int \frac{d\mathbf{k}_{1234} dt}{(2\pi)^8} \langle \psi_1(0) \eta_2(0) \psi_3(t) \eta_4(t) \rangle \overline{|k_1|} \overline{|k_3|} (\mathbf{k}_1 \cdot \mathbf{k}_2 + k_2^2) (\mathbf{k}_3 \cdot \mathbf{k}_4 + k_4^2). \end{aligned}$$

We note that the third term above, that can be decomposed by Wick's theorem, vanishes because it is supported at the zero frequency ω_4 imposing $k_4 = 0$. The last term can also be analyzed using Wick's theorem. Noting that the pair-correlations are supported at the zero sum of the involved wavenumbers, we find that the last term equals

$$\int \frac{d\mathbf{k}_{1234} dt}{(2\pi)^8} [\langle \psi_1(0)\psi_3(t) \rangle \langle \eta_2(0)\eta_4(t) \rangle + \langle \psi_1(0)\eta_4(t) \rangle \langle \eta_2(0)\psi_3(t) \rangle] \times \overline{|k_1|} \overline{|k_3|} (\mathbf{k}_1 \cdot \mathbf{k}_2 + k_2^2) (\mathbf{k}_3 \cdot \mathbf{k}_4 + k_4^2). \quad (\text{E.13})$$

Using the correlation functions from Eq. (1.13) and noting the vanishing of the terms containing δ -functions supported at the zero frequency, we can write (E.13) as

$$\int \frac{d\mathbf{k}_{12}}{(2\pi)^3} \left[\overline{|k_1|}^2 (\mathbf{k}_1 \cdot \mathbf{k}_2 + k_2^2)^2 \left(\frac{\Omega_1 k_2}{4k_1 \Omega_2} \right) [n_1 n_{-2} \delta(\Omega_1 - \Omega_{-2}) + n_{-1} n_2 \delta(\Omega_{-1} - \Omega_2)] - \frac{1}{4} \overline{|k_1|} \overline{|k_2|} (\mathbf{k}_1 \cdot \mathbf{k}_2 + k_2^2) (\mathbf{k}_1 \cdot \mathbf{k}_2 + k_1^2) [n_1 n_{-2} \delta(\Omega_1 - \Omega_{-2}) + n_{-1} n_2 \delta(\Omega_{-1} - \Omega_2)] \right] = 0,$$

where we introduced the shorthand notation: $n(\pm \mathbf{k}_i, t) = n_{\pm i}(t)$ and $\Omega_{\pm \mathbf{k}_i} = \Omega_{\pm i}$. Above we used that for surface waves $\Omega_{\mathbf{k}}$ is an increasing function of $|\mathbf{k}|$ and that δ -functions imply $\Omega_1 = \Omega_2$ and $k_1^2 = k_2^2$. We find that λ_2 can be written as

$$\lambda_2 = \int \frac{d\mathbf{k}_{12} dt}{2(2\pi)^4} k_1^2 k_2^2 \langle \psi_1(0)\psi_2(t) \rangle - \int \frac{d\mathbf{k}_{123} dt}{(2\pi)^6} \overline{|k_1|} k_3^2 (\mathbf{k}_1 \cdot \mathbf{k}_2 + k_2^2) \langle \psi_1(0)\eta_2(0)\psi_3(t) \rangle. \quad (\text{E.14})$$

The calculation of the above terms demands the account of the interactions. We now consider the terms in λ_3 that can be calculated by the direct use of Wick's theorem.

E.7 Calculation of the fourth-order terms in λ_3

We consider λ_3 from (1.3). Using the expression (1.10) for the velocity, we obtain

$$\begin{aligned}
 \lambda_3 = & - \int \frac{d\mathbf{k}_{123}}{(2\pi)^6} k_1^2 k_2^2 (\mathbf{k}_2 \cdot \mathbf{k}_3) \int_0^\infty dt \int_0^t dt_1 \langle \psi_1(0) \psi_2(t) \psi_3(t_1) \rangle \\
 & + \int \frac{d\mathbf{k}_{1234}}{(2\pi)^8} \int_0^\infty dt \int_0^t dt_1 \left[\overline{|k_1|} (\mathbf{k}_1 \cdot \mathbf{k}_2 + k_2^2) k_3^2 \langle \psi_1(0) \eta_2(0) \psi_3(t) \psi_4(t_1) \rangle \right. \\
 & \times (\mathbf{k}_3 \cdot \mathbf{k}_4) + k_1^2 \overline{|k_2|} (\mathbf{k}_2 \cdot \mathbf{k}_3 + k_3^2) (\mathbf{k}_2 \cdot \mathbf{k}_4 + \mathbf{k}_3 \cdot \mathbf{k}_4) \langle \psi_1(0) \psi_2(t) \eta_3(t) \psi_4(t_1) \rangle \\
 & \left. + k_1^2 k_2^2 (\mathbf{k}_2 \cdot \mathbf{k}_4) \overline{|k_3|} \langle \psi_1(0) \psi_2(t) \psi_3(t_1) \eta_4(t_1) \rangle \right]. \tag{E.15}
 \end{aligned}$$

One can use Wick's theorem for the last three terms. Employing the identity

$$\int_0^\infty dt \int_0^t dt_1 \exp[i\omega_1 t + i\omega_2 t_1] = \frac{i\pi[\delta(\omega_1) - \delta(\omega_1 + \omega_2)]}{\omega_2}, \tag{E.16}$$

one finds that part of the obtained terms contain δ -functions supported at the zero frequency and they vanish because of the vanishing of the integrand there. Let us consider the rest of the terms. For the first of the fourth-order terms in (E.15) one finds

$$\begin{aligned}
 & \int \frac{d\mathbf{k}_{12}}{(2\pi)^4} \overline{|k_1|} \left\{ |k_1|^2 (\mathbf{k}_1 \cdot \mathbf{k}_2 + k_2^2) \left[\frac{n_{-1} n_2 \delta(\Omega_{-1} - \Omega_2)}{\Omega_2} + \frac{n_{-2} n_1 \delta(\Omega_{-2} - \Omega_1)}{\Omega_{-2}} \right] \right. \\
 & \left. - k_2^2 (\mathbf{k}_1 \cdot \mathbf{k}_2 + k_2^2) \left[\frac{n_{-1} n_2 \delta(\Omega_{-1} - \Omega_2)}{\Omega_{-1}} + \frac{n_{-2} n_1 \delta(\Omega_{-2} - \Omega_1)}{\Omega_1} \right] \right\} \frac{\Omega_1 \pi}{4k_1} (\mathbf{k}_1 \cdot \mathbf{k}_2) = 0,
 \end{aligned}$$

where the equality of the frequencies implies the equality of the wavelengths. Analogously, for the second Gaussian term one finds

$$\begin{aligned}
 & \int \frac{\Omega_2 \overline{|k_2|} d\mathbf{k}_{23}}{(4\pi)^3 k_2} \left\{ |k_2|^2 (\mathbf{k}_2 \cdot \mathbf{k}_3 + k_3^2)^2 \left[\frac{n_{-3} n_2 \delta(\Omega_{-3} - \Omega_2)}{\Omega_{-3}} + \frac{n_{-2} n_3 \delta(\Omega_{-2} - \Omega_3)}{\Omega_3} \right] \right. \\
 & \left. - k_3^2 (\mathbf{k}_2 \cdot \mathbf{k}_3 + k_3^2) (\mathbf{k}_2 \cdot \mathbf{k}_3 + k_2^2) \left[\frac{n_{-3} n_2 \delta(\Omega_{-3} - \Omega_2)}{\Omega_2} + \frac{n_{-2} n_3 \delta(\Omega_{-2} - \Omega_3)}{\Omega_{-2}} \right] \right\} = 0.
 \end{aligned}$$

Finally, the third Gaussian term contains only δ -functions supported at the zero frequencies, so it also produces zero. We conclude that λ_3 can be written as

$$\lambda_3 = - \int \frac{d\mathbf{k}_{123}}{(2\pi)^6} k_1^2 k_2^2 (\mathbf{k}_2 \cdot \mathbf{k}_3) \int_0^\infty dt \int_0^t dt_1 \langle \psi_1(0) \psi_2(t) \psi_3(t_1) \rangle. \quad (\text{E.17})$$

E.8 Summary

As a result of the calculation in the previous subsections, adding equations (E.14) and (E.17), one can write λ as a sum over the terms which calculation involves the wave interactions. Using Fourier representation over the frequency one finds

$$\begin{aligned} \lambda &= \frac{1}{2} \int \frac{k_1^2 k_2^2 d\mathbf{k}_{12} d\omega}{(2\pi)^5} \langle \psi_1(\omega) \psi_2(\omega = 0) \rangle \\ &- \int \frac{d\mathbf{k}_{123} d\omega_{12}}{(2\pi)^8} |k_1| k_3^2 (\mathbf{k}_1 \cdot \mathbf{k}_2 + k_2^2) \langle \psi_1(\omega_1) \eta_2(\omega_2) \psi_3(\omega = 0) \rangle \\ &- \int \frac{d\mathbf{k}_{123} d\omega_{123}}{(2\pi)^9} k_1^2 k_2^2 (\mathbf{k}_2 \cdot \mathbf{k}_3) \langle \psi_1(\omega_1) \psi_2(\omega_2) \psi_3(\omega_3) \rangle \frac{i\pi [\delta(\omega_2) - \delta(\omega_1)]}{\omega_3}, \end{aligned} \quad (\text{E.18})$$

where we introduced shorthand notation $d\omega_{ijl} = d\omega_i d\omega_j d\omega_l \dots$ and used in the last term the identity (E.16) and the proportionality of the correlation function to $\delta(\omega_1 + \omega_2 + \omega_3)$.

F Interaction terms containing the products of three fields

To calculate the interaction terms of the third order we use (E.8), Wick's decomposition and Fourier transformed version of (1.13). The second term in (E.18) can be written with the help of (E.8) as

$$\begin{aligned}
& - \int \frac{d\mathbf{k}_{1234}d\omega_{123}}{(2\pi)^{11}} \overline{|k_1|} k_3^2 (\mathbf{k}_1 \cdot \mathbf{k}_2 + k_2^2) \left(\overline{|k_4|} - \frac{\mathbf{k}_4 \cdot \mathbf{k}_3}{|k_3|} \right) \langle \psi(\mathbf{k}_1, \omega_1) \eta(\mathbf{k}_2, \omega_2) \psi(\mathbf{k}_4, \omega_3) \\
& \eta(\mathbf{k}_3 - \mathbf{k}_4, -\omega_3) \rangle = - \int \frac{d\mathbf{k}_{12}d\omega_1}{(2\pi)^3} \overline{|k_1|} (\mathbf{k}_1 + \mathbf{k}_2)^2 (\mathbf{k}_1 \cdot \mathbf{k}_2 + k_2^2) \left(\overline{|k_1|} - \frac{\mathbf{k}_1 \cdot (\mathbf{k}_1 + \mathbf{k}_2)}{|\mathbf{k}_1 + \mathbf{k}_2|} \right) \\
& \left(\frac{\Omega_1 |k_2|}{4\Omega_2 |k_1|} \right) [n_1 \delta(\omega_1 + \Omega_1) + n_{-1} \delta(\omega_1 - \Omega_{-1})] [n_2 \delta(-\omega_1 + \Omega_2) + n_{-2} \delta(\omega_1 + \Omega_{-2})] \\
& + \frac{1}{4} \int \frac{d\mathbf{k}_{12}d\omega_1}{(2\pi)^3} \overline{|k_1|} (\mathbf{k}_1 + \mathbf{k}_2)^2 (\mathbf{k}_1 \cdot \mathbf{k}_2 + k_2^2) \left(\overline{|k_2|} - \frac{\mathbf{k}_2 \cdot (\mathbf{k}_1 + \mathbf{k}_2)}{|\mathbf{k}_1 + \mathbf{k}_2|} \right) \\
& \times [n_1 \delta(\omega_1 + \Omega_1) - n_{-1} \delta(\omega_1 - \Omega_{-1})] [n_{-2} \delta(\omega_1 + \Omega_{-2}) - n_2 \delta(\omega_1 - \Omega_2)], \tag{F.1}
\end{aligned}$$

where to show that the remaining contraction vanishes, one should use that $\langle \psi(\mathbf{k}, \omega = 0) \rangle$ is representable as an integral over $\langle \psi(\mathbf{k}, t) \eta(\mathbf{k}', t) \rangle$ which in the Gaussian approximation vanishes by (1.13). Using $\Omega_{-\mathbf{k}} = \Omega_{\mathbf{k}}$ and noting that the terms supported at $\Omega_{\mathbf{k}} = 0$ vanish, one may rewrite the above as

$$\begin{aligned}
& - \frac{1}{4} \int \frac{d\mathbf{k}_{12}}{(2\pi)^3} \overline{|k_1|} (\mathbf{k}_1 + \mathbf{k}_2)^2 (\mathbf{k}_1 \cdot \mathbf{k}_2 + k_2^2) \left(\overline{|k_1|} - \frac{\mathbf{k}_1 \cdot (\mathbf{k}_1 + \mathbf{k}_2)}{|\mathbf{k}_1 + \mathbf{k}_2|} \right) \left[n_1 n_{-2} \delta(\Omega_1 - \Omega_{-2}) \right. \\
& \left. + n_{-1} n_2 \delta(\Omega_2 - \Omega_{-1}) \right] + \frac{1}{4} \int \frac{d\mathbf{k}_{12}}{(2\pi)^3} \overline{|k_1|} (\mathbf{k}_1 + \mathbf{k}_2)^2 (\mathbf{k}_1 \cdot \mathbf{k}_2 + k_2^2) \left(\overline{|k_2|} - \frac{\mathbf{k}_2 \cdot (\mathbf{k}_1 + \mathbf{k}_2)}{|\mathbf{k}_1 + \mathbf{k}_2|} \right) \\
& \times [n_1 n_{-2} \delta(\Omega_1 - \Omega_{-2}) + n_{-1} n_2 \delta(\Omega_2 - \Omega_{-1})] = \frac{1}{4} \int \frac{d\mathbf{k}_{12}}{(2\pi)^3} \overline{|k_1|} (\mathbf{k}_1 + \mathbf{k}_2)^2 (\mathbf{k}_1 \cdot \mathbf{k}_2 + k_2^2) \\
& \left(\overline{|k_2|} - \overline{|k_1|} + \frac{k_1^2 - k_2^2}{|\mathbf{k}_1 + \mathbf{k}_2|} \right) \left[n_1 n_{-2} \delta(\Omega_1 - \Omega_{-2}) + n_{-1} n_2 \delta(\Omega_2 - \Omega_{-1}) \right] = 0, \tag{F.2}
\end{aligned}$$

where we used that δ -functions imply $\Omega_1 = \Omega_2$ and $k_1 = k_2$. Let us now consider the last term in (E.18) that can be written as

$$i\pi \int \frac{d\mathbf{k}_{123}d\omega_{23}}{\omega_3 (2\pi)^9} k_1^2 k_2^2 \mathbf{k}_3 \cdot (\mathbf{k}_2 - \mathbf{k}_1) \langle \psi(\mathbf{k}_1, \omega = 0) \psi(\mathbf{k}_2, \omega_2) \psi(\mathbf{k}_3, \omega_3) \rangle. \tag{F.3}$$

Substituting (E.8) we find

$$\begin{aligned}
& i\pi \int \frac{d\mathbf{k}_{1234} d\omega_{234} k_1^2 k_2^2 \mathbf{k}_3 \cdot (\mathbf{k}_2 - \mathbf{k}_1)}{\omega_3 (2\pi)^{12}} \left(\overline{|k_4|} - \frac{\mathbf{k}_4 \cdot \mathbf{k}_1}{|k_1|} \right) \langle \eta(\mathbf{k}_1 - \mathbf{k}_4, -\omega_4) \psi(\mathbf{k}_2, \omega_2) \psi(\mathbf{k}_3, \omega_3) \\
& \times \psi(\mathbf{k}_4, \omega_4) \rangle = i\pi \int \frac{d\mathbf{k}_{23} d\omega_3}{\omega_3 (2\pi)^4} (\mathbf{k}_2 + \mathbf{k}_3)^2 k_2^2 \mathbf{k}_3 \cdot (2\mathbf{k}_2 + \mathbf{k}_3) \left(\overline{|k_3|} - \frac{\mathbf{k}_3 \cdot (\mathbf{k}_2 + \mathbf{k}_3)}{|\mathbf{k}_2 + \mathbf{k}_3|} \right) \frac{\Omega_3}{4i|k_3|} \\
& \times [n_2 \delta(\omega_3 - \Omega_2) - n_{-2} \delta(\omega_3 + \Omega_{-2})] [n_3 \delta(\omega_3 + \Omega_3) + n_{-3} \delta(\omega_3 - \Omega_{-3})] + i\pi \int \frac{d\mathbf{k}_{23} d\omega_3}{\omega_3 (2\pi)^4} \\
& \times (\mathbf{k}_2 + \mathbf{k}_3)^2 k_2^2 \mathbf{k}_3 \cdot (2\mathbf{k}_2 + \mathbf{k}_3) \left(\overline{|k_2|} - \frac{\mathbf{k}_2 \cdot (\mathbf{k}_2 + \mathbf{k}_3)}{|\mathbf{k}_2 + \mathbf{k}_3|} \right) \left(\frac{\Omega_2}{4i|k_2|} \right) \\
& \times [n_2 \delta(\omega_3 - \Omega_2) + n_{-2} \delta(\omega_3 + \Omega_{-2})] [n_3 \delta(\omega_3 + \Omega_3) - n_{-3} \delta(\omega_3 - \Omega_{-3})], \tag{F.4}
\end{aligned}$$

where the term involving the contraction $\langle \eta(\mathbf{k}_1 - \mathbf{k}_4, -\omega_4) \psi(\mathbf{k}_4, \omega_4) \rangle$ corresponding to $\langle \psi(\mathbf{k}, \omega = 0) \rangle$, vanishes as was shown in the analysis of the previous term, where we omitted the terms supported at the zero frequency. Taking the integral over ω_3 , omitting the terms supported at the zero frequency, we find

$$\begin{aligned}
& i\pi \int \frac{d\mathbf{k}_{23}}{(2\pi)^4} (\mathbf{k}_2 + \mathbf{k}_3)^2 k_2^2 \mathbf{k}_3 \cdot (2\mathbf{k}_2 + \mathbf{k}_3) \left(\overline{|k_3|} - \frac{\mathbf{k}_3 \cdot (\mathbf{k}_2 + \mathbf{k}_3)}{|\mathbf{k}_2 + \mathbf{k}_3|} \right) \\
& \times \left[\frac{n_2 n_{-3} \delta(\Omega_2 - \Omega_{-3})}{4i|k_3|} + \frac{n_{-2} n_3 \delta(\Omega_{-2} - \Omega_3)}{4i|k_3|} \right] + i\pi \int \frac{d\mathbf{k}_{23}}{(2\pi)^4} \\
& \times (\mathbf{k}_2 + \mathbf{k}_3)^2 k_2^2 \mathbf{k}_3 \cdot (2\mathbf{k}_2 + \mathbf{k}_3) \left(\overline{|k_2|} - \frac{\mathbf{k}_2 \cdot (\mathbf{k}_2 + \mathbf{k}_3)}{|\mathbf{k}_2 + \mathbf{k}_3|} \right) \\
& \times \left[-\frac{n_{-2} n_3 \delta(\Omega_3 - \Omega_{-2})}{4i|k_2|} - \frac{n_2 n_{-3} \delta(\Omega_2 - \Omega_{-3})}{4i|k_2|} \right] = 0, \tag{F.5}
\end{aligned}$$

where zero is obtained in the same way as with the previous term. The result of this appendix is that λ can be written as

$$\lambda = \frac{1}{2} \int \frac{k_1^2 k_2^2 d\mathbf{k}_{12}}{(2\pi)^4} \int \frac{d\omega}{2\pi} \langle \psi(\mathbf{k}_1, \omega) \psi(\mathbf{k}_2, \omega = 0) \rangle. \tag{F.6}$$

G Continuity of the PDF of particle-velocity gradient for $St = St^*$

To prove the continuity of the PDF $\mathcal{P}(x, \alpha)$ for $St = St^*$ we first notice that the limit $St \rightarrow St^*$ is equivalent to $\tilde{w} \rightarrow 0$. The limit $\tilde{w} \rightarrow 0$ of the solution Eq. (2.9) in the small-Stokes number regime is $p(x) = C_1 f(x) I_{0,w}(x)$, where

$$f(x) = \frac{(w-x)^{m-1}}{(w+x)^{m+1}x^2} \exp\left[-\frac{\nu - \Delta\nu}{2x}\right], \quad (\text{G.1})$$

where $I_{0,w}(x)$ is the characteristic function of the interval $(0, w)$. To study the limit of the solution Eq. (2.11), let us consider the limits $p_1(x)$ and $p_2(x)$ when $\tilde{w} \rightarrow 0$. The latter is easily obtained as

$$p_2(x) \sim \exp\left[\frac{(\nu - \Delta\nu)\pi}{4\tilde{w}}\right] f(x). \quad (\text{G.2})$$

Now let us rewrite $p_1(x)$ as

$$p_1 = \frac{|w-x|^{m-1}}{|w+x|^{m+1}(x^2 + \tilde{w}^2)} \exp\left[-n \arctan\left(\frac{\tilde{w}}{x}\right)\right] \\ \times \int_{-w}^x \frac{|w+y|^{m+1}(\nu - 2y)dy}{|y-w|^{m-1}(w^2 - y^2)} \exp\left[n \arctan\left(\frac{\tilde{w}}{y}\right)\right]. \quad (\text{G.3})$$

As $\tilde{w} \rightarrow 0$, then $p_1(x) = \mathcal{O}(1)$ if $x < 0$ and

$$p_1(x) \sim 2 \exp\left[\frac{(\nu - \Delta\nu)\pi}{4\tilde{w}}\right] \tilde{w}^2 f(x), \quad (\text{G.4})$$

for $x > 0$. To obtain the last asymptotic one takes into account that the main contribution in the integral (G.3) is brought by the right small vicinity of $y = 0$, say $(0, s)$ and apply

$$\int_0^s \exp\left[-\frac{1}{\delta} \arctan\left(\frac{y}{\delta}\right)\right] dy \sim \int_0^s \exp\left(-\frac{y}{\delta^2}\right) \sim \delta^2, \quad (\text{G.5})$$

for all $s > 0$ and small δ . The continuity of the solution of Eq. (2.8) in the limit $\tilde{w} \rightarrow 0$ is therefore guaranteed by the conditions

$$C = \frac{C_1}{2\tilde{w}^2 \exp[\nu - \Delta\nu\pi/(4\tilde{w})]}, \quad C_2 = 2C\tilde{w}^2. \quad (\text{G.6})$$

This conditions are indeed equivalent to the normalization conditions

$$\int p(x)dx = 1, \quad \int q(x)dx = 0, \quad (\text{G.7})$$

where $q = -[C + (1/(4\tau^2) + s_0/\tau - x^2)p]$. To this notice that Eq. (2.8) can be written as

$$\left\{ \left[\frac{s^2}{\tau^2} - \left(\frac{1}{4\tau^2} - x^2 \right)^2 \right] p + Cx^2 \right\}_x + \nu q = 0. \quad (\text{G.8})$$

It follows that

$$\int_{-x}^x q(y)dy = -\frac{1}{\nu} \left[\frac{s^2}{\tau^2} - \left(\frac{1}{4\tau^2} - x^2 \right)^2 \right] [p(x) - p(-x)]. \quad (\text{G.9})$$

Thus, the second condition in Eq. (G.7) is equivalent to

$$\lim_{x \rightarrow \infty} x^4 [p(x) - p(-x)] = 0. \quad (\text{G.10})$$

According to Eq. (2.11) $p(x)$ is written as the sum of p_1 and p_2 , whose asymptotic behavior is

$$p_1(x) \sim \frac{1}{x^2} + \frac{P_1^+}{x^4}, \quad x \rightarrow \infty, \quad p_1(x) \sim \frac{1}{x^2} + \frac{P_1^-}{x^4}, \quad x \rightarrow -\infty, \quad \text{and} \quad (\text{G.11})$$

$$p_2(x) \sim \frac{P_2^+}{x^4}, \quad x \rightarrow \infty, \quad p_2(x) \sim \frac{P_2^-}{x^4}, \quad x \rightarrow -\infty. \quad (\text{G.12})$$

Notice that $P_2^- = 0$, $P_2^+ = \exp[(\nu - \Delta\nu)\pi/4\tilde{w}]$. Thus Eq. (G.10) becomes

$$C_2 = \frac{C(P_1^+ - P_1^-)}{P_2^+}. \quad (\text{G.13})$$

In the limit $\tilde{w} \rightarrow 0$,

$$P_1^- = o(P_1^+), \quad P_1^+ \sim 2\tilde{w}^2 P_2^+, \quad (\text{G.14})$$

and we obtain

$$C_2 \sim 2\tilde{w}^2 C, \quad (\text{G.15})$$

which implies the continuity of PDF. Normalization of $p(x)$ in the limit $\tilde{w} \rightarrow 0$ is equivalent to the first condition in Eq. (2.8).

H The derivation of Lyapunov moments

The behavior of the Lyapunov moments γ_n , defined as $\langle R^n \rangle \sim \exp(\gamma_n t)$ is determined by a closed system of $2(n+1)$ equations

$$\frac{d}{dt} \langle R^{n-i} V^i \rangle = (n-i) \langle R^{n-i-1} V^{i+1} \rangle - \frac{i}{\tau} \langle R^{n-i} V^i \rangle + \frac{i}{\tau} (\alpha + s_0) \langle R^{n-i+1} V^{i-1} \rangle, \quad (\text{H.1})$$

$$\frac{d}{dt} \langle \alpha R^{n-i} V^i \rangle = (n-i) \langle \alpha R^{n-i-1} V^{i+1} \rangle - \left(\frac{i}{\tau} + \nu \right) \langle \alpha R^{n-i} V^i \rangle - \frac{i}{\tau} s_0 \langle \alpha R^{n-i+1} V^{i-1} \rangle, \quad (\text{H.2})$$

where $i = 0, 1, \dots, n$. The n -th Lyapunov moment γ_n is the largest solution of this system of this system

$$\det \begin{bmatrix} \mathbf{A} & \mathbf{C} \\ \mathbf{D} & \mathbf{B} \end{bmatrix} = 0, \quad (\text{H.3})$$

here \mathbf{A} and \mathbf{B} are tri-diagonal matrices with the elements

$$\begin{aligned} A_{i,i} &= \gamma_n + i/\tau & i &= 1, n \\ A_{i,i-1} &= -is_0/\tau & i &= 2, n \\ A_{i,i+1} &= i - n & i &= 1, n - 1 \\ B_{i,i} &= \gamma_n + \nu + i/\tau & i &= 1, n \\ B_{i,i-1} &= is_0/\tau & i &= 2, n \\ B_{i,i+1} &= i - n & i &= 1, n - 1 \end{aligned} \quad (\text{H.4})$$

and \mathbf{C} and \mathbf{D} are sub-diagonal matrices with the elements $C_{i,i-1} = -i/\tau$ for $i = 2, n$ and $D_{i,i-1} = i(s_0^2 - s^2)/\tau$ for $i = 2, n$.

In the limit $\text{St} \rightarrow 0$ one recovers the Lyapunov moments of fluid tracers [43]:

$$\gamma_n = \sqrt{\left(\frac{\nu}{2}\right)^2 + s^2(n^2 - n)} - \frac{\nu}{2}. \quad (\text{H.5})$$

Notice that for fluid tracers the sign of the separation R is preserved, and hence the moments $\langle R^n \rangle$ and $\langle |R|^n \rangle$ coincide. The asymptotic linear behavior of γ_n for large n is the hallmark of the presence of an upper bound for velocity gradients.

תקציר

עבודה זו עוסקת במספר תופעות פיזיקאליות שטורבולנציה היא האלמנט המרכזי בהן. המונח טורבולנציה, מתייחס למערכות עם מספר רב של דרגות חופש הרחק משיווי משקל. כל בעיה עומדת בפני עצמה, אך בכולן המערכות הנדונות הן מחוץ לשיווי משקל. כמו כן, בכולן אני מתרכזת בהתפלגויות פרקטליות במרחב הפיזיקאלי או במרחב הפאזה. בתחילת העבודה, אני דנה בהיווצרות צברי חלקיקים בתוך זרם כתוצאה מקומפרסיביליות ואינרציה. לאחר מכן אני מתרכזת בטורבולנציה במערכות דו ממדיות. בחלק זה, אני בודקת את טבעם הפרקטלי של מסלולי משתנים סקלרים פסיביים בשדות מהירות קרצנניים חלקים. בנוסף, אני חוקרת את מדרוג האנרגיה במערכת מערבולות מאולצת. בחלק הבא, אני מראה איך במערכות לא ליניאריות, ומחוץ לשיווי משקל, ניתן להשתמש באנליזה של פונקציונאל העבודה כדי לחקור מערכות אלו. האנליזה בה אני נעזרת מטפלת באירועים נדירים הקובעים את צורת הזנב של פונקצית ההתפלגות. אירועים נדירים אלו מייצגים את קצב ייצור העבודה האנומלי, ובהתאם לכך מכילים מידע על קונפיגורציות ספציפיות של המערכת. לבסוף, אני מציעה שיטה חדשה לשימוש בערבוב בתנאי אי שיווי משקל בכדי להאיץ את התכנסות אלגוריתם MCMC אל עבר מצב שיווי משקל.



מכון ויצמן למדע

WEIZMANN INSTITUTE OF SCIENCE

Thesis for the degree
Doctor of Philosophy

עבודת גמר (תזה) לתואר
דוקטור לפילוסופיה

Submitted to the Scientific Council of the
Weizmann Institute of Science
Rehovot, Israel

מוגשת למועצה המדעית של
מכון ויצמן למדע
רחובות, ישראל

By
Marija Vucelja

מאת
מריה ווצליה

פרקטלים ואירועים נדירים במערכות רחוקות משיווי משקל
Fractals and rare events in non-equilibrium systems

Advisor:
Prof. Gregory Falkovich

מנחה:
פרופ' גריגורי פלקוביץ

July, 2010

אב תש"ע